



**Biological Effects of Low Power Microwave Radiation on Proteins and Cells:
Modelling and Experimental Evaluation**

**A thesis submitted in fulfilment of the requirements for the degree of
Doctor of Philosophy**

SOHNI SINGH JAIN

M.Phil. (Computational Biology) University of Delhi, India

**School of Engineering
College of Science, Engineering and Health
RMIT University**

June 2018

DECLARATION

I certify that except where due acknowledgement has been made, the work is that of the author alone; the work has not been submitted previously, in whole or in part, to qualify for any other academic award; the content of the thesis/project is the result of work which has been carried out since the official commencement date of the approved research program; any editorial work, paid or unpaid, carried out by a third party is acknowledged; and, ethics procedures and guidelines have been followed.

I acknowledge the support I have received for my research through the provision of an Australian Government Research Training Program Scholarship.

Sohni Singh Jain

June 2018

ACKNOWLEDGEMENTS

I dedicate this thesis to *my mother, my husband, and my two beautiful sons Chaitanya and Viraj*. Their constant support, patience and encouragement have helped me to complete this research project successfully. A special thanks to my Husband **Ravi** who has patiently supported me and remained by my side in good and tough times.

I would like to acknowledge the important contributions of the following people and organisations during the entire course of my PhD research project. First, my highest and most sincere acknowledgement goes to my main supervisor, Dr Elena Pirogova, for providing me with the opportunity to undertake this PhD study under her supervision. Her constant encouragement and support during my candidature were indispensable. I want to thank her for showing patient support and assistance so that I can get the best benefits from this study.

Secondly, I sincerely acknowledge my consultant, **Dr Vuk Vojisavljevic**, and my supervisors **Prof. Andy Ball** and **Dr Sara Barachi** for their consistent assistance, guidance and support at every stage of my research at RMIT University.

Thirdly, I am thankful for the research facilities offered by RMIT University, mainly by the School of Electrical and Computer Engineering, College of Science, Engineering and Health and RMMF, RMIT University.

I also acknowledge the support I have received for my research through Australian Postgraduate Award scholarship, Australian Government Research Training Program scholarship, School of Computer and Electrical Engineering (SECE) top-up scholarship and Australia Centre for Electromagnetic Bioeffects Research (ACEBR) for financial support. I also acknowledge the paid editorial assistance of Dr Bradley Smith.

Finally, my acknowledgement also goes to my family-like friends **Sonia, Varun, Deepika and Dheeraj** for their unswerving love. You guys mean a lot to me. Thanks for always around me to help and support.

Sohni Singh Jain

June 2018

ABSTRACT

Rapid growth in telecommunication and related technologies has resulted in increased exposure of human population to low power non-ionising Electromagnetic Radiation (EMR). This research is focussed on studying biological effects of low power EMR at the molecular and cellular levels. Radiofrequency/Microwave (RF/MW) radiation has been integrated into modern telecommunication systems, health (medical devices) and even food technology. However, the increasing rate of exposure to RF/MW radiation (especially exposures from mobile phones) has raised a health concern and stimulated much research into biological and health effects of MWs and the mechanisms of interaction between MW radiation and living matter. The primary objectives of this project are: (i) to improve our understanding of the impact of low power MWs (1.8 GHz - 2.6 GHz) emitted by handheld mobile communication devices on ion channel proteins, isolated enzymes and yeast cells; and (ii) determine the safe thresholds of induced biological effects.

This project has two arms (computational and experimental) and is undertaken via the sequentially linked four sub-studies: (i) Molecular simulation of Conotoxin protein exposed to low strengths static and oscillating electric fields; (ii) *in-vitro* evaluation of MW radiation (frequencies 2.1 GHz, 2.3 GHz and 2.6 GHz and powers -10, 0 and 17dBm) on biological activity of L-Lactate Dehydrogenase and Catalase enzymes; (iii) *in-vitro* evaluation of changes in growth rate of yeast cells exposed to MW radiation (frequencies 1.8GHz and 2.1GHz and powers -10, 0, and 17dBm, and (iv) *in-vitro* evaluation of MW radiation (frequency 1.8 GHz and powers -10, 0, 17 dBm) on bioactivity of TRP ion channel proteins (expressed in epithelial cells). The findings are summarised as follows:

(i) *in-silico* analysis show that conformational changes in Conotoxin occur under the exposure to weak static and oscillating electric fields of particular strengths;

(ii) low power MW radiation induces modulating (inhibition and promotion) effects on LDH and Catalase enzyme kinetics at the particular frequencies and powers of exposures. The results indicate the frequency- and power-dependence of the observed biological effects;

(iii) low power MW radiation induces cell proliferation or inhibition on yeast cells growth depending on the exposure parameters, and

(iv) effects of MW exposures at the particular powers induce n Ca^{2+} ion influx and affects gating function of TRP ion channel proteins.

In essence, this study demonstrated that even non-thermal microwave exposures produce modulating effects at the molecular and cellular levels. The outcomes of this study will assist in understanding the bioeffects of low power MWs and their interaction with biological media. It will also assist in identifying thresholds of MW exposures affecting the selected proteins and cells, and will be useful in providing much-needed evidence on defining safe exposure limits. Further investigation of the mechanism of action of microwaves of different frequency and power combinations is proposed for future work as an extension of this project.

TABLE OF CONTENTS

DECLARATION	II
ACKNOWLEDGEMENTS	III
ABSTRACT	III
TABLE OF CONTENTS	VI
LIST OF TABLES	IX
LIST OF FIGURES	X
CHAPTER 1: INTRODUCTION	1
1.1 MOTIVATION	1
1.2 OBJECTIVE	4
1.3 COMPUTATIONAL STUDY	6
1.4 EXPERIMENTAL INVESTIGATION	6
1.5 THESIS COMPOSITION	9
CHAPTER 2: LITERATURE REVIEW	11
2.1 INTRODUCTION	11
2.2 A BRIEF OVERVIEW OF THE ELECTROMAGNETIC SPECTRUM AND EMR	11
2.3 LOW-POWER EMR AND MOBILE COMMUNICATION TECHNOLOGY	14
2.4 HEALTH CONCERNS AND EXPOSURE GUIDELINES	17
2.4A IN-SILICO (MOLECULAR MODELLING) STUDIES	21
2.4B IN VITRO STUDIES.....	22
2.4C IN VIVO ANIMAL AND HUMAN STUDIES	28
2.5 SUMMARY	32
CHAPTER 3: EFFECTS OF STATIC AND TIME-VARYING ELECTRIC FIELDS ON THE CONFORMATION OF CONOTOXIN PROTEIN: A MOLECULAR MODELLING STUDY	33
3.1 INTRODUCTION	33
3.2 COMPUTATIONAL MODELLING STUDY	34
3.2.1 MODEL SYSTEM: CONOTOXIN PEPTIDE	34
3.2.2 PARAMETERS OF EXTERNAL STATIC AND TIME-VARYING ELECTRIC FIELDS	34
3.2.3 MOLECULAR MODELLING APPROACH: MOLECULAR DYNAMICS SIMULATION	36
3.2.4 STATIC AND TIME-VARYING EXTERNAL ELECTRIC FIELDS.....	36
3.3 RESULTS AND DISCUSSION	39
3.3.1 STUDY ONE: EXTERNAL STATIC ELECTRIC FIELD OF 0.01 V/NM, 0.001 V/NM AND 0.0001 V/NM	39
3.3.2 STUDY TWO: EXTERNAL STATIC ELECTRIC FIELD OF 0.000055 V/M, 0.00123 AND 1E+9	42
3.3.3 STUDY THREE: EXTERNAL TIME-VARYING ELECTRIC FIELD AT 4.7E-8 V/NM, 6E-9 V/NM, 2E-9 V/NM	46
3.3.4 SECONDARY STRUCTURE ANALYSIS OF CONOTOXIN PEPTIDE UNDER TIME-VARYING ELECTRIC FIELDS	48
3.3.5 CONOTOXIN CLUSTER ANALYSIS.....	50
3.4 CONCLUDING REMARKS	53

3.4.1 THE CONCLUSION FROM STUDY 1	53
3.4.2 THE CONCLUSION FROM STUDY 2	53
3.4.3 THE CONCLUSIONS FROM STUDY 3	54
CHAPTER 4: EFFECTS OF LOW POWER MICROWAVE RADIATION ON KINETICS OF L-LACTATE DEHYDROGENASE AND CATALASE ENZYMES	55
4.1 INTRODUCTION	55
4.2 EXPERIMENTAL EVALUATION <i>IN VITRO</i>	55
4.2.1 TRANSVERSE ELECTRO-MAGNETIC (TEM) CELL EXPOSURE SYSTEM	55
4.2.2 LACTATE DEHYDROGENASE (LDH)	58
4.2.3 CATALASE ENZYME	60
4.3 RESULTS AND DISCUSSION	61
4.3.1 CHANGES IN LDH ENZYME CATALYTIC ACTIVITY	62
4.3.2 CHANGES IN CATALASE ENZYME	63
4.4 CONCLUDING REMARKS	67
CHAPTER 5: EFFECTS OF MICROWAVES AT 1800MHZ AND DIFFERENT LOW POWERS ON YEAST CELLS	69
5.1 INTRODUCTION	69
5.2 EXPERIMENTS AND ANALYSIS	69
5.2.1 MODEL SYSTEM: YEAST	69
5.2.2 YEAST GROWTH PHASES	70
5.2.3 MICROWAVES EXPOSURE PARAMETERS	71
5.2.5 YEAST CELL SAMPLE PREPARATION FOR TEM	72
5.2.6 CELL COUNT AND VIABILITY	72
5.2.7 FLUORESCENCE MICROSCOPY	72
5.3 RESULTS AND DISCUSSION	74
5.3.1 SPECTROPHOTOMETRIC ANALYSIS OF YEAST SAMPLES	74
5.3.2 IMAGE ANALYSIS OF YEAST CELLS	79
5.3.3 TEM STUDY OF YEAST CELLS	82
5.4 CONCLUDING REMARKS	85
CHAPTER 6: LOW POWER MICROWAVES INDUCE CHANGES IN FUNCTIONAL PROPERTIES OF TRPV4, A MECHANICALLY ACTIVATED ION CHANNEL	88
6.1 INTRODUCTION	88
6.2 MATERIALS AND METHODS	89
<i>GSK1016790A Agonist</i>	<i>89</i>
<i>Cell culture and Ca²⁺ measurement protocol</i>	<i>89</i>
<i>Preparation of cells for Transmission Electron Microscopy</i>	<i>90</i>
<i>Statistical Analysis</i>	<i>90</i>
<i>Exposure System Setup</i>	<i>90</i>
6.3 RESULTS AND DISCUSSION	91
6.3.1 <i>Agonist (GSK1016790A) response of TRPV4 ion channel protein at room temperature when irradiated for 4 hrs and 2hrs at 1800 MHz and 17 dBm</i>	<i>91</i>

6.3.2	Agonist GSK1016790A response of TRPV4 ion channel protein at 25°C after 2 and 4 hrs of exposure at 1800 MHz and 0 dBm	93
6.3.3	The average maximum response of TRPV4 ion channel at 25°C irradiated for 4 and 2 hrs at 1800 MHz and -10 dBm.	94
6.3.4	The average maximum response of TRPV4 ion channel at room temperature (25°C ±2°C) when irradiated for 4 hrs and 2 hrs at 1800 MHz and 17 dBm.....	96
6.3.5	Agonist GSK1016790A response of TRPV4 ion channel protein at body temperature (37°C ±2.5°C) and 4hrs and 2 hrs of irradiation at 1800 MHz and 17 dBm.....	98
6.4	TEM ANALYSIS OF HEK-293 CELLS.....	102
6.5	CONCLUDING REMARKS.....	104
	CHAPTER 7: CONCLUSION AND FUTURE DIRECTIONS.....	106
7.1	CONCLUSIONS.....	106
	EFFECTS OF LOW POWER MICROWAVES RADIATION ON KINETICS OF L-LACTATE DEHYDROGENASE (LDH) AND CATALASE ENZYMES (CHAPTER 4)	108
7.2	FUTURE WORK.....	110
	PUBLICATIONS.....	112
	REFERENCES.....	113

LIST OF TABLES

Table 2.1 Effects of low power MW radiation in the frequency range of 450MHz –2GHz	25
Table 2.2. Effects of MW of varying SAR and duration at the cellular level	26
Table 2.3: Findings of latest research studies on the effects of low-power MW radiation	29
Table 3.1: The SAR values of the MW exposures limits based on the ICNIRP limit	35
Table 3.2: Microwaves simulations parameters for Static Electric field in the range of 17, 0 and -10 dBm	35
Table 3.3: Simulations parameters used to simulate Conotoxin for the time-varying electric field at the microwave frequency 1800 MHz and electric strengths of 17 dBm, 0 dBm and -10 dBm	35
Table 3.4: Distance between the Ramachandran Angles (Phi and Psi) sets calculated for static electric fields of selected strengths vs no-field condition	39
Table 5.1. Exposure System and Sample Preparation for Spectrophotometric Analysis	71
Table 5.2: Chi-square test results	79

LIST OF FIGURES

Figure 2.1: Electromagnetic radiation – the propagation of energy in the form of electromagnetic waves through a medium [30].	12
Figure 2.2: Electromagnetic spectrum showing the entire range of wavelength and frequency [30].	13
Figure 2.3: Working Principle of mobile call [34].	15
Figure 3.1: RMSD data calculated for No-field vs static electric field of 0.01 V/nm exposure.	40
Figure 3.2: Change of the radius of gyration (Rg) during MD simulation for No-field (black line) vs electric field 0.01V/nm (red line) conditions.	41
Figure 3.3: Cladogram of Conotoxin peptides conformations: no-field (NF) and different electric fields conditions.	41
Figure 3.4: Conotoxin backbone's RMSD evolution over the 1000 ps simulation time at different strengths 0.00123, 0.000055 and 1e+9 V/m compared to the no-field condition.	43
Figure 3.5: The radius of gyration (Rg) of Conotoxin peptide under the stress of external electric fields of 0.000055, 0.00123, and 1e+9 V/m compared to the no-field condition.	43
Figure 3.6: Peptide-water interactions represented by the radial distribution functions. The line colour is representative of the electric field strength: 1e+9 V/m (red), 0.00123 V/m (green), 0.000055 V/m (blue), no-field (black).	44
Figure 3.7: Snapshots of Conotoxin conformation at no-field condition (A, B), electric fields of 0.00123 V/m (C, D) and 1e+9 V/m (E, F) at 500 ps and 1000 ps respectively. The white colour encodes non-polar residues; green colour encodes polar residues, red colour encodes acidic residues and blue - basic residues. The arrow indicates the direction of the electric field.	45
Figure 3.8: Conotoxin structural deviations vs simulation time at the frequency 1800 MHz and different field strengths. RMSD values of peptide's C α -atoms with a field amplitude of 4.7e-8 V/nm, 6e-9 V/nm, 2e-9 V/nm and with zero field conditions at 300 K.	46
Figure 3.9: Conotoxin structural deviations during the simulations time at the field frequency 1800 MHz and different strengths. RMSF values calculated for each amino acid of Conotoxin peptide at the field strengths 4.7e-8 V/nm, 6e-9 V/nm, 2e-9 V/nm and "no- fie	47
Figure 3.10: The secondary structure of lysozyme at different field strengths and "no-field" conditions. Distribution of secondary structure elements over the Conotoxin sequence at frequencies of 1.800 GHz and power of 4.7e-8 V/nm (purple), 6e-9 V/nm (blue), 2e-9 V	48
Figure 3.11: Peptide-water interactions represented by radial distribution functions The line colour is representative of the electric field strength: 4.7e-8 V/m (blue), 2e-9 V/m (red), 6e-9 V/m (blue), no-field (violet).	49
Figure 3.12: Schematic diagram showing the number of clusters sampled at the different field strengths during the simulation.	50
Figure 3.13: Snapshots of Conotoxin conformation at no-field condition (A, B), electric fields of 0.00123 V/m (C, D) and 1e+9 V/m (E, F) at the last frame of each repeat.	52
Figure 4.1: Experimental set up showing exposure camera, signal generator, controller, cuvette holder and spectrophotometer [20].	56
Figure 4.2: The position of the sample and the direction of the electric field inside the TEM cell; b. The vertical distance from the top of the cell to the sample is 22 cm. b Field pattern at the position of the sample (top view)[109].	56
Figure 4.3: PDB structure of LDH M tetramer (LDH5) from human[164].	59
Figure 4.4: PDB structure of catalase from <i>Saccharomyces cerevisiae</i> [165].	60

Figure 4.5: Relative change in the rate of reaction of NADH for irradiated vs non-irradiated LDH at different frequencies and powers	62
Figure 4.6: Relative change of Dissociation constant of H ₂ O ₂ for irradiated vs non-irradiated Catalase samples at the frequencies of 2.1 GHz, 2.3 GHz, and 2.6 GHz at 17 dBm and -10 dBm	63
Figure 4.7: Relative change of dissociation constant of H ₂ O ₂ for irradiated vs non-irradiated Catalase at 2600 MHz and five different powers of 0 dBm, -20 dBm, -30, -40, and -50 dBm	64
Figure 4.8: Relative change in absorption at 1800 MHz and power of 0, -10 and 17 dBm	65
Figure 4.9: Relative change in absorption at 2100 MHz and power of 0, -10 and 17 dBm	65
Figure 4.10: Changes in the absorption of Catalase at 1800 MHz and power of -10 dBm, 0 dBm and 17 dBm compared with Control (Non-irradiated) sample	66
Figure 4.11: Changes in the absorption of Catalase at 2100 MHz MHz and power of -10 dBm, 0 dBm and 17 dBm compared with control (non-irradiated) samples.	67
Figure 5.1: Typical Yeast Growth Curve of Saccharomyces [87].....	70
Figure 5.2 A) Initial image from the microscope B) Final image generated by ImageJ software	73
Figure 5.3: OD600 of control and a test sample of yeast cells irradiated at 1800MHz and selected power of 0, -10 and 17 dBm	74
Figure 5.4: Cell viability of control yeast vs test yeast samples irradiated at 1800MHz and powers -10, 0, and 17 dBm	75
Figure 5.5: Change in yeast cells growth under MW exposures at the different frequency, and power	76
Figure 5.6: Changes in absorbance of yeast cells exposed to different frequencies of 1800 MHz and powers of 17 dBm, 0 dBm and -10 dBm6.	77
Figure 5.7: Changes in absorbance of yeast cells exposed to different frequencies of 2100 MHz and powers of 17 dBm, 0 dBm and -10 dBm. I : Irradiated samples, and NR :Non-irradiated.....	77
Figure 5.8: Change in concentration of yeast over the period of 6 hours; irradiated vs non-irradiated samples (%)	78
Figure 5.9: Change in concentration of yeast over the period of 6 hours; irradiated vs non-irradiated samples (%)	79
Figure 5.10: Effect of irradiation at 1800MHz and -10dBm on the circularity of yeast sample at the end of 6th hour of the growth phase.....	80
Figure 5.11: Effect of irradiation at 1800 MHz and 17dBm on the circularity of yeast sample at the end of 5th hour of the growth phase	80
Figure 5.12: Elongation factor distribution among the irradiated vs non-irradiated yeast sample at the end of 6th hour of growth phase: [a] irradiated at 1800MHz and -10dBm; and [b] irradiated at 1800MHz and 17dBm.....	82
Figure 5.13: Transmission Electron Microscope (TEM images of control yeast samples (unexposed after 6 hours) with a well-organised nucleus and cell membrane.	83
Figure 5.14: Transmission Electron Microscope (TEM) images of yeast cells irradiated at 1800 at -10 dBm showing dividing cells (DC) after exposure and other cells.....	83
Figure 5.15: Transmission Electron Microscope (TEM) images of yeast cells irradiated at 1800 at 0 dBm. Loss of cell membrane (CM) and diffused nucleus(N).....	84
Figure 5.16: Transmission Electron Microscope (TEM) images of yeast cells irradiated at 1800 at 17 dBm. Arrows are showing affected nucleus (N) and cell membrane (CM) after exposure.....	84
Figure 6.1: Agonist (GSK1016790A) response of TRPV4 ion channel protein at 25°C when irradiated for 4 hr at 1800 MHz and 17 dBm.....	92

Figure 6.2: Agonist (GSK1016790A) response of TRPV4 ion channel protein at 25°C, when irradiated for 2 hr at 1800 MHz and 17 dBm.....	92
Figure 6.3: Agonist GSK1016790A response of TRPV4 ion channel protein at 25°C, when irradiated for 4hr at 1800 MHz and 0 dBm.....	93
Figure 6.4: Agonist GSK1016790A response of TRPV4 ion channel pro attain 25°C when irradiated for 2 hr at 1800 MHz and 0 dBm.	94
Figure 6.5: Agonist GSK1016790A response of TRPV4 ion channel protein at 25°C when irradiated for 4 hrs at 1800 MHz and -10 dBm. At all four concentrations of GSK1016790A, we do not find any changes in channel response.	95
Figure 6.6: Agonist GSK1016790A response of TRPV4 ion channel protein at 25°C when irradiated for 2 hrs at 1800 MHz and -10 dBm. The black line corresponds to control and red line to irradiated sample.....	96
Figure 6.7: Effect of different radiation powers and times of exposure on TRPV4 responses to its selective agonist. (A&B) show the effect of 1800 MHz and 17 dBm radiation upon 4 hrs and 2 hrs respectively. (C&D) show the effect of 1800 MHz and 0 dBm radiation upon 4 hrs and 2 hrs respectively. (E&F) show the effect of 1800 MHz and -10 dBm of radiation upon 4 hrs and 2 hrs respectively.	97
Figure 6.8: Agonist GSK1016790A response of TRPV4 ion channel protein at 37°C when irradiated for 4 hrs and 2hrs respectively at 1800 MHz and 17 dBm	100
Figure 6.9: Effect of different radiation powers and times of exposure on TRPV4 responses to its selective agonist, (A&B) show the effect of 1800 MHz and 17 dBm radiation upon 4 hrs and 2 hrs respectively. (C&D) show the effect of 1800 MHz and 0 dBm radiation upon 4 hrs and 2 hrs respectively. (E&F) show the effect of 1800 MHz and -10 dBm of radiation upon 4 hrs and 2 hrs respectively.	101
Figure 6.10: TEM micrographs show control and HEK-293 cells exposed at 1800 MHz and powers of 17 dBm, 0 dBm, -10 dBm exposed at 37 °C for 4 hrs. Figure a: shows control HEK-293 cells kept at 37 °C, Figure B: HEK-293 cells exposed at 1800 MHz and 17 dBm, Figure C: HEK-293 cells exposed at 1800 MHz and 0 dBm, Figure D: HEK-293 cells exposed at 1800 MHz and -10 dBm.	103
Figure 6.11: TEM micrographs show the control and HEK-293 cells exposed at 1800 MHz and powers of 17 dBm, 0 dBm, -10 dBm exposed at 37 °C for 2 hrs. Figure A: shows control HEK-293 cells kept at 37 °C, Figure B: HEK-293 cells exposed at 1800 MHz and 17 dBm, Figure C: HEK-293 cells exposed at 1800 MHz and 0 dBm, Figure D: HEK-293 cells exposed at 1800 MHz and -10 dBm	104

CHAPTER 1: INTRODUCTION

1.1 Motivation

There is a proverb, do not believe your doubt, and do not doubt your belief. Technology usually plays a twin role, to serve and make life easier, and to protect from any predicted undesirable effects, natural or artificial. Most scientific investigations or even discoveries are initiated from doubt and concluded as knowledge. Today there is a doubt about the safety of the radio frequency wireless technology. Is modern mobile communication equipment/technology affecting biological systems?

Penetration of mobile communication technology in everyday life is alarming. Leading public health organisations, such as the World Health Organisation (WHO) and National Health and Medical Research Council (NHMRC), Australia, are sceptical about safety assurances coming from mobile phone manufacturers and telecom service providers. Effects of low power radiofrequency (RF) and microwave (MW) exposure depend upon the nature of the exposure, proximity to the source, and the time of exposure. However, the fact that constant exposure to low power microwaves is affecting every part of our day-to-day life and influencing over 85% of the global population cannot be denied.

We are familiar with effects of long-term exposure to high power RF and MW radiation, i.e. heating effects on body and tissue, but there is little or negligible information about the health effects of long-term exposure to low power RF and MW radiation. Modern mobile communication operates at low power RF and MW frequencies (3G, 4G), which do not produce any heating effects [1]. Affordable advanced RF wireless technology revolutionised various industries and found applications in defence, medicine, food technology, and mobile telecommunication. From 2005 to 2015, mobile phone penetration increased by 200%. In 2015, the mobile phone penetration was 60%, 5 billion worldwide mobile users are expected by 2019[2], and it will reach the 6 billion mark by 2020. It is also expected that in 2020, the global penetration of mobile phone will be 100%, meaning that the number of mobile phone subscriptions will be equal to the number of inhabitants. The exponential rise in penetration of mobile technology in our daily life creates a pressing need to investigate and evaluate the impact of long-term exposure to low power RF and MW radiation at the cellular and molecular levels on biological systems, including humans.

Mobile phone radiation is a subset of the non-ionizing part of the electromagnetic spectrum. Non-ionizing radiation does not have sufficient energy to break chemical bonds to produce its effect. Hence, the mechanism by which non-ionizing radiation, especially at low powers, interacts with biological material is still a matter of research. It is considered that tissues nearest to the mobile antenna can absorb this energy, which may contribute to changes in the standard biological functioning of the living organism [3] [4] [5]. There is evidence suggesting that, even at low powers, RF and MW radiation can affect the normal biological processes in the human body. In addition, anecdotal and scientific studies show biological and possible health effects associated with mobile phone towers and antennas. However, the research data available are still insufficient to reach conclusions regarding the health issues related to low power radiation. Many studies have been conducted to examine the relationship between RF radiation and biological effects [6] [7]; however, to date, the results have been inconclusive.

There is an ongoing scientific debate about the existence of “non-thermal” effects induced by long-term exposure to low-level RF and MW emitted by mobile phones. With recent advancements in telecommunications, the exposure to RF and MW radiation has raised to a level never before seen. The operating frequency of commercial mobile communication is in the range of 450-2700 MHz, with peak powers ranging from 0.1 to 2 Watts. The existing 4G network operates within the frequency range of 1800-2600 MHz. To accommodate the meteoric rise in the usage of mobile communication and to provide quality and reliable services, telecom industries have to employ a higher frequency band, known as a 5G network, which will include frequency bands currently used in 4G (1800-2600 MHz) and frequencies above 5000 MHz. This further raises an ongoing concern among scientific and public communities about the safety of low-power exposure and its long-term biological and possible health effects on various biological systems, including humans and other animals.

Possible health effects of increased exposure to weak (low-power) RF/MWs has received significant media coverage and raised concerns among the public, the scientific community and healthcare regulatory bodies [8-10]. In response to public concerns, in 1996 the WHO established the International Electromagnetic Fields (EMF) Project to assess the scientific evidence of possible health effects of EMFs (low-frequency and high-frequency EMFs). Specific studies have been identified to address the problem of localised exposure. The project has established a formal mechanism for reviewing the research results and conducting risk assessments of EM exposures. It is also developing public information materials and

bringing together standards groups worldwide in an attempt to harmonise international exposure standards.

A committee on Electromagnetic Energy Public Health Issues (CEMEPHI) under the Australian parliamentary committee, the Environment, Communications, Information Technology and the Arts References Committee, received submissions and evidence from some scientists and health professionals as well as community organisations and individuals [11]. Some claimed that there is ample evidence of biological and adverse health effects associated with non-thermal levels of exposure to electromagnetic radiation (EMR), while others concluded that no clear relationship had been established.

The Australian Radiation Protection and Nuclear Safety Agency (ARPANSA) specifies exposure limits to RF electromagnetic energy (EME) at the frequencies used in mobile phones [12]. On 4 July 2003, ARPANSA commenced the centralised Electromagnetic Radiation (EMR) Health Complaints Register. The Register collects reports of health concerns related to possible EMR field exposures in the range of 0-300 GHz. Since its commencement, it has received 126 reports. The register collected more than 70 reports in 2012-13 and 2013-14 alone [13]. These data indicate that, with a spike in technology, exposure-related health issues are increasing and need further detail investigation.

Based on the body of evidence on biological effects induced by low-power MWs, there is a general agreement within the scientific community that a new approach to protecting the public health is required. The scientific community has built these conclusions upon published reports documenting the following [14]:

1. Bioeffects and adverse health effects are demonstrated using low-power microwaves at levels significantly below the existing exposure standards.
2. Public safety limits issued by the International Commission on Non-Ionizing Radiation Protection (ICNIRP) ICNIRP, Institute of Electrical and Electronics Engineers (IEEE) and American National Standards Institute (ANSI) [15] [16, 17] are not sufficient to protect the public from prolonged, low-intensity exposures.
3. Exposure standards require urgent attention and revisions to protect public health worldwide.

It is worth mentioning here that the Bio-initiative report (last updated in March 2014) describes that 88% of papers published show adverse effects of radiation and just 12% of

published papers show that there is no effect of RF/MW radiation. The report also warns about risks based on the specific evidence of bio-effects, including a change in behavioural response, cardiovascular disorders, inflammatory responses, and brain tumours [18]. Research activities focused on studying the effects of RF/MW exposure and its possible bio-effects can be classified into five major categories, each addressing a specific question:

1. Understanding the mechanism by which low-level MW radiation produces bioeffects.
2. Determining the specific bioeffects due to MW radiation, which may be helpful to identify a related response mechanism in biological systems.
3. Determining whether the biological effects can impact human health.
4. Determining whether there is an association between mobile phone radiation and cancer.
5. Identifying indirect/secondary effects on human health which do not result directly from an interaction between the mobile phone radiation and biological systems.

It is, therefore, essential to improve our understanding of the biological effects of low-power RF/MW radiation used in 3G and 4G mobile networks at the molecular and cellular levels. Furthermore, it is equally critical to confirm that the currently used safety standards for the operating frequency range are indeed sufficient to protect living organisms from ever increasing electromagnetic pollution.

Responding to public concern, the Australian Centre for Electromagnetic Bioeffects Research (ACEBR) embarked on a 5-year research program to promote Australia's EME health both in the immediate future and through the development of human research capacity in this field into the future [19]. The ACEBR is a National Health and Medical Research Council (NHMRC) Centre of Research Excellence. This research project is a part of a more extensive research program initiated by the ACEBR and through the collaborative efforts of leading Australian universities and research institutes.

1.2 Objective

The current body of knowledge is not sufficient to reach a consensus and draw conclusions explaining adverse effects of low-level RF/MW radiation. There is an increasing need to study and evaluate the impact of weak RF radiation at cellular and molecular levels.

The primary objective of conducting the present research is to investigate the effects of low-power electromagnetic radiation in the range of 900MHz-2.6GHz on proteins and cells,

and in particular enzymes and ion-channel proteins. In this research project, a study was made of conformational and functional changes taking place in selected enzymes, yeast and mammalian cells due to the effects of MWs of different frequencies, power, and exposure duration (given energy dose).

Laboratory studies on animals *in-vivo* and cell cultures *in-vitro* have shown that weak static and varying electric fields may have effects on several biological processes. For example, they may alter hormone and enzyme levels and the rate of movement of some chemicals through living tissue. Although these changes do not appear to constitute a health hazard, they need further investigation in order to elucidate the possible mechanisms of actual effects, including the long-term effects. Some effects of RF radiation on biological processes can be reversible and, thus, do not impact human health. However, the significance of investigating non-thermal RF biological effects at the molecular level should not be underestimated.

This PhD research is focused on recent reports confirming that even weak RF/MW radiation can induce modulating effects on various biological systems [20] [21]. The author has studied the biological effects of low-power static and electromagnetic fields (RF/MW radiation used in 3G and 4G mobile networks) on selected model systems: proteins, yeast cells, and human cells. This research work includes irradiation of selected enzymes and cells with low-power MW used in 3G and 4G networks. Powers used were 17, 0 and -10 dBm, and frequencies of 1.8GHz, 2.1GHz, 2.3GHz and 2.6GHz, and their different combinations. *In vitro* evaluation of thermal receptor sensitivity of Transient Receptor Potential (TRP) ion channel proteins are of particular interest to the project, because members of this channel superfamily play an essential role in sensory transduction processes in vertebrates, including humans [22] [23] [24].

This research project has two arms, computational and experimental; and investigation includes *in silico* and *in vitro* sub-studies as follows:

- ***In silico*** study to evaluate the effects of applied external static and oscillating electric fields of different strengths on the conformation of Conotoxin peptide (2efz.pdb) at the nanoscale level.
- ***In vitro*** studies to evaluate experimentally the effects of MW radiation of different frequencies and powers on the biological activity of the selected enzymes (L-Lactic

dehydrogenase and Catalase), yeast (*Saccharomyces cerevisiae*) cells and TRPV4-ion channels proteins expressed in Hek-293 cells.

1.3 Computational Study

A computational method such as Molecular Dynamic (MD) simulation presents a useful insight into the analysis of effects of external electric field (stressor) on a protein's structure and its functional properties. In the computational study presented here, the effects of applied static and oscillating fields of different strengths on Conotoxin protein are simulated using MD technique. The simplicity of Conotoxin structure, i.e. 16 amino acids in length, and its wide range of therapeutic applications [25] makes it an ideal model to study its conformational changes under the electric field of different strengths.

The author studied the protein structure at the nanoscale range, as the structure of the biomolecule is directly related to the change in its function. This means that any change in the final structure of the Conotoxin protein due to static electric or electromagnetic fields may complement the change in functionality of the protein. This is crucial to this study, as proteins are the building blocks of any living organism and play a vital role in maintaining the normal biochemical reactions inside the body.

Conformational changes in the Conotoxin protein exposed to the electric fields were evaluated using multiple parameters, comprising Ramachandran Angles (phi and psi), Root Mean Square Deviation (RMSD), Radius of Gyration (Rg), and peptide water interactions represented by Radial Distribution Function (RDF). The author also studied protein unfolding which affects the formation of hydrogen bonds between residues during simulations, and which in turn affects RMSD and Rg values. A novel Dynamic Time Warping (DTW) method was introduced and employed to evaluate the conformational changes in exposed Conotoxin proteins and to compare these with the protein under standard un-exposed conditions. Conotoxin's structure was evaluated to establish the relation between applied external EMF and change in protein structure under the influence of applied EMFs.

1.4 Experimental Investigation

Within the experimental *in vitro* studies, the effects of low power MW exposures have been evaluated on the kinetics of L-Lactic dehydrogenase and Catalase enzymes irradiated at the frequencies of 1.8, 2.1, 2.3 and 2.6 GHz and powers 0dBm, -10 dBm and 17dBm, using the

commercial Transverse Electro-Magnetic (TEM) cell. The selected metabolic enzymes play an essential role in the biological processes in living cells. Enzymes control several complicated biochemical reactions and maintain the overall health and well-being of living organisms. Lactic dehydrogenase (LDH) enzyme is extensively present in blood cells and heart muscles and is a marker of common injuries and disease. Catalase is a crucial enzyme: it helps to protect the cell from oxidative damage by reactive oxygen species (ROS), hence protects living cells from unstable oxidising molecules. It is found in all types of living organisms. Catalase helps to catalyse the decomposition of hydrogen peroxide into water and oxygen. Kinetics of Catalase was studied under the low power MW exposure at the frequencies of 1.8 GHz and 2.1 GHz, and powers of -10dBm, 0dBm, and 17dBm. Absorption coefficients of Catalase were measured at a fixed time interval in test samples and compared with control samples to analyse modulating effects of applied irradiation. Furthermore, we also tested the relationship between the frequency and power of applied exposures on the enzyme reactions. The inhibitory and excitatory effects observed at the frequencies of 2.1, 2.3, and 2.6 GHz and selected powers indicate that power and frequency of applied irradiation induce effects on the enzymatic reactions independently of each other.

In addition to the studies mentioned above, evaluation was also made of the effects of the specific MW exposure on the structural and functional behaviour of *Saccharomyces cerevisiae* yeast. The objective of this study was to test the hypothesis that low-power MW radiation can produce modulating effects on cell growth. Previous research using photospectroscopy assessment shows that low-power RF/MW exposure induces modulating effects on the studied biological models [19, 26, 27]. Here, the author used (TEM) to investigate further the changes in the cell wall and internal organelles of selected yeast cells induced by low-level mobile phone radiation. Yeast cell samples were exposed at the frequency of 1.8GHz and three powers -10 dBm, 0 dBm and 17 dBm. Cell growth rate and morphology of yeast cell samples were compared to non-irradiated samples. *S. cerevisiae* yeast type II (YSC2-Sigma) was selected for its fast growth rate (~120 min doubling time). The SAR values of the MW exposures used in this study were below and above the standard safety limit (SAR of 2.0 W/kg) based on the International Commission on Non-Ionizing Radiation Protection (ICNIRP)' standards [16]. The safety limit for exposure to mobile phone emissions is set by determining the lowest level of exposure known to cause health hazards and then adding a safety margin. Yeast cell growth was analysed based on cell count, optical density and cell viability, population doubling time, cell circularity and cell elongation. The growth cycles of yeast cell

samples (test and control) were captured at regular intervals for photospectroscopy and scanning electron microscopy (SEM) assessments. The obtained results were analysed statistically using two-way repeated ANOVA.

Research studies suggest that different cells respond differently to applied radiation. Non-thermal radiation does not have enough energy to influence the cell chemistry directly but may alter biological pathways affecting specific biological actions. Thus, the author extends her research work to study the effects of low-power MW exposure on mammalian cells. Transient receptor potential cation channel subfamily V member 4 (TRPV4) is an ion channel protein encoded by the TRPV4 gene. TRPV4 channel is a calcium-permeable cation channel that is detectable in both sensory and non-sensory cells. TRPV4 is a non-selective cation channel that is expressed in various tissues, including epithelial and endothelial cells, which can be activated by different stimuli such as heat, hypotonic stress, GSK1016790A, derivatives of arachidonic acids and shear stress. TRPV4 is identified as an osmotically activated channel. For its wide range of implications from osmoregulation to thermo-sensing, the author used TRPV4 stably expressed in Hek-293 cells to better understand the thermal/non-thermal nature of the interaction between the applied MW exposure and cells.

The present sub-study was aimed at evaluating the effects of low-power MW radiation at 1.8GHz and powers of 17, 0 and -10 dBm (47, 6 and 2 V/m, respectively). In this study, Ca²⁺ imaging and confocal microscopy were used to investigate the effects of MW at the frequency of 1800 MHz and power of 17dBm on TRPV4 channel gating in response to its selective agonist GSK1016790A and hypotonic stress. To understand the effects of exposure on the bioactivity of TRPV4 channel proteins, the channel response was recorded at a pre-defined time interval. Gating function of an exposed TRPV4 sample of variable concentrations (40 mOsm, 80 mOsm, 160 mOsm, 280 mOsm) was recorded and compared with a control sample to establish whether there are any changes in the thermal sensation and thermoregulation.

Summarising the above-presented experimental and computational studies conducted within this PhD research, the author aims to answer the following research questions:

1. Whether low power RF/ MW frequencies can affect the catalytic activity of enzymes L-Lactate dehydrogenase (LDH) and Catalase; proliferation and conformation of yeast cells and bioactivity of TRP ion channels?

2. What is the relation between frequency and power of applied radiation and how it affects the activity of the selected proteins and cells?
3. Relation and the relative effect of parameters including frequency, power, exposure duration (dose/energy) absorbed by cells in the biological activity of TRPV4 ion channel proteins?
4. What are the safety thresholds of powers used in the studied MW exposures?

The expected outcomes of this research are to identify the particular effects of low-power MW on selected model systems and whether there is any relationship between frequency and power and their effects on irradiated samples. This research will open up areas for further investigation and thus assist in providing inputs to guidelines on identifying the safety limits for long-term exposure to low-power MW radiation.

1.5 Thesis Composition

This PhD thesis is primarily dedicated to improving the understanding of effects of low-power MW radiation at the frequencies used in the 3G/ 4G mobile networks on selected biomolecules and cells. An outline of the chapters of the thesis is presented as follows:

Chapter 1 – Introduction and motivation

Chapter 2 - Literature review

The chapter discusses the basic principles of EMR, mobile phone radiation range and associated health effects, and relevant research updates. In this chapter, the author will also summarise guidance for various experiments. The author will then present an overview of the strategies that are implemented to answer the identified research questions.

Chapter 3 - Computational study

This chapter presents a study of *In silico* simulation of protein (Conotoxin: 2efz.pdb) under the different strengths of static and varying electric fields. In this part, the author studies the conformational changes in Conotoxin (3D structure obtained from the protein data bank) [28]. Several approaches were applied, including a novel DTW, to evaluate the changes in the peptide backbone over the period of simulation. This knowledge can further be extended to explore applications of external static or oscillating electric fields and to explain the possible

bio-effects of low-power microwaves, radio frequencies, pulsed electric fields and electro-hydrodynamic drying on the biochemical composition.

Chapter 4 - Experimental evaluation using enzyme model systems

The influence of low-power MW radiation on LDH and Catalase enzymes was studied to observe the changes in the rate of reactions when exposed to irradiation. It is important to evaluate the changes in enzymatic reaction time, as these reactions play a vital role in maintaining the standard biochemical and physiological functions of the body.

Chapter 5 – Experimental evaluation using a yeast model system

The author investigated the effects of selected frequencies and powers on yeast cell proliferation and their internal organisation. This study was aimed at evaluating the hypothesis that low-power MWs produce modulating effects in *Saccharomyces cerevisiae* yeast by affecting their growth cycle, bioactivity, conformation and viability. The effects of MW radiation were investigated at 1800 MHz and powers -10 dBm, 0 dBm and 17 dBm on the growth rate, morphology and internal organisation of the yeast.

Chapter 6 – Experimental evaluation using mammalian cells

The author investigated the influence of MW exposure on TRPV4 ion channel protein expressed in Hek-293 cells, to gain a better understanding of the thermal/non-thermal nature of the interaction of MWs with healthy epithelial cells. The author studied the response of the Ca²⁺ ion channel when cells were exposed to electromagnetic radiation and compared with the standard response time. Scanning Electron Microscopy (SEM) and Transmission electron microscopy (TEM) were employed to evaluate changes in the surface and internal organisation of HEK-293 treated with irradiation.

Chapter 7 – Conclusions and recommended future works.

CHAPTER 2: LITERATURE REVIEW

2.1 Introduction

In the previous chapter, the author highlighted the importance of studying the effects of low-power electromagnetic radiation (EMR) in the radiofrequency and microwave range on biological systems. The author further summarised the motivation behind the focus area of her PhD research project. In this chapter, the author discusses the current body of knowledge, including a subject's background, theoretical contributions and substantive research findings. In the later subsection 2.4, the author also reviews the latest published studies and methodical contributions for evaluating the effects of low-power microwave radiation on various biological model systems, including on humans. Based on the available literature and research work, the author progressively attempts to identify the existing research gaps that have motivated the present research. This chapter is organised into the following sections:

2.2 A brief overview of Electromagnetic Spectrum and EMR

2.3 Low-power EMR and mobile communication technology

2.4 Health concern and exposure guidelines:

- a. *In-Silico* Molecular modelling and studies.
- b. *In-vitro* studies.
- c. *In-vivo* studies

2.2 A brief overview of the electromagnetic spectrum and EMR

Electromagnetic radiation (EMR) is a specific form of the more general electromagnetic field, where energy is emitted and absorbed by charged particles as it travels through space in waveform [29]. Accelerated atomic particles produce a time-varying electric and magnetic field. EMR is associated with an electromagnetic field that moves away from its source. EMR has both electric and magnetic field components, oscillating with a 90° degree phase difference from each other perpendicular to the direction of wave propagation or energy.

Electromagnetic waves are typically described by any of the following three physical properties: frequency (f), wavelength (λ), and photon energy (e). Frequency is defined as the number of oscillations or cycles per second, whereas the term wavelength is defined as the distance between consecutive corresponding points of the same phase, such as crests or troughs of a wave. Plank's equation defines the inversely proportional relationship between wavelength and frequencies [5]:

$$e = hf = hc/\lambda \quad \text{Equation 2.1}$$

where $c = 299792458$ m/s is the speed of light in a vacuum; and $h = 6.62606896(33) \times 10^{-34}$ J·s = $4.13566733(10) \times 10^{-15}$ eV·s is Plank's constant.

Figure 2.1 describes the interaction between the electric field (red) and magnetic field (blue) in electromagnetic waves. The interaction between electromagnetic field, charges and currents are defined by the Lorentz force law shown in Equation 2.2.

$$F = q * (E + v * x * B) \quad \text{Equation 2.2}$$

where force, F , enforced on a particle of electric charge, q , with an instantaneous velocity, v , E is an electric field, B is a magnetic field.

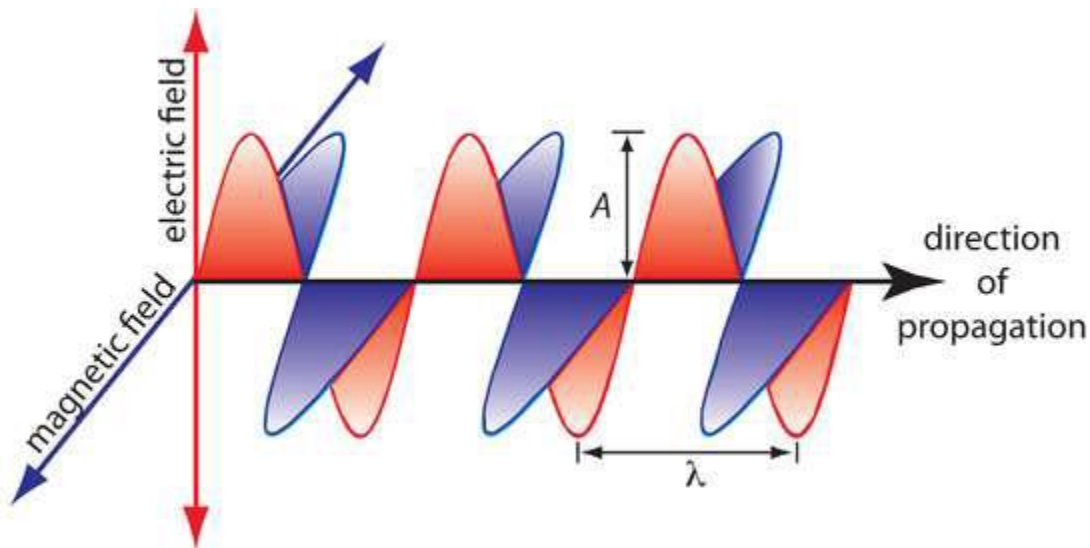


Figure 2.1: Electromagnetic radiation – the propagation of energy in the form of electromagnetic waves through a medium [30].

Depending on their frequency (measured in cycles per second (Hertz) and corresponding wavelength (measured in meters), EM waves are mapped onto the electromagnetic spectrum. The electromagnetic spectrum is divided into seven broad categories: *Radio waves, Microwave, Infrared, Visible light, Ultraviolet, X-rays, and Gamma rays*. Some of these classifications are further divided into subcategories. The electromagnetic spectrum, as shown in Figure 2.2, covers the frequencies ranging from 1 Hz to above 10^{25} Hz, which corresponds to wavelengths from thousands of kilometres down to a fraction of the size of an atomic nucleus.

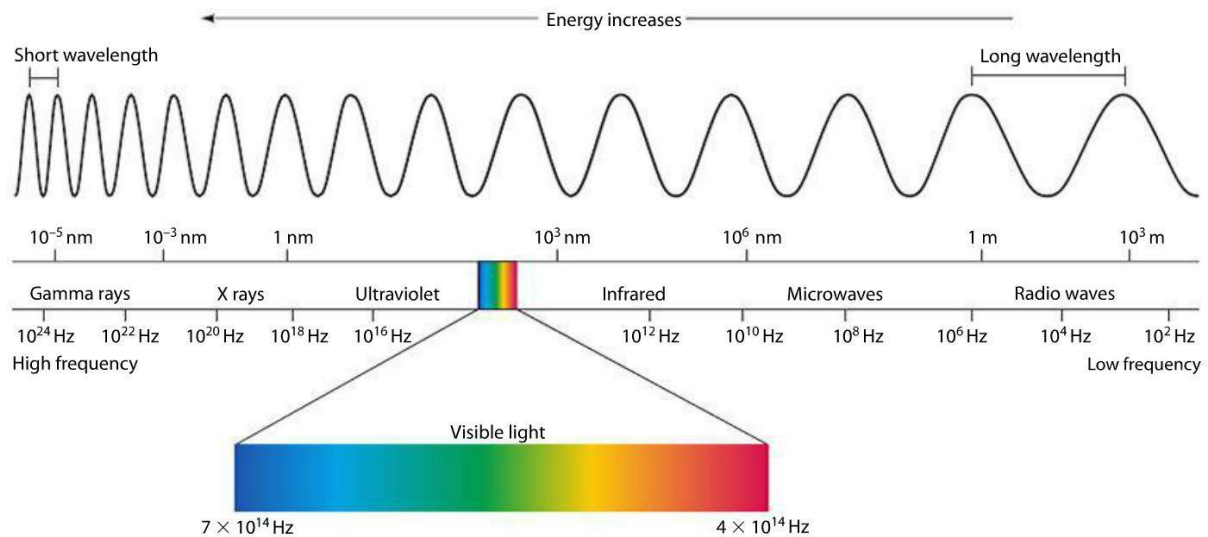


Figure 2.2: Electromagnetic spectrum showing the entire range of wavelength and frequency [30].

The electromagnetic field (EMF) is viewed as the combination of an electric field and a magnetic field. The electrical field is produced by a voltage gradient and is measured in volts per meter. The magnetic part is generated by any flow of current and is measured in Tesla. Electromagnetic power is the rate at which energy is consumed or produced, and it is the product of voltage and current [16]. Power density, also known as the power flux density, is a distribution of power over a particular area (mW/cm^2). The unit used to measure how much the body absorbs EMF radiation is called the *Specific Absorption Rate* (SAR). The SAR is usually expressed in units of watts per kilogram (W/kg) or milliwatts per gram (mW/g). The international exposure guidelines' limit level is reported as a maximum SAR of $2 \text{ W}/\text{kg}$ by ICNIRP [17] and $1.6 \text{ W}/\text{kg}$ by IEEE [15]. According to ICNIRP, the threshold for biological effects is seen at SAR values above $4 \text{ W}/\text{kg}$ [17]. However, this temperature rise falls within the normal range of human thermoregulatory capacity. A SAR value of $4 \text{ W}/\text{kg}$ is associated with a temperature increase of more than 1°C . Although the sensitivity of tissues to thermal damage varies widely, irreversible effects occur above SAR of $4\text{W}/\text{kg}$.

One of the main characteristics that define an electromagnetic field (EMF) is its frequency or its corresponding wavelength. These properties also determine their ability to travel through objects, their heating effects and their effects on living tissue. EMR is described as a stream of mass-less particles called photons. Each photon has a certain energy level and is travelling in a wave-like pattern at the speed of light. Oscillation rate in Hertz defines the energy level of each type of photon. The rate of oscillation is inversely proportional to the

distance each photon travels in meters. Higher photon energy means higher frequency of oscillation and shorter wavelength. Thus, radio waves contain photons with the lowest energy level, while Gamma rays have the highest energy level in the spectrum [31].

Energy transmitted through EM waves is broadly divided into two categories:

1. *Ionising Radiation:* is electromagnetic waves that carry enough energy to break molecular/ chemical bonds between molecules and ionise atoms; whereas
2. *Non-ionising radiation:* is low-frequency EM Waves that do not have sufficient energy to break molecular/ chemical bonds and ionise atoms.

Gamma rays and X-rays are examples of ionising radiation, whereas radiation from microwaves, radiofrequency fields and the ELF is found at a relatively long wavelength and classified as non-ionizing radiation. Non-ionizing radiation ranges from 0 to approximately 3×10^{11} Hz. Radiation above 3×10^{11} Hz is considered as ionising radiation [32].

The scope of this PhD research work is limited to investigating the effects of radio waves and microwaves which fall under the non-ionizing radiation range. The focus of the study is biological effects of non-ionizing EMR in the frequency range used for mobile communication technologies.

2.3 Low-power EMR and Mobile communication technology

Since the evolution of the Universe, there has been electromagnetic radiation. We are always surrounded by different types of natural electromagnetic radiation. Naturally occurring radio waves are generated by lightning or by astronomical objects, whereas artificial radiowaves and microwaves are generated, transmitted and received for any and all wireless communication, electrical generators and even home appliances. Artificially generated radiowaves are used for fixed and mobile radio communication, broadcasting, radar and other navigation systems, communications satellites, computer networks and many other applications. Radiowaves have a frequency ranging from 3KHz to 300GHz for wavelength ranges from 100km to 1mm. Radiofrequency radiation, more commonly known as radiowaves, can be artificially generated, controlled, transmitted and received. Moreover, radiowaves can penetrate haze, rain, cloud, snow and smoke without any distortion, so they are used for transferring data and audio/ video transmission.

Similar to infrared (IR), the primary effect of absorption of radiowaves by materials is to heat them. However, IR causes surface heating, whereas radio waves penetrate and deposit

the energy inside the body or biological tissues [33]. In today's world, we are regularly exposed to numerous sources of radiowaves such as powerlines, smart meters, computers, conductive water pipes, microwave ovens, **mobile phones**, cordless communication devices, phone towers, and even devices in our neighbours' homes. The comforting part is that the radiowaves are very low-power EMR and the heating effect is same as any other form of heat; thus, the focus of the present study is directed to non-thermal effects of radiowaves/microwaves.

As discussed in Section 1.1, the exponential worldwide increase in usage of wireless telecommunication devices, mainly mobile phones, has resulted in increased human exposure to radiofrequency (RF) fields. Mobile phones (3G and 4G mobile networks) are low-powered radiofrequency transmitters, operating at frequencies between 450MHz and 2700MHz with peak powers in the range of 0.1 to 2 watts. Mobile phones communicate by transmitting radiowaves through a network of fixed antennas, called base stations. For broadcasting, high RF power is generally required to maximise the area of coverage. Close to the antennas, electric field strengths can reach several hundred volts per meter. Cellular networks cause low levels of electromagnetic fields in public areas. Handsets and cell phones, however, might cause significantly higher peak levels of exposure during use.

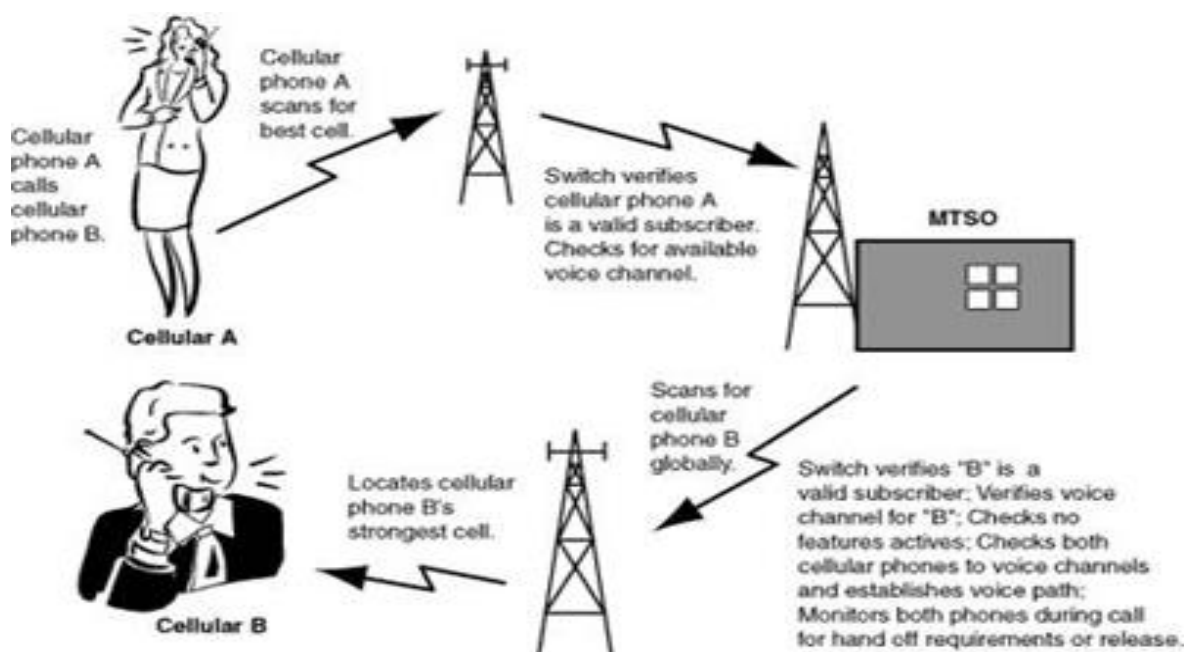


Figure 2 3: Working Principle of mobile call [34]

Figure 2.3 describes the working of mobile phones. A mobile phone device converts voice, text, multi-media messages or data calls into radio frequencies (RF). Mobile phone base stations transmit and receive these RF signals and connect callers to other phones and other

networks. The mobile phone network is divided into thousands of overlapping, individual geographic areas or ‘cells’, each with a base station. During talks, Global System for Mobile Communication (GSM) users are exposed to low-power RF or microwave (MW) radiation (depending on the operational frequency range). To maximise the coverage, these frequencies of human-made origin have a complex amplitude distribution over time. For instance, there are 124 different channels/frequencies, which are used in GSM900 technology used in 2G (2nd Generation) mobile technology. They differ by 0.2 MHz in the frequency range between 890 MHz and 915 MHz. The base station supplies frequency to a mobile phone user depending on the number of connected users. The base station can change the frequency during the same talk. In contrast to GSM phones, mobile phones of the 3G (3rd generation) network use UMTS (Universal Mobile Telecommunications System) wideband signal. 3G/ UMTS (in Europe) mobile communication technology operates at frequencies between 1900 MHz to 2200 MHz. It is anticipated that UMTS may have higher biological effects because of the eventual “effective” frequency windows [35]. The 4G (4th Generation) and 5G systems in mobile technology are specified to operate in the 2 and 3.6 GHz licensed bands for mobility [36].

3G mobile phones operate at lower power levels than both GSM and CDMA handsets. The maximum power from a 3G phone (2100 MHz) is 0.125 W produced over a 5 MHz bandwidth, whereas GSM phones (900 and 1800 MHz) emit an average power of 0.25 and 0.125 W over a 0.2 MHz bandwidth, and CDMA handsets (800 MHz) have a maximum power of 1 W. With adaptive power control technology, handsets operate at the lowest power necessary for good quality and reliable radio communications. Typically, handsets are held against the head while a call is made. The distance from the antenna to the head is only about 2 cm or less. Therefore, the user is in the near-field of the source, and simple field calculations are not appropriate to assess the exposure level. RF exposure limits for mobile phone users are given regarding the Specific Absorption Rate (SAR) – the rate of RF energy absorption per unit mass of the body [37] [38].

In Australia, the current mobile frequency bands can be broken into 800, 900, 1800 and 2100MHz (2G and 3G networks). As the demand for data transmission, speed and coverage increased significantly over the years, the carriers moved from 2G (900/1800 MHz bands) to 3G (1900- 2200MHz) frequency bands. With the introduction of the 4G mobile network, the carriers began turning off their GSM 1800 MHz service and using the space to operate a 4G service. The Australian Radiation Protection and Nuclear Safety Agency (ARPNSA) specifies

exposure limits to RF at the frequencies used for mobile phones [39]. The SAR limit in Australia for mobile phone handsets is set at 2W/kg of tissue averaged over 10 grams.

2.4 Health Concerns and Exposure Guidelines

As discussed in Chapter 1, the mobile phone radiation is non-ionising radiation and does not have sufficient energy to break chemical bonds, so the mechanism by which this low-power radiation interacts with biological material is still a matter of research. It is considered that tissues nearest to the mobile antenna can absorb this energy and may contribute to the changes in the standard biological functioning of a living organism [3] [4] [5]. There is circumstantial evidence described in various scientific reports suggesting that even low-power RF and MW radiation can affect the standard biological processes in human body. Furthermore, anecdotal and scientific studies show biological and possible health effects associated with mobile towers and antennas. A large number of research studies had been conducted worldwide to elucidate the effects of low-power RF radiation from mobile phones on biological processes, which can ultimately affect human health. In this section, the author has gathered and categorised the recent relevant research reports to identify research gaps in the current state-of-the-art literature, and to develop and guide the present study.

The tissue heating is the principal mechanism of interaction between RF energy and the human body. The heating effects produced by RF and MW are well known, extensively studied and well characterised. There is a number of different applications developed based on the heating effects produced by high-power RF/MW radiation which is used in the food industry, defence and medical applications (i.e. RF ablation). However, radiation emitted by mobile phone devices and other telecom technologies is at a low-power level and complies with safety standards (no heating effect requirement, $<1^{\circ}\text{C}$ in surface heating).

Mobile phones operating at various frequency bands and low powers produce RF energy which is absorbed by the skin and other superficial tissues, resulting in negligible temperature rise in the brain or any other organs of the body [40]. It has been reported that the increasing use of smartphone possibly targets several biochemical processes leading to health problems [11]. These effects vary from those as simple as behavioural changes, which can be corrected by changing lifestyle, to those as complex as the development of brain cancer [41]. Despite this information, knowledge of the exact mechanisms underlying interaction between

biological systems is crucial for understanding physiology as well as for possible prevention, diagnostics and therapy of pathological state.

In the last twenty years, a particular interest arose in the weak (low-level) non-thermal and non-ionising EMR [42]. A significant number of peer-reviewed papers were published exploring the harmful effects of ionising EMR, but still very little is known about the effects of low-level, non-ionising radiation. Our level of understanding of the mechanisms of interaction of EMR with biological systems decreases as we move from extracellular (membrane) to intracellular (protein, DNA) components.

There is evidence that long-term exposure to low-level RF and MW radiation can be dangerous to health [15] [39] [43] [44]. According to a study conducted by Brazilian researchers, RF radiation may result in the development of cancers in humans [45]. According to the study, more than 80 percent of the people who have died in Belo Horizonte, Brazil from brain cancer lived less than 500 meters away from 300 identified cell phone base stations in the city.

In response to public concerns, in 1996 the WHO established the International Electromagnetic Fields Project to assess the scientific evidence on the possible health effects of EM fields. The WHO also identifies and promotes research priorities for radiofrequency fields and health to fill gaps in knowledge through its research agendas. Specific studies have been identified to address the problem of localised exposure. The project has established a formal mechanism for reviewing the research results and conducting risk assessments of EM exposure. The WHO promotes dialogue among scientists, governments, industry and the public to raise the level of understanding about the potential adverse health risks of mobile phones. The WHO is also developing public information materials, and bringing together standards groups worldwide in an attempt to harmonise international exposure standards. The WHO FS^o 193 suggests that there is evidence that long-term exposure to low-level radiofrequency and microwave radiation can be dangerous to health [46].

Epidemiological research examining potential long-term risks from RF exposure has mostly looked for an association between brain tumours and mobile phone use [47] [48] [49]. As epidemiological studies can only assess those cancers that become evident within shorter time periods, it was reported that no association had been suggested. Though it is a fact that many cancers remain undetectable for many years after the interactions that led to a tumour,

results of animal studies consistently show there is no increased cancer risk of long-term exposure to RF fields.

However, the WHO 2010 RF Research Agenda included cellular research aiming to elucidate the potential impacts of new, emerging technologies on health through the associated mechanistic understanding. It recommends dosimetry and cellular studies aimed at better communicating the current state of understanding of the biological and health effects of RF at the genetic and protein levels [46] [39] [50]. The call for *in vitro* cellular research acknowledges the current lack of understanding regarding the potential of low-level (non-thermal) RF to interact with the healthy functioning of an individual. Moreover, this knowledge will help to anticipate the potential impacts of new and emerging technologies on health through the associated mechanistic understanding.

The WHO also conducted a large-scale multinational epidemiology study coordinated in over 13 countries through the International Agency for Research on Cancer (IARC). In 2014, WHO reported the epidemiological studies that have been completed or are ongoing, including case-control studies and prospective cohort studies examining a number of health endpoints in adults. The most extensive retrospective case-control study to date on adults, by Interphone, coordinated by IARC, was designed to determine whether there are links between use of mobile phones and head and neck cancers in adults [51]. While an increased risk of brain tumours is not established, the increasing use of mobile phones and the lack of data for mobile phone use over time periods longer than 15 years warrant further research on mobile phone use and brain cancer risk [41]. In particular, with the recent popularity of mobile phone use among younger people, and therefore a potentially longer lifetime of exposure, the WHO has promoted further research on this group.

Increased public concern has also promoted further investigation of biological and associated health effects of exposure to low-power RF radiation emitted by mobile phones (3G and 4G mobile networks) [52] [53] [54]. Studies have been focused on effects of RF radiation in the range of 800MHz -2400MHz at a relatively low exposure density (average SAR near 2.0 W/Kg) on biochemical processes in various biological systems [55] [56] [57].

Researchers have investigated the effects of RF fields on brain electrical activity (EEG), cognitive function, sleep, heart rate (ECG) and blood pressure in volunteers [43]. To date, the research does not suggest any consistent evidence of adverse health effects from exposure to

low-power RF fields at the levels below those that cause tissue heating. Furthermore, research has not been able to provide support for a causal relationship between exposure to RF fields and self-reported symptoms, or “electromagnetic hypersensitivity”. There are some indications of an increased risk of glioma for those who reported the highest 10% of cumulative hours of mobile phone use, although there was no consistent trend of increasing risk with greater duration of use. The researchers concluded that biases and errors limit the strength of these conclusions and prevent a causal interpretation [43].

Intensive international research has found no conclusive or convincing evidence of adverse health effects of mobile phone use. However, an increasing number of research studies have demonstrated the existence of biological effects of low-power RF and MW radiation at the molecular and cellular levels. Barnes and Greenebaum in 2017 presented that low-power FR/MW waves may affect a biological system, causing a biological effect, without necessarily causing an adverse change in health [58]. Hence, the concern remains, and it is unclear whether the accumulative biological effects caused by long-term exposure to low-level/power RF can lead to health effects, adverse or therapeutic [46]. As such, there is a need for more research focussing on the mechanism of interaction of RF fields with bio-molecules and cells.

Since 1996, the Australian Government has provided \$1 million per year to the Electromagnetic Energy (EME) program. This program supports research into and provides information to the public about health issues associated with mobile phones, mobile phone base stations and other communication devices and equipment. The Australian government conducted an inquiry into the safety of mobile phone technology[59]. The inquiry found no substantiated scientific evidence of health effects from mobile phones and their base stations. The inquiry reiterated that mobile phones must comply with strict safety guidelines established by the government.

ARPANSA commenced centralised the Electromagnetic Radiation (EMR) Health Complaints Register on 4 July 2003. The Register collects reports of health concerns related to possible EMR field exposure in the range of 0-300 GHz. Since its commencement, it has received 126 reports. The register collected more than 70 reports in the year 2012-13 and 2013-14 alone [60]. This data indicates that, with a spike in technology, exposure-related health issues are increasing and need further detail investigation.

2.4a *In-silico* (molecular modelling) studies

Electric and time-varying electric fields can affect biological systems. An external current field increases the permeability of the cell membrane in the course of several biological processes [61] [62]. Exposure to radio waves at the frequencies used in communication technology may affect the proteins in many different ways. For example, via the interactions of the receptor protein, dipole moments change with the external oscillating electric fields [63] [64]. In general, charged and polar residues can directly interact with an oscillating electric field, and this may lead to some perturbation in proteins. Computational studies, based on MD simulations, suggest that proteins exposed to high static electric fields undergo significant conformational changes sufficient to produce functional changes [65] [63] [66].

In recent years, it has been shown that weak static electric fields could be used in various food technology and therapeutic medical applications (pain relief and chronic inflammatory autoimmune disorders) [67] [68]. However, for the development of an effective treatment, a better understanding of the influence of static electric fields at the molecular and cellular levels is required. In recent years, several *in-silico* studies were conducted to investigate the effects of varying static [63, 69, 70] and oscillating electric fields [25, 71] [72] on selected proteins and peptides. These studies were aimed to elucidate the mechanistic response of selected proteins to applied electric field exposure. *In-silico* approaches were also helpful in studying the effects of electromagnetic fields on proteins' denaturation and stability. It is worth mentioning here that experimental monitoring of these effects is very challenging, due to the short time frame of a nanosecond (ns) [69] [73] [74] [75] [76]. Computational or *in-silico* methods present powerful tools that enable a mechanistic understanding of interactions between external fields and molecules or cells [70].

Molecular modelling methods are now used routinely to investigate the structure, dynamics, surface properties, and thermodynamics of inorganic, biological, and polymeric systems. The types of biological activity that have been investigated using molecular modelling include protein folding, enzyme catalysis, protein stability, conformational changes associated with the biomolecular function, and molecular recognition of proteins, DNA, and membrane complexes [77] [78].

With the increase in the strength (power) of the static field, the potential also increases. Research shows that external stress related to EMR at different levels can alter a protein's

structure [71]. A number of research studies were conducted to evaluate the effects of static and oscillating EMFs on the living matter [79]. Research studies investigated mostly acute effects of static electric fields, and showed only the effects associated with body hair movement and discomfort from spark discharges. However, chronic or prolonged effects of static electric fields have not been adequately investigated [80]. Most of the studies done were at high field strength, which is beyond the scope of the present study. Of particular interest to this study are biological and possible health effects of low strength static electric fields ($f = 0\text{Hz}$). A computational modelling approach was applied for the present research to understand the mechanism of molecular interaction in the biological system (protein molecule) with applied electrical fields.

Proteins are the building blocks of living cells, and their structure is directly correlated to their function(s) [25]. Any change in the conformation of a protein leads to changes in its functional performance and thus, may result in altering of a particular biological process. Molecular Dynamics, or MD simulation, is a powerful computational tool to study the interaction of atoms and molecules under external stimuli for a fixed period. There are only a few studies in biological sciences performed using the MD approach [66] [69] [70] that have provided a detailed description of the effects of applied exposures at the atomic level within the nanoseconds time period. MD simulation can efficiently model atomic and molecular interactions occurring in biological systems and effects of external stimuli on molecules and cells. NAMD and GROMACS (Groningen Machine for Chemical Simulations) are the two most commonly used software applications to simulate and study the effects of peptide and proteins at nanoscale level [67] [81] [82] [83].

The molecular modelling approach could be a breakthrough in this research and can help in understanding the mechanistic aspect of low power radiation by capture effects at the nanoscale level. Nevertheless, much work needs to be done to design an algorithm to mimic the real nature of electromagnetic radiation.

2.4b In vitro studies

Experimental research on the effects of RF radiation is extensive and heterogeneous. It includes both studies of cell cultures and tissues (*in vitro*) and laboratory animals (*in vivo*), as well as human subjects (*in vivo* clinical studies). A number of these studies were focused on functional changes in the brain and the effects of RF fields on cognition. Any measurable

change in a biological system initiated by a specific stimulus is referred to as the biological effect of the stimuli. However, it is not necessary for every biological effect to contribute to a biological or health hazard. Several reports indicate that EMR from mobile phones at non-thermal levels might elicit a biological effect in target cells or tissues. Whether or not these biological effects lead to adverse health effects (including cancer) is unclear. To date, there is limited scientific evidence of health issues and no mechanism by which mobile phone radiation could influence cancer development [59] [84] [77] [85] [86]. The research findings on changes at the molecular level associated with the development of cancer are inconsistent and contradictory. Nevertheless, other biological effects of low-power RF radiation are neither rejected nor denied.

Yeast cells are frequently used as a model system for in-vitro studies, as yeast is a simplest eukaryotic organism with a nucleus. Many essential cellular processes in yeast and humans are the same, which makes yeast suitable to study basic molecular processes transferrable to biological process in humans [87]. There have been a number of experiments conducted to study the growth pattern of yeast cells exposed to MW radiation [88, 89]. For instance, researchers [90, 91] evaluated the effects of low-power MW radiation on bacteria and yeast strains and reported that the yeast cell growth rate was affected by applied exposure. It was shown that microwave radiation induces frequency-specific effects on the yeast growth rate, i.e. increase up to 15% at the frequency 41.6 GHz and decrease to 38% at 41.8 GHz.

French et al. [92] developed a theoretical mechanism by which RF radiation from mobile phones could induce cancer, via the chronic activation of the heat shock response. Upregulation of heat shock proteins (HSPs) is a standard defence response to cellular stress. However, chronic expression of HSPs is known to induce or promote oncogenesis, metastasis and resistance to anti-cancer drugs. The authors suggest that repeated exposure to mobile phone radiation acts as repetitive stress leading to continuous expression of HSPs in exposed cells and tissues, which in turn affects their normal regulation, and thus cancer can result. This hypothesis provides the possibility of a direct association between mobile phone use and cancer, and thus provides a principal focus for future experimentation [93] [94].

Studies at the cellular level have shown that non-thermal effects of MWs at levels lower than the ICNIRP (International Commission for Non-Ionizing Radiation Protection) safety standards depend on several physical and biological parameters. Frequency-dependent effects of non-thermal MWs from GSM mobile phones on 53BP1/ γ -H2AX foci and chromatin

conformation in human lymphocytes were observed [95] UMTS MWs induce significant adverse effects in human lymphocytes, similar to effects of heat shock and GSM MWs at the particular frequencies. The obtained results are in line with the hypothesis that UMTS MWs may affect cells more efficiently than GSM MWs, because of the nature of the signal [95]. The effects of MWs from mobile phones on 53BP1/ γ -H2AX foci persisted up to 72 hrs following exposure of lymphocytes. Long-lasting adverse effect on these critical cells of the immune system can have a relationship with health risk from mobile telephony [96].

A number of studies report that EMFs alter the proliferation rate of cells, as well as the rate of DNA, RNA, and protein synthesis [53, 59, 93, 97-100]. The biochemical processes are strongly affected by changes in cytosolic ion concentrations (especially calcium), and such changes can be induced by RF microwave radiation [101, 102]. It has been shown that RF fields modulated by extremely low frequencies (ELF) decrease cytosolic calcium ion concentration [103]. In some experiments, this effect was at the maximum power densities between 0.6 and 1mW/cm² [103]. In one study [104], the GSM signals tested were the RF carrier signals, pulsed at ELF and the power densities 0.436-0.060mW/cm². It is known that cell proliferation, DNA, RNA, and protein synthesis are connected with increased cytosolic ion concentrations (especially calcium) and with depolarisation of the plasma membrane. The effects of external EMFs on the cytosolic ion concentrations appear to be connected with the interaction between the external field and the cation channels of the plasma membrane, which results in irregular gating of these channels [104]. A biophysical mechanism for this interaction has been proposed [104]. According to this mechanism, ELF fields of the order of a few V/m can gate electro-sensitive channels on a cell's plasma membrane irregularly and therefore disrupt cell function. In addition, pulsed fields are shown to be more bioactive than continuous ones. Therefore, according to one study [105], the ELF component of a GSM signal, due to the pulse repetition frequency at 217 Hz, with a mean electric field intensity of the order of 6 V/m, can disrupt cell function and consequently affect the reproductive capacity of a living organism. Two significant findings of these studies are that the effects of EMF are waveform-specific and cell type-specific [106].

The limited number of studies on oxidative enzyme systems has yielded mixed results. Exposure of suspension of the membrane-bound enzyme Cytochrome oxidase to sinusoidal modulated MWs at 2.45 GHz with SAR of 26 W/kg did not significantly affect its activity during the exposure [107]. Findings of other *in vitro* studies reveal that MWs at particular frequencies and powers induce changes in the enzyme's kinetics. The modulation of the rate

of change in corresponding biochemical reactions which these enzymes catalyse is directly affected by the change in enzyme kinetics [108] [109] [110]. *In vitro* studies also show that membrane structure and functionality could be altered upon exposure to RF fields [111]; and hence it is safe to suggest that low-power radio waves may affect a biological system, without necessarily causing an adverse change in health [58]. Findings of a few relevant *in vivo* studies investigating effects of low-power MW are summarised in Tables 2.1 and 2.2.

In the last five years, an increased number of *in vitro* studies have been conducted to evaluate the health effects of low-power RF radiation [27, 35, 37, 38, 112]. Interestingly, a more significant number of published studies have reported health effects associated with mobile phone radiation as opposed to studies reporting no effects [18]. In one recent study [113], researchers investigated the effects of mobile phone radiation on semen parameters (semen volume, sperm concentration and count). The effects of MW exposure at 2.4 GHz were studied on ejaculated semen donated by healthy volunteers (20-30 years old). The researchers screened and documented the information from a total of 794 young men in 2013, followed by 666 and 568 in 2014 and 2015, respectively. The findings of this three-year study reveal that semen quality, concentration, motility and morphology were all significantly affected by exposure [113]. It was also reported that mobile phone radiation damages DNA indirectly, by the leakage of digestive enzymes from lysosomes or by the production of reactive oxygen species (ROS) [114].

Table 2.1 Effects of low power MW radiation in the frequency range of 450MHz –2GHz

Frequency	Power density	Cells/Tissues	Effect
915 MHz	1mW/g	Human Neuroblastoma [115]	A significant increase in the efflux of calcium ions
450 MHz	0.29 mW/g	Calcium efflux from awake cat cerebral cortex [104]	Increased end-tidal CO ₂ excretion

837 MHz to 1909.8 MHz	5mW/g	Chromatin in human cells [116]	The microwave irradiation of human cells induces the significant increase of Heterochromatin granules quantity parameter
905 MHz	0.5 mW/g	Saccharomyces cerevisiae [89]	Significant reduction of colony growth compared to non-irradiated strains after all exposure times
1800MHz	0.06mW/g	Deoxyribonucleic Acid Damage Vis-à-vis Genotoxicity in Brain of Fischer Rats [117]	Chronic microwave radiation exposure at low-level induces DNA damage
9.9 GHz	1mW/g	Biochemical Changes in Rat Brain Radiation [118]	Decrease activity of protein kinase

It is evident from research studies that different cells respond differently to applied radiation, which may lead to alterations in complex biological processes [119]. Cellular and animal studies reveal that EMFs produce both thermal and non-thermal biological effects [120]. Non-thermal radiation does not have enough energy to influence the chemistry of cells directly but plays a vital role in altering particular biological pathways, which indirectly affects specific biological actions. It is reported that RF radiation could affect cell membrane proteins and trigger an increase in intracellular Ca²⁺ ions [121] [122]. Changes in Ca²⁺ signalling occurs almost immediately after EMR exposure [123]. The thermal mechanisms that may convey detection of microwaves by mammals are the heating of tissues by microwave exposure, which can be detected by thermal receptors in the skin and elsewhere in the body and central nervous system (CNS) [58]. The identification of a family of transient receptor potential (TRP) ion channels which are gated by specific temperatures has been a significant advance in the elucidation of the molecular mechanisms of thermo-sensitivity. Research has revealed a family of TRP proteins that sense heat and cold at the cellular level [124].

Table 2.2. Effects of MW of varying SAR and duration at the cellular level

Study	Exposure power, SAR and time	Exposure Temp.	Effects
[125]	SAR of 1, 2 and 4 W/kg for 1,2, and 3 days respectively	37.06 +/- 0.5°C	<ol style="list-style-type: none"> mRNA and protein expression of proneural genes NGN1 and NEUROD were decreased with UP-regulation of their inhibitor HES1 after exposure. Neurite outgrowth of eNSC differentiated neurons was inhibited after 4 W/kg RF exposure for 3 days.
[126]	The power density of 50 mW/cm ²	37.0 °C	<ol style="list-style-type: none"> The structure of BBB has damaged, and permeability of ions and low molecular weight molecules were increased. Decreased in occluding mRNA and protein along with increased Tyr phosphorylation
[56]	Power density of 10, 30, 50 and 100 mW/cm ²	37+/-0.5 °C	Microwave Radiation induces apoptosis in the neural cell through the mitochondria-mediated caspase-3 pathway.
[57]	SAR of 0.607W/kg for 4 and 24 hr	37°C	<ol style="list-style-type: none"> Cell viability decreased Cell proliferation inhibited and apoptosis induced Mitochondrial membrane potential decreased

It is important to note that there are a number of studies showing biological effects of RF exposure, whereas studies focused on investigating the direct health effects of RF radiation are inconclusive. The possibility of a direct relationship between mobile phone use and carcinogenic processes, reproduction and development, the cardiovascular system and longevity, are ruled out by a good number of researchers. These studies have found minimal and reversible biological and physiological effects which do not necessarily lead to diseases or injuries. In addition, the research findings on changes at the molecular level associated with the development of cancer are inconsistent and contradictory [127]. *In vitro* studies of non-thermal effects of RF often report conflicting results [128] [129] [130]. Some studies suggest that RF exposure, even at a power lower than the standard recommended exposure levels, can change processes of gene and/or protein expression in certain types of cells. However, the biological consequences of most of the changed genes/proteins are still unclear and need to be further explored to make an evidence-based conclusion on their health effects. There is a lack of understanding of the long-term accumulating effects of RF radiation at the genetic and protein levels which might lead to health effects [131] [6] [132] [133]. The potential sources of inconsistency in reporting of research findings include differences in experimental protocols,

temperature control, exposure parameters, cytogenetic techniques, and sensitivity of different cell types to applied radiation.

2.4c In vivo animal and human studies

Since 1990, until the first decade of the 21st century, about 93% of *in vivo* studies published have shown no significant short- or long-term effects of applied irradiation. Furthermore, the average survival of irradiated groups of animals was not affected in some 96% of studies [134]. No convincing evidence has been presented for acute or chronic effects of RF on other physiological and biochemical parameters in animals. Thus, during the first decade of the 21st century, the general conclusion has been that no consistent or essential effects of RF could be demonstrated in whole animals at the radiation level below the international safety standards. However, a surge in the usage of mobile phones and unprecedented development in telecommunication technology have forced the scientific community to review the effects of RF exposures. Extended hours of mobile phone usage, penetration of mobile phones, and higher frequency and power density are some new parameters used by the scientific community to analyse the effects. In 2014, the WHO stated: "With a large number of mobile phone users, it is important to investigate, understand and monitor any potential public health impact [135]." WHO also recognise that the research done to date shows some connection between mobile phone use and health effects [135].

Recent *in vivo* studies [18, 37, 112-114] demonstrate that anthropogenic RF radiation is capable of eliciting post-neurotomy pain in animals. Experimental rats were exposed at 915 MHz and a power density 756 ± 8.5 mW/m² for 10 minutes, once per week for eight weeks. The RF exposure was attenuated to deliver an average power density equal to that measured at 39 meters from a local mobile phone tower. In another study [47], single- and double-strand DNA breakages were observed in brain cells of rats exposed to continuous and pulsed MWs at 2.45 GHz and a power density 2mW/cm². This field provided an average whole-body SAR of 1.2 W/kg, which is below the safety standard (the SAR limit in Australia for mobile phone handsets is 2W/kg of tissue averaged over 10 grams). The authors conclude that the observed cumulative DNA damage in cells in the central nervous system could lead to accelerated ageing and neurodegenerative disorders [136].

Microarray analysis was performed on the ovaries of 4 days-old female *Drosophila melanogaster* exposed to mobile phone radiation for 30 mins at SAR of 0.15 W/kg. The

findings reveal that ROS cellular content was increased, with 168 genes being differentially expressed. As reported, the applied radiation is capable of inducing critical cytopathic effects and altering fundamental genetic programs and networks in *Drosophila melanogaster* [6]. In another study [137], researchers irradiated mouse NIH/3T3 and human U-87 MG cells by MW radiation at 1800 MHz and a power density of 1209 mW/m². The results show that MW exposure induces apoptosis-related events such as ROS burst and more oxidative DNA damage, which lead to p53-dependent caspase-3 activation through release of cytochrome c from mitochondrion [138]. This finding is critical, as it is known that ROS can damage various cellular compartments resulting in DNA damage and apoptosis.

A study on monoamine neurotransmitters and their vital regulating enzymes in a rat brain show that low-power MWs alter the level of brain monoamine neurotransmitters at mRNA and protein levels, which may cause learning and memory disturbances [37]. In this study, rats were exposed to MWs at 900 MHz and 1800 MHz for 30 days, 2 hours/day and five days/week. The levels of monoamine neurotransmitters were detected using LC-MS/MS in the hippocampus of all experimental animals [37]. In an *in vivo* animal study [139], the effects of 935 MHz radiation were studied on fertilisation and embryonic development in mice. The ovulating mice were irradiated for 4 hours and 2 hours per day for three consecutive days, and then ova were harvested for *in vitro* fertilisation, to observe the changes if any in fertilisation rate. Compared to control groups, a reduction in fertilisation rate was observed in exposed groups [139]. The effects of MWs on body hormones in pregnant rats have also been reported. When four groups of rats, including forty new off-springs, were irradiated at 900, 1800 and 2450 MHz, it was observed that the levels of plasma prolactin, progesterone and oestrogen were decreased, whereas the levels of uterine oxidative stress in pregnant rats and their offspring were increased [114]. However, the mechanisms underlying the observed effects have not been reported. It was also shown that long-term use of mobile phones could have various health problems ranging in their severity from headaches to brain cancer [136]. DNA damage due to lower-power MW radiation may be the cause of cancer and also the loss of fertility, as previously reported [4]. Table 2.3 summarises some of the recent *In-vivo* research on the effect of low-power MW radiation.

Table 2.3: Findings of the latest research studies on the effects of low-power MW radiation

Study	Exposure (SAR or power density)	Frequency	Effect
Tang J et al., 2015 [140]	0.016 W/Kg	900 MHz	Impaired spatial memory and damages BBB permeability in rats
Eris AH, et al., 2015 [141]	608 mW/m ²	900 MHz	Retarder learning and deficit in special memory in rats.
Li HJ, et al., 2015 [142]	5, 10, 20 mW/cm ²	2.856 GHz	Long-term, chronic MW exposure could induce dose-dependent deficit of spatial learning and memory in rats
Aydogan F, Unlu, 2015 [56]	0.4 W/kg	2.1 GHz	Exposure to 2100 MHz RF radiation causes salivary gland damage to some extent and especially with more prolonged exposure duration.

TRPV ion channel proteins play a significant role in the sensory function in our body. TRPV1 ion channel protein was investigated for long-time exposure at 900 and 1800 MHz in a rat model [114]. In the study, 24 adult rats were divided into control, and test groups irradiated at 900 MHz and 1800 MHz exposure. Samples were irradiated for 6 min/5days of the week for one year. The study concludes that mitochondrial oxidative stress, programmed cell death and Ca⁺² entry pathway through TRPV1 activation were increased. At 2450 MHz, the response of the brain was studied in rats. Single- and double-strand DNA breakages were observed in brain cells of rats exposed to continuous and pulsed MWs at 2.45 GHz and a power density 2 mW/cm² [47]. The study reports detrimental changes in the rat brain leading to lowering of learning and memory and expression of anxiety behaviours, with falls in brain antioxidant enzyme systems.

A study group of human volunteers has been selected for various demographic data including age, gender, dietary pattern, smoking habit, alcohol consumption, duration of mobile phone use and average daily mobile phone usage [143]. The objective of the study was to analyse various antioxidants in the plasma of individuals exposed to low-power EM radiation. The analysis reveals significant attrition in glutathione (GSH) concentration ($p < 0.01$), activities of catalase (CAT) ($p < 0.001$) and superoxide dismutase (SOD) ($p < 0.001$), and rise in lipid peroxidation (LOO) when compared to controls. Multiple linear regression analyses reveal a significant association between reduced GSH concentration ($p < 0.05$), CAT ($p <$

0.001) and SOD ($p < 0.001$) activities and high MN frequency ($p < 0.001$) and LOO ($p < 0.001$) with increasing RF power density [143].

The results of a recent research study conducted in the USA by the National Institute of Health (NIH) under the National Toxicology Program (NTP) reveal that there is higher confidence in the association between the mobile phone radiation and development of cancer in rats [114] [144]. This study shows that about 2 to 3 percentage of male rats exposed to cell phone radiation developed malignant glioma brain tumours, and 5 to 7 percentage of exposed rats developed *schwannoma* tumours in their heart.

Several questions need to be answered at the genetic and protein levels. For example, there is a lack of scientific research and information on whether mobile phone radiation initiates any biochemical changes/responses in human volunteers. Studies have been done using a wide range of biological model and exposure protocols, resulting in a pool of research articles, but it is impossible to compare results obtained from different types of study. Secondly, there is limited research on gene and protein expression, individual sensitivity, and effects on DNA and the blood-brain barrier. Few studies have been conducted using human volunteers to examine the related biochemical responses [35, 145]. This is the reason why the effect of radiation from handheld wireless communication devices on human physiology is considered to be still unknown.

Some studies report the effects of EMR exposure on embryo development, behaviour, and biochemical and immune systems in animals and humans. However, the health consequences of these biological changes are still unclear and need to be further explored [18]. The health effects of low-power RF and MW radiation need to be further researched, as findings of different studies remain inconclusive and are sometimes conflicting. The reasons for inconsistent results are due to difficulties in comparing and validating reported research studies. In RF radiation research studies, researchers employ different research methods, including different experimental protocols of radiation exposure and its dosimetry. Often, the parameters of exposure (generated field strength, SAR, and power density) are not reported, and the temperature not monitored, resulting in difficulty in comparing published results. Furthermore, currently there is no clear understanding of the mechanism(s) underpinning the interaction of low-level RF radiation with biological processes, which is a considerable constraint in directional studies of non-thermal effects of RF radiation [145]. Despite the inconsistent nature of the observed effects, in 2011, based on an increased risk for glioma, a

malignant type of brain cancer associated with wireless phone use [94], the WHO/ IARC classified RF EM fields as possibly carcinogenic to humans under Group 2B, a category used when a causal association is considered credible but when chance, bias or confounding results cannot be ruled out with reasonable confidence.

2.5 Summary

In this chapter, the author has discussed the fundamental principles of electromagnetic radiation with a focus on non-ionizing radiation. The author has also discussed in detail the frequency range used for mobile telecommunication. Based on the current body of knowledge, the author discussed research on the possible health effects and regulations for service providers to use such radiation protectively. Later in this chapter, various research approaches used by the research community have been discussed in detail. In the next chapters, the author will discuss an *in-silico* study conducted to investigate the effects of static and oscillating electric fields on the conformation of Conotoxin protein, and *in vitro* evaluation of RF radiation on selected proteins and cells.

CHAPTER 3: EFFECTS OF STATIC AND TIME-VARYING ELECTRIC FIELDS ON THE CONFORMATION OF CONOTOXIN PROTEIN: A MOLECULAR MODELLING STUDY

3.1 Introduction

This chapter presents *in silico* studies performed to model the conformation of a selected peptide, Conotoxin, under the influence of applied external static and time-varying electric fields.

Molecular Dynamics (MD) simulation is a computational method frequently used in biological science to study the interaction of atoms and molecules under a fixed period. MD simulation can efficiently model atomic and molecular interactions occurring in biological systems and effects of external stimuli on molecules and cells. Computational studies, based on MD simulations, suggested that proteins exposed to high strength static electric fields undergo significant conformational changes sufficient to affect the functionality of these proteins [65] [63] [66].

Initially, the author studied the effects at 0.01, 0.001 and 0.0001 V/nm on the conformation of Conotoxin peptide. In this work, a novel Dynamic Time Warping (DTW) method was employed to evaluate the conformational changes [146]. In the follow-up study, the author further simulated the effects of the static electric fields of three different strengths $1e+9$, 0.00123 and 0.000055 V/nm on the structural stability and conformation of Conotoxin peptide [146]. The effects were also studied when Conotoxin was simulated under time-varying electric fields of strengths $2e-9$, $6e-9$ and $4.7e-8$ V/m and the calculated frequency equivalent to 1800 MHz. The findings showed that applied time-varying (oscillating) electric field of $4.7e-8$ V/m (the highest strength) produced changes in conformation of Conotoxin, whereas at $6e-9$ V/m minor changes were observed, which were then stabilized during the simulation. The results show that the applied field at the lowest strength $2e-9$ does not induce any change in the conformation of Conotoxin.

3.2 Computational modelling study

3.2.1 Model System: Conotoxin Peptide

Conotoxin generally consists of 15-30 amino acids and includes between 2 and 3 disulphide bridges. Conotoxins are a family of Cys-enriched peptides found in several marine snails from the genus *Conus*. Many neurological diseases are being associated with functional changes within specific subclasses of nicotinic acetylcholine receptors. α -Conotoxins act as competitive antagonists of the nicotinic acetylcholine receptor and express significant painkilling effects. Conotoxin target and block potentially a wide range of ion channel proteins (a type of cell membrane proteins), such as voltage-gated sodium channels (Nav), voltage-gated calcium channels (Cav), voltage-gated potassium channels (Kv), nicotinic acetylcholine receptors (nAChRs) as well as other membrane receptors. The simplicity of Conotoxin structure, i.e. 16 amino acids in length, and its wide range of therapeutic applications [25] make it an ideal model to study its conformational changes under the electric field of different strengths. It is a useful molecular tool to study the properties of their target in healthy as well as in diseased states. In this study, we downloaded Conotoxin (2efz.pdb) from the Protein data bank. This Conotoxin belongs to M-superfamily and has typical Cys framework (-CC-C-CC-), and one of the eight major superfamilies found in the venom of cone snail. Conotoxin has an increasing therapeutic interest in peptide-based drugs.

3.2.2 Parameters of external static and time-varying electric fields

Table 3.1 presents electric field parameters used in this computational study for simulating Conotoxin peptide. As can be seen from Table 1, the SAR values employed here were below and above the standard safety limit (SAR of 2.0 W/kg - introduced by the International Commission on Non-Ionizing Radiation Protection (ICNIRP)). The safety limit for exposure to mobile phone emissions is set by determining the lowest level of exposure known to cause health hazards and then adding a safety margin.

Table 3.1: The SAR values of the MW exposures limits based on the ICNIRP limit

Power, dBm	Power density, mW/cm ²	Electric field, V/m	Electric field, V/nm	Specific Absorption Rate (SAR)
-10	0.00121	2	2e-9	0.0078
0	0.01210	6	6e-9	0.0700
17	0.606	47	4.7e-8	4.314

Table 3.2 shows the electric field strengths used in this *in-silico* study to create an external static electric field inside the system. The strengths were calculated as the power equivalent to the selected powers, as follows: -10 dBm (2e-9 v/nm), 0 dBm (6e-9 v/nm) and 17 dBm (4.7e-8 v/nm).

Table 3.2: Microwaves simulations parameters for Static Electric field in the range of 17, 0 and -10 dBm

System	Electric Field Strength	Temperature (K)	Duration (ns)
Conotoxin (2efz.pdb)	2e-9	300	1
	6e-9	300	1
	4.7e-8	300	1

Table 3.3: Simulations parameters used to simulate Conotoxin for the time-varying electric field at the microwave frequency 1800 MHz and electric strengths of 17 dBm, 0 dBm and -10 dBm

System	Field frequency (MHz)	Field Strength V/nm	Duration of simulation (ns)	Temperature (K)	Number of replicates
Conotoxin (2efz.pdb)	1800	2e-9	10	300	3
	1800	6e-9	10	300	3
	1800	4.7e-8	10	300	3

Table 3.3 shows the parameters used to create the time-varying electric field at the frequency 1800 MHz field strengths equivalent to the powers 17 dBm, 0 dBm and -10 dBm.

The Conotoxin was simulated for 10ns, and three replicates were used to analyse the conformation of the peptide for each studied parameter.

3.2.3 Molecular Modelling Approach: Molecular Dynamics Simulation

Computations based on molecular models are playing an increasingly important role in biology, chemistry, and biophysics. Since only an insufficient number of properties of biomolecular systems is accessible for measurements by experimental means, computer simulations offer an opportunity to complement experimental studies by providing insights into mechanistic aspects of a particular biological process and understanding of interactions between biomolecules (cells) and external stimuli. Computational approaches not only provide information on the averaged values but also distributions and time series of any definable quantity. In this study GROMACS software [83] was used to simulate the Conotoxin under static and time-varying electric field, with the changes in the peptide conformation being studied. GROMACS is an acronym for GRONingen Machine for Chemical Simulations. It is a very active programme for molecular dynamics (MD) simulations. Here, it is implemented with the static and time-varying algorithms, which provide a suitable environment to study the behaviour of the molecular system under the influence of applied stimuli (electric fields) and evaluate the changes occurring in the molecule in a fraction of seconds.

The electric fields (static and oscillating) were introduced through .mdp file described in detail elsewhere [147]. GROMACS molecular dynamics package [83] was extended to include a pulsed, time-varying electric field [148].

$$E(t) = E0 \exp \left[-\frac{(t-t_0)^2}{2\sigma^2} \right] \cos[\omega(t - t_0)] \quad \text{Equation 3.1}$$

Where, sigma is the pulse width, and t is the time after the pulse maximum at t^0 . The angular frequency $\omega = 2\pi c/\lambda$ was varied in the microwave regime as described above.

3.2.4 Static and Time-Varying External Electric Fields

Simulation parameters applied for static and time-varying electric field are discussed in detail separately. For static electric field, simulation of Conotoxin was conducted for 1000 ps to stabilise the molecule, whereas overall simulation time used for time-varying electric field simulation of Conotoxin was 10ns with three repeats for each selected power. When Conotoxin was simulated to study the effects of the static electric field on its structure, the higher field

strengths were used for which the induced effects can be seen even at the brief period of simulation, namely 1000 ps.

Simulation Parameters for Conotoxin under Static Electric Fields

MD simulations were performed using the GROMACS software package, version 4.5.3 [74]. Conotoxin peptide (PDB ID 2EFZ) along with four alpha-Conotoxin peptides were used in this study (PDB IDs: 2JUQ, 2JUR, 2JUS, 2JUT) to evaluate and compare the structural changes in these peptides under the applied exposures. The CHARMM27 [75, 149] force field and TIP3P [150] water models were adopted for the simulation of the peptide and solvent respectively. Conotoxin(2efz.pdb). The starting geometry of Conotoxin was taken from the Protein Data Bank (PDB ID 2EFZ.pdb) [76] was downloaded from the PDB database and placed at the centre of a periodic 6.3X6.3X6.3nm transferable intermolecular potential 3-Point (TIP3P) water box [150] containing 21,333 water molecules. Sodium ions (Na⁺) were introduced to neutralise the system. The system was first energy minimised with the protein frozen using the steepest descent for 20000 steps. Then, two 600 ps equilibrations were carried out at the constant temperature, constant volume (NVT) and constant pressure (NPT) ensemble, while keeping the protein fix. The converging criterion of energy minimisation was a maximum force value of 10 KJ/nm/mol. All electric fields were applied in the same arbitrary direction, i.e. along the x-axis (1,0,0) of the starting equilibrated conformation. Finally, the production MD simulations were run for 1000ps with the temperature maintained at 300 K and time constant of 0.1 ps. The pressure was maintained at 1atm with a time constant of 0.5ps [151]. A 2-fs time step was used in all MD simulations. A cut off of 1 nm was applied to short-range non-bonded interactions, and for long-range electrostatic interactions, the particle mesh Ewald (PME) method [152] was used with a grid spacing of 0.12nm and the 4th order interpolation.

A novel Dynamic Time Warping (DTW) method was introduced and employed to evaluate the conformational changes in Conotoxin exposed to static electric fields of different strengths. The DTW method [153] is a dynamic programming algorithm based on warping the time scale of one series, S , onto another series, Q [154]. The algorithm consists of the following steps:

1. Firstly, a Distance matrix is calculated using the following process:

$$D(i, j) = d(i, j) + \min \begin{cases} D(i-1, j) \\ D(i-1, j-1) \\ D(i, j-1) \end{cases} \quad \text{Equation 3.2}$$

Where $D(i,j)$ is the Euclidean distance between the points i and j .

2. Secondly, the DWT algorithm is searching for optimal warping path, and finally calculates the DWT distance as follows:

$$DTW(S, Q) = \min \left\{ \sqrt{\sum_1^K \frac{W_k}{K}} \right. \quad \text{Equation 3.3}$$

Where W_k and K represent weights for each part and normalising factors.

Root mean square deviation (RMSD) of the backbone atoms was calculated to determine the starting/initial structure of Conotoxin peptide. The radius of gyration (Rg) and protein–water molecules interactions were calculated to evaluate the response of the protein to the applied electric fields. Structural changes occurring in Conotoxin were analysed during simulation using the STRIDE algorithm [155], which is implemented within the visual molecular dynamics (VMD) software package [156]. VMD is a molecular graphics program designed for the display and analysis of molecular assemblies, such as proteins and nucleic acids.

Simulation parameters for Conotoxin under the time-varying electric fields

MD simulations were performed to study the structural changes in Conotoxin when the time-varying electric field of $2e-9$ V/nm, $6e-9$ V/nm and $4.7e-8$ V/nm (Table 3) were applied at frequency 1800 MHz and field strengths equivalent to the powers 17 dBm, 0 dBm and -10 dBm. The structures were solvated in an SPC water box. The Conotoxin peptide was centred in a cubic simulation box with edge lengths of $111\text{\AA} \times 111\text{\AA} \times 111\text{\AA}$. Overall ionic strength was maintained using 150 mM NaCl, 218 Na^+ ions and 203 Cl^- ions were added to the Conotoxin system. The systems were then energy minimised over 2000 steps using the steepest descent minimisation algorithm and further equilibrated (with heavy atoms restrained) for 100 ps of NPT equilibration each using the Berendsen thermostat at 300K. The pressure was isotopically maintained at 1.0 bar using the Berendsen barostat [157] [40]. Electrostatic interactions between non-covalent atoms were computed using particle-mesh Ewald (PME) [75] [41]. All MD simulations were performed using Gromacs (Version 4.5.5) [83] [74]. All MD simulations in this study were performed using the Amber 99SB-ILDN force

field [158] [43]. All data analysis was performed by using the VMD software package.

3.3 Results and Discussion

3.3.1 Study one: External Static Electric Field of 0.01 V/nm, 0.001 V/nm and 0.0001 V/nm

Presented below are the results obtained when Conotoxin peptide was simulated at three different electric strengths 0.01 V/nm, 0.001 V/nm and 0.0001 V/nm.

A. *Ramachandran Angles and DTW Analysis*

The conformational changes in Conotoxin peptide exposed to the static electric fields were evaluated using, the distances between the Ramachandran angles (Phi and Psi) sets calculated for two different scenarios: static electric field of different strengths *vs* no-field condition (Table 3.2).

Table 3.4: Distance between the Ramachandran Angles (Phi and Psi) sets calculated for static electric fields of selected strengths vs no-field condition

No-field	No-field vs 0.01 V/nm	No-field vs 0.001 V/nm	No-field vs 0.0001 V/nm
0	437.1026	10.6668	2.1083

As seen from data presented in Table 3.4, the most significant change in conformation of Conotoxin is observed for exposure at the field strength 0.01V/nm.

Changes in Ramachandran angles for the particular peptide bonds were also analysed statistically to determine the significance of the changes in the exposed *vs* non-exposed Conotoxin. Pairwise t-test analysis was used here. The t-test revealed that conformational change in Conotoxin is only significant for the static electric field of 0.01 V/nm: $t(14)=1.77$, $p=0.05$ for Phi angles; and $t(14)=2.53$, $p=0.01$ for Psi angles. The other two strengths of the applied static electric field induced **no statistically significant conformational change in Conotoxin peptide**.

B. *Root Mean Square Deviation (RMSD) and Radius of Gyration (Rg) Analysis*

The RMSD of the backbone atoms was calculated to determine the conformational

changes in Conotoxin under the electric field 0.01V/nm during the MD simulations. Figure 3.1 represents the RMSD plots for the static electric field vs No-field conditions. As observed in Figure 3.1, the applied electric field 0.01V/nm induces conformational changes in the studied Conotoxin peptide.

Conformational changes in Conotoxin were studied further by calculating the radius of gyration (Rg). The calculated Rg data for No-field and electric field conditions are plotted and shown in Figure 3.2. As can be seen from Figure 3.2, the conformation of Conotoxin peptide is affected by the applied electric field 0.01V/nm.

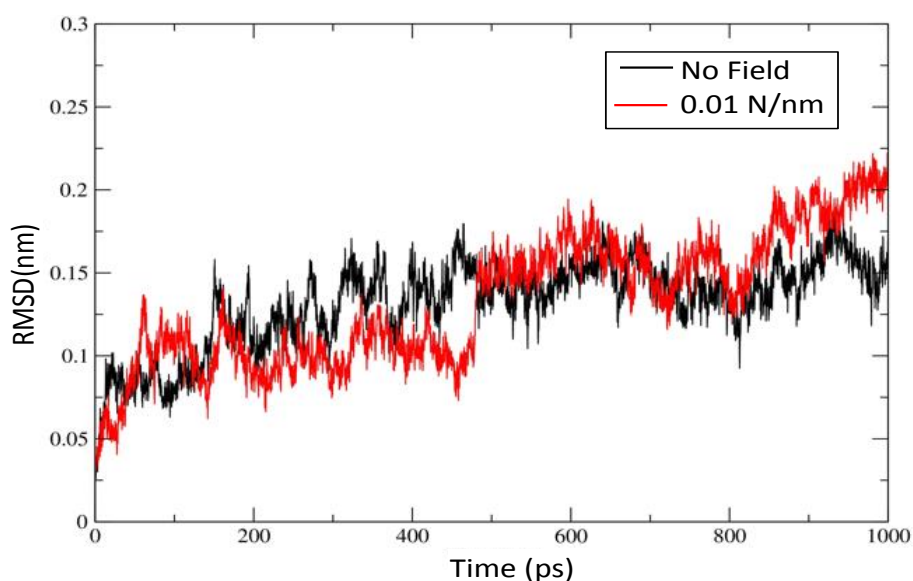


Figure 3.1: RMSD data calculated for No-field vs static electric field of 0.01 V/nm exposure

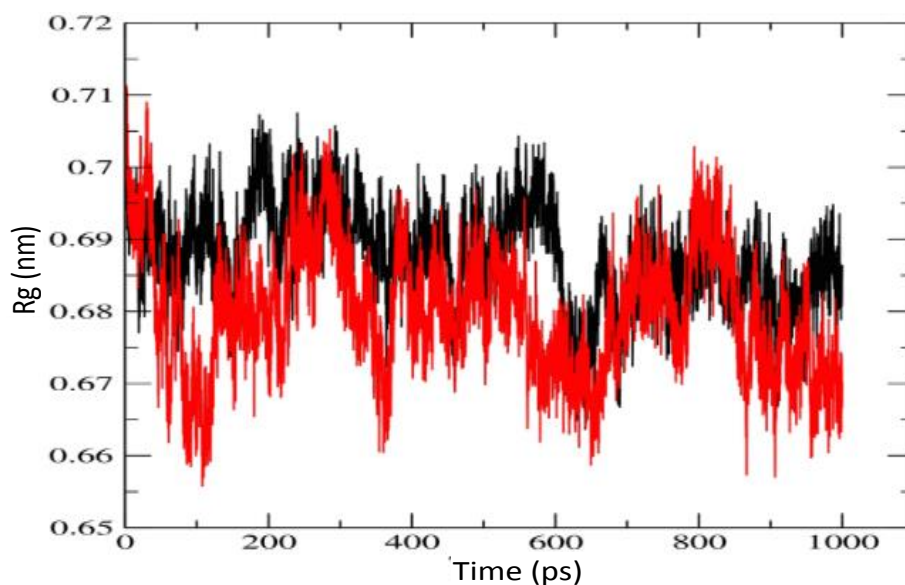


Figure 3.2: Change of the radius of gyration (Rg) during MD simulation for No-field (black line) vs electric field 0.01V/nm (red line) conditions.

C. Distance analysis of Homologues Conotoxin Peptides

Using the DTW analysis, the effects of static electric fields were further studied on the selected four homologues Conotoxin peptides (2JUQ, 2JUR, 2JUS, 2JUT). These homologues peptides have similar biological activities and similar structures. Their starting geometries were downloaded from the PDB (No-field condition), simulated in the static electric field of the different strengths 0.01, 0.001, 0.0001 V/nm. For all sixteen conformations, Ramachandran angles (Phi-Psi) were calculated. DTW was used for each pair of Ramachandran angles. The distance matrix is constructed:

$$|a|_{i,j} = DTW(i,j) \quad \text{Equation 3.4}$$

where i and j are the i^{th} and j^{th} set of Ramachandran angles.

The cladogram was created to cluster Conotoxin peptides based on the similarity of their conformations with respect to the changes in the distances for No-field vs different strengths of electric field conditions.

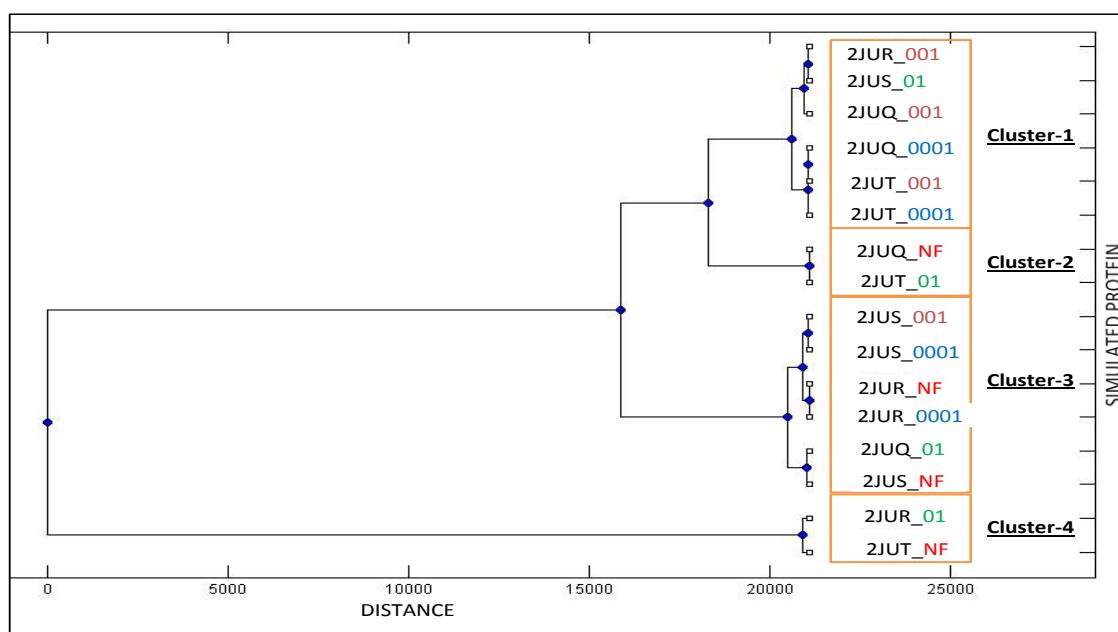


Figure 3.3: Cladogram of Conotoxin peptides conformations: no-field (NF) and different electric fields conditions

Figure 3.3 represents the change in conformations of selected Conotoxin peptides at the

different field strengths compared to no-field condition (NF). From the cladogram, it can be seen that analysed four Conotoxin peptides are clustered into four major groups. According to the DTW distances the following specific observations were made:

1. Static electric fields induce different structural changes in peptides having the similar structures. For instance, the 2JUQ peptide can be seen in four different groups. This means that that applied electric field induces changes in the distance matrix and hence, changes its conformation.
2. The changes in distance matrix are different and dependent on the strength of the applied static electric field for each analysed Conotoxin peptides.
3. The most significant change in distance matrix can be observed (regrouping) with the electric field 0.01V/nm.

3.3.2 Study two: External Static Electric Field of 0.000055 V/m, 0.00123 and 1e+9

Further to our analysis with static electric fields, we simulated Conotoxin peptide using an additional range of electric fields. Three different electric strengths -of 0.000055 V/m, 0.00123 and 1e+9 V/m were used.

A. Root Mean Square Deviation (RMSD) and Radius of Gyration (Rg) Analysis

RMSD for the Conotoxin backbone was calculated to evaluate structural variations in the protein under the applied static electric fields. Also, Rg of Conotoxin that represents the distribution of atoms in space relative to their centre of mass was calculated. Rg gives the information about the changes in the shape and size of a given protein. As can be seen from Figure 3.4, when simulated that electric field of 0.000055 V/m produces no change in RMSD compared to the no-field condition. However, electric fields of 0.00123 and 1e+9 V/m induce significant changes in RMSD.

It can also be observed from Figure 3.5 that the calculated Rg values are higher for the electric field strength of 1e+9 V/m when compared to the other two lower strengths external electric field. Higher Rg value is likely due to the loss of secondary structure and unfolding of Conotoxin peptide, which is also can be seen in the snapshots taken at 500ps and 1000ps for each of the simulation (Figure 3.7B). When Conotoxin is exposed to the electric field 0.00123 V/m, a minor increase in Rg can be observed, whereas at 0.000055 V/m no change in Rg is

visible when compared to the no-field condition.

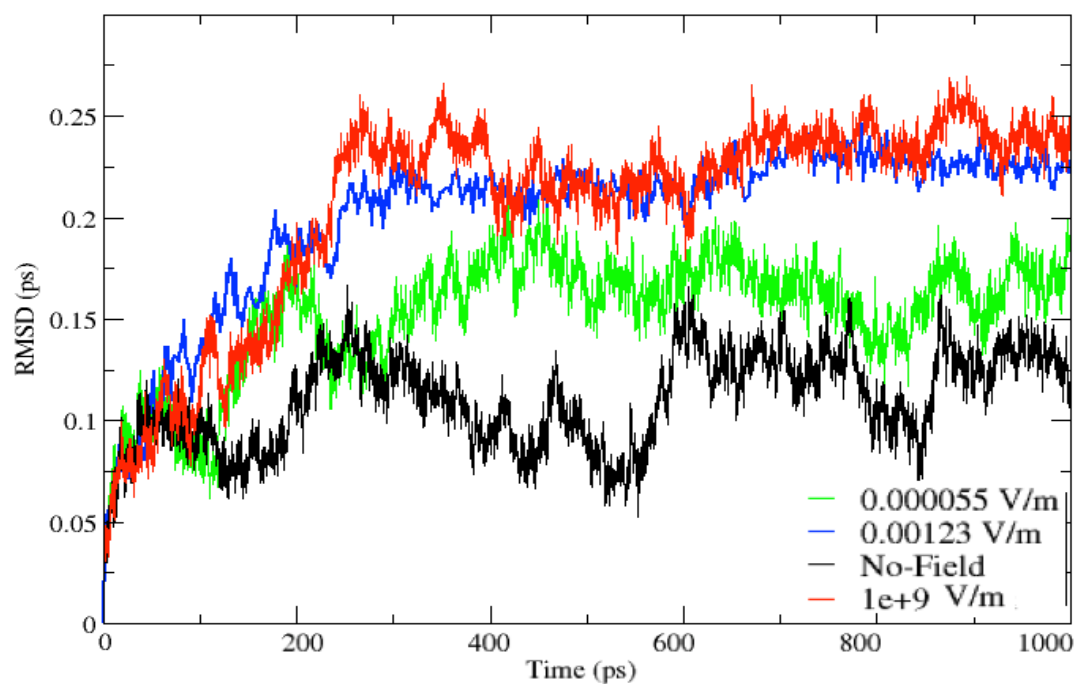


Figure 3.4: Conotoxin backbone's RMSD evolution over the 1000 ps simulation time at different strengths 0.00123, 0.000055 and 1e+9 V/m compared to the no-field condition

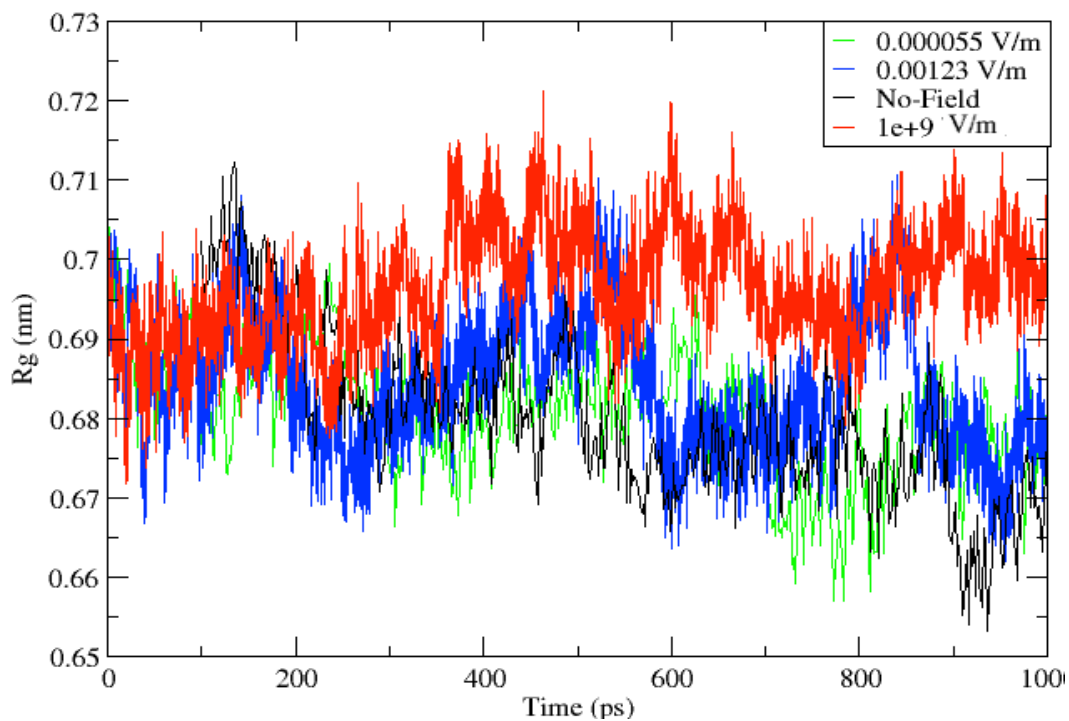


Figure 3.5: The radius of gyration (Rg) of Conotoxin peptide under the stress of external electric fields of 0.000055, 0.00123, and 1e+9 V/m compared to the no-field condition

B. Radial Distribution Functions (RDFs) and Conotoxin conformation

Accumulation of water molecule around the protein plays a significant role in protein's final conformation and ultimately contributes to its functions. It is critical to understand the protein's interaction with water molecules when it is exposed to the electric field of different strengths. The interaction between Conotoxin and water molecules was evaluated by calculating the radial distribution functions (RDFs). Referring to Figure 3.6, the RDFs between Conotoxin peptide and water exhibit 2 separate peaks, the first sharp peak at ~ 0.19 and second less significant at ~ 0.4 , that indicate a hydrogen bond between Conotoxin and water molecules, which leads to the formation of a hydration shell. The sharp water-protein peak at 0.19 suggests the accumulation of water molecules around the protein molecule, which decreases with the decrease in electric field strength (Figure 3.6). This result implies that Conotoxin peptide is more solvated at the field of the higher strength $1e+9$ V/m, whereas at the low field strengths peptide folds or coils which make the protein less exposed to water molecules.

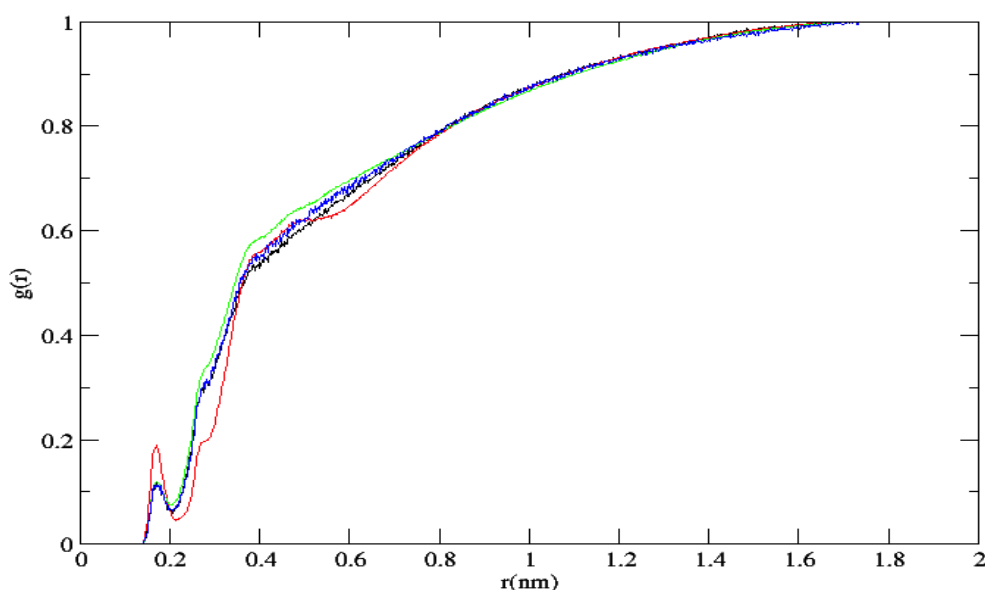


Figure 3.6: Peptide-water interactions represented by the radial distribution functions. The line colour is representative of the electric field strength: $1e+9$ V/m (red), 0.00123 V/m (green), 0.000055 V/m (blue), no-field (black)

As can be observed from the snapshot taken at 500 ps and 1000 ps (Figures 3.7A and 3.7B respectively), for 1ns simulation of Conotoxin at “no-field” condition, there is no change in protein conformation during the simulation. However, at the static electric field 0.00123 V/m, particularly towards the end of the simulation (Figures 3.7E and 3.7F), Conotoxin starts

losing its structure. At the electric field $1\text{e}+9$ V/m, a significant unwinding of Conotoxin can be seen (Figures 3.7E and 3.7F), which has resulted in the increased hydrogen bonding between the protein and water molecules discussed above and shown in Figure 3.6. These results imply that Conotoxin is changing its secondary structure only when exposed to the fields $1\text{e}+9$ V/m and 0.00123 V/m.

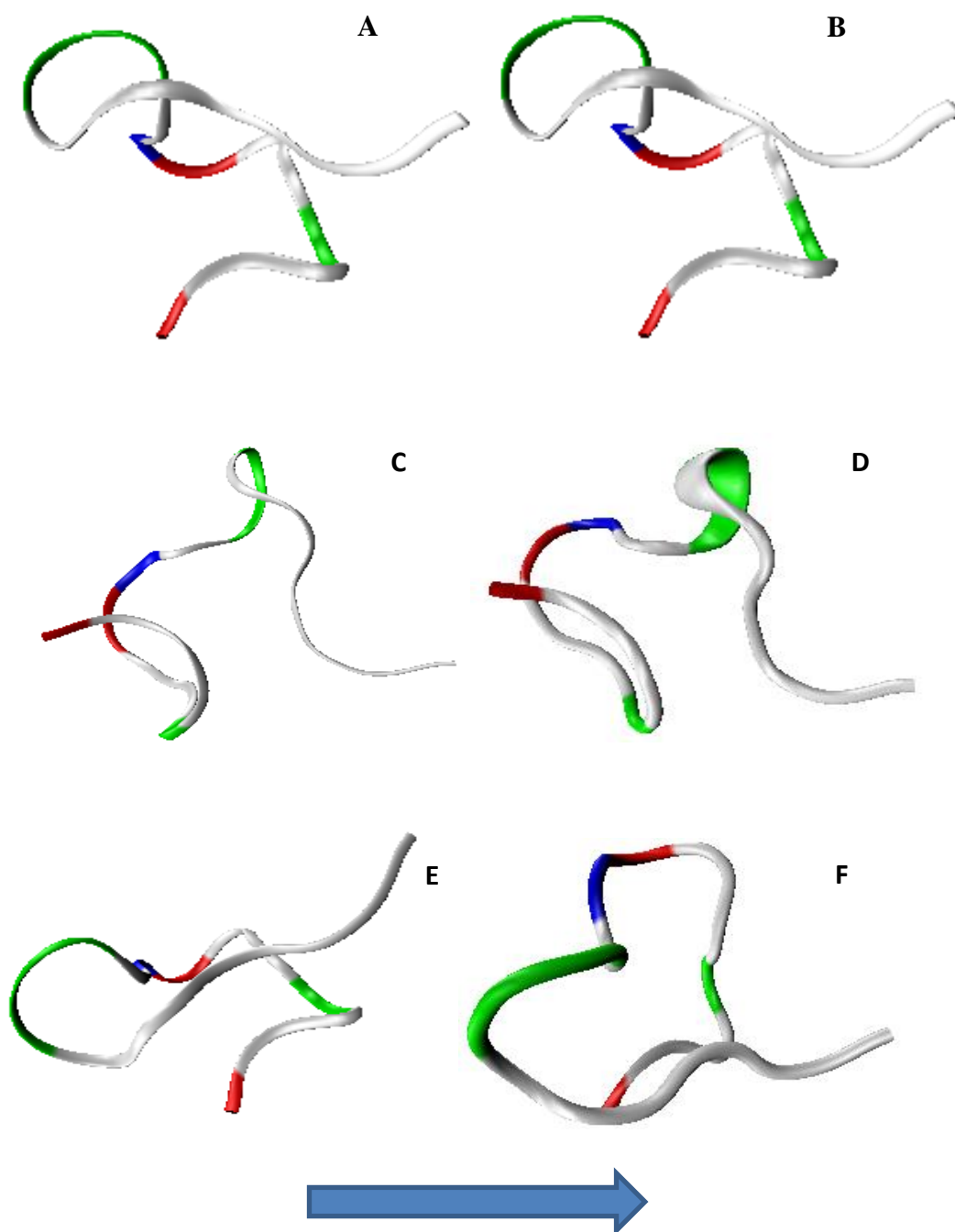


Figure 3.7: Snapshots of Conotoxin conformation at no-field condition (A, B), electric fields of 0.00123 V/m (C, D) and $1\text{e}+9$ V/m (E, F) at 500 ps and 1000 ps respectively. The white colour

encodes non-polar residues; green colour encodes polar residues, red colour encodes acidic residues and blue - basic residues. The arrow indicates the direction of the electric field.

3.3.3 Study three: External Time-varying Electric Field at $4.7e-8$ V/nm, $6e-9$ V/nm, $2e-9$ V/nm

A. RMSD and Root mean square fluctuation (RMSF) of Conotoxin

RMSD for the Conotoxin backbone was calculated to evaluate structural variations in the peptide under the applied time-varying electric fields (external stressor). RMSF and radial distribution curve of Conotoxin were analysed to study the distribution of atoms in space relative to their centre of mass. We also studied the accumulation of water molecules around the peptide by analysing the distribution of water molecules as it plays a significant role in peptide's final conformation and function.

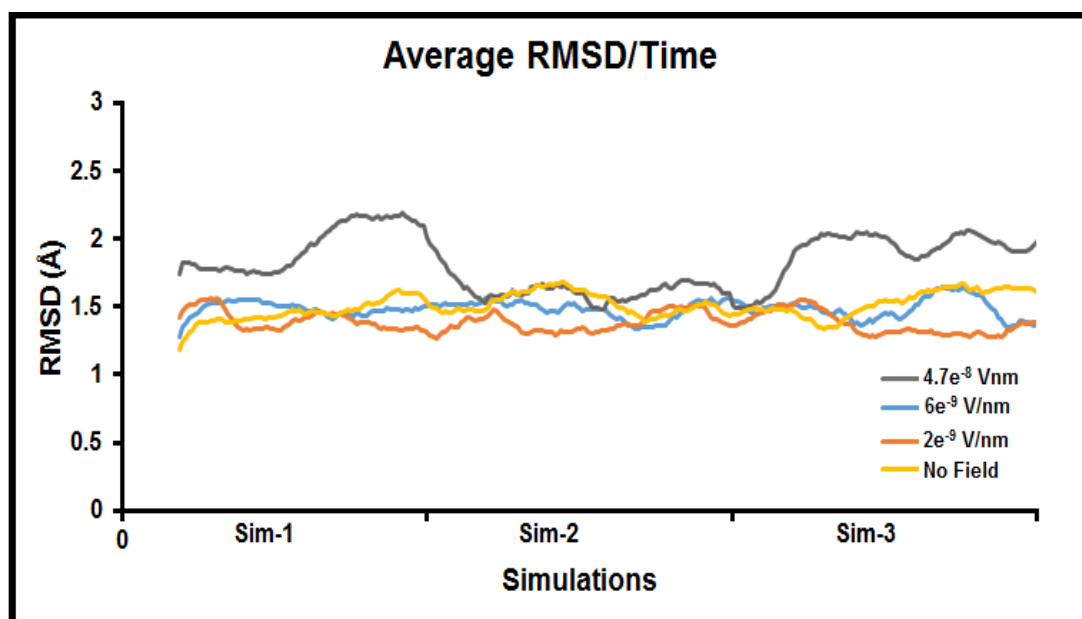


Figure 3.8: Conotoxin structural deviations vs simulation time at the frequency 1800 MHz and different field strengths. RMSD values of peptide's $C\alpha$ -atoms with a field amplitude of $4.7e-8$ V/nm, $6e-9$ V/nm, $2e-9$ V/nm and with zero field conditions at 300 K

The effect of the applied fields on Conotoxin's structure was examined in detail. Conotoxin's structural changes were considered according to the time course of the peptide's RMSD ($C\alpha$ root mean square deviation relative to the Conotoxin's final structure at "no-field" condition), in the RMSF of individual residues and the % of peptide's secondary structure. Figure 3.8 showed the time evolution of the peptide's backbone deviation under the field at the

frequency 1800 MHz and three different powers ($P_1 = 4.7 \times 10^{-8}$ V/nm, $P_2 = 6 \times 10^{-9}$ V/nm, and $P_3 = 2 \times 10^{-9}$ V/nm) and compared to peptide backbone at “no-field” structure. The field at the power P_1 (equal to 17 dBm) induces the maximum deviation in backbone structure as compared to the fields at the powers $P_2 = 6 \times 10^{-9}$ V/nm (equal to 0 dBm) and $P_3 = 2 \times 10^{-9}$ V/nm (equal to -10 dBm). Fields at P_2 and P_3 induce no change in the backbone structure and are aligned with the structure at “no-field” condition, which suggests that at these powers the generated fields produce no effect on the backbone of the Conotoxin peptide structure during the whole simulation time (30 sec).

We have three repeats for 10ns simulations which are represented as Sim-1, Sim-2 and Sim-3 (Figure 3.8). As can be seen from Fig.1 the structural deviation occurred during each simulation during the last 2ns simulation time, i.e. in between 8 to 10 ns in Sim-1, 18-20 ns in Sim-2 and 28-30 ns in Sim-3.

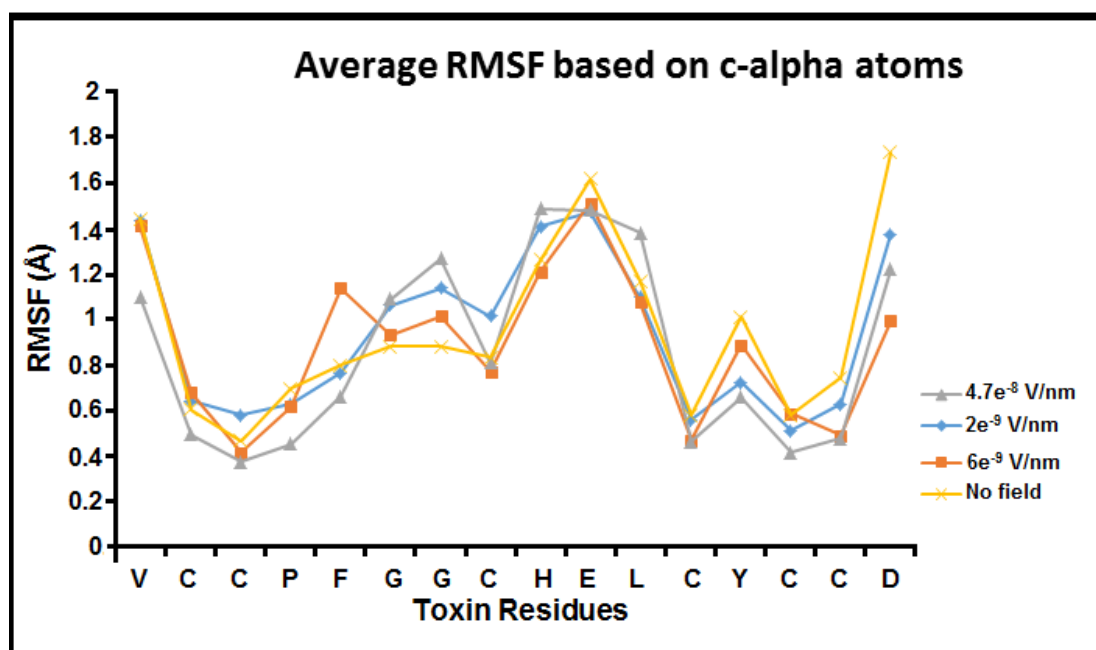


Figure 3.9: Conotoxin structural deviations during the simulations time at the field frequency 1800 MHz and different strengths. RMSF values calculated for each amino acid of Conotoxin peptide at the field strengths 4.7×10^{-8} V/nm, 6×10^{-9} V/nm, 2×10^{-9} V/nm and “no- fie

It is important to see which peptide regions undergo the significant structural fluctuations induced by the oscillating field and if there is a field-strength dependency effect. Figure 3.9 depicts the excess $C\alpha$ -atom fluctuations Δ RMSF (after subtracting the zero field RMSFs).

3.3.4 Secondary structure analysis of Conotoxin peptide under time-varying electric fields

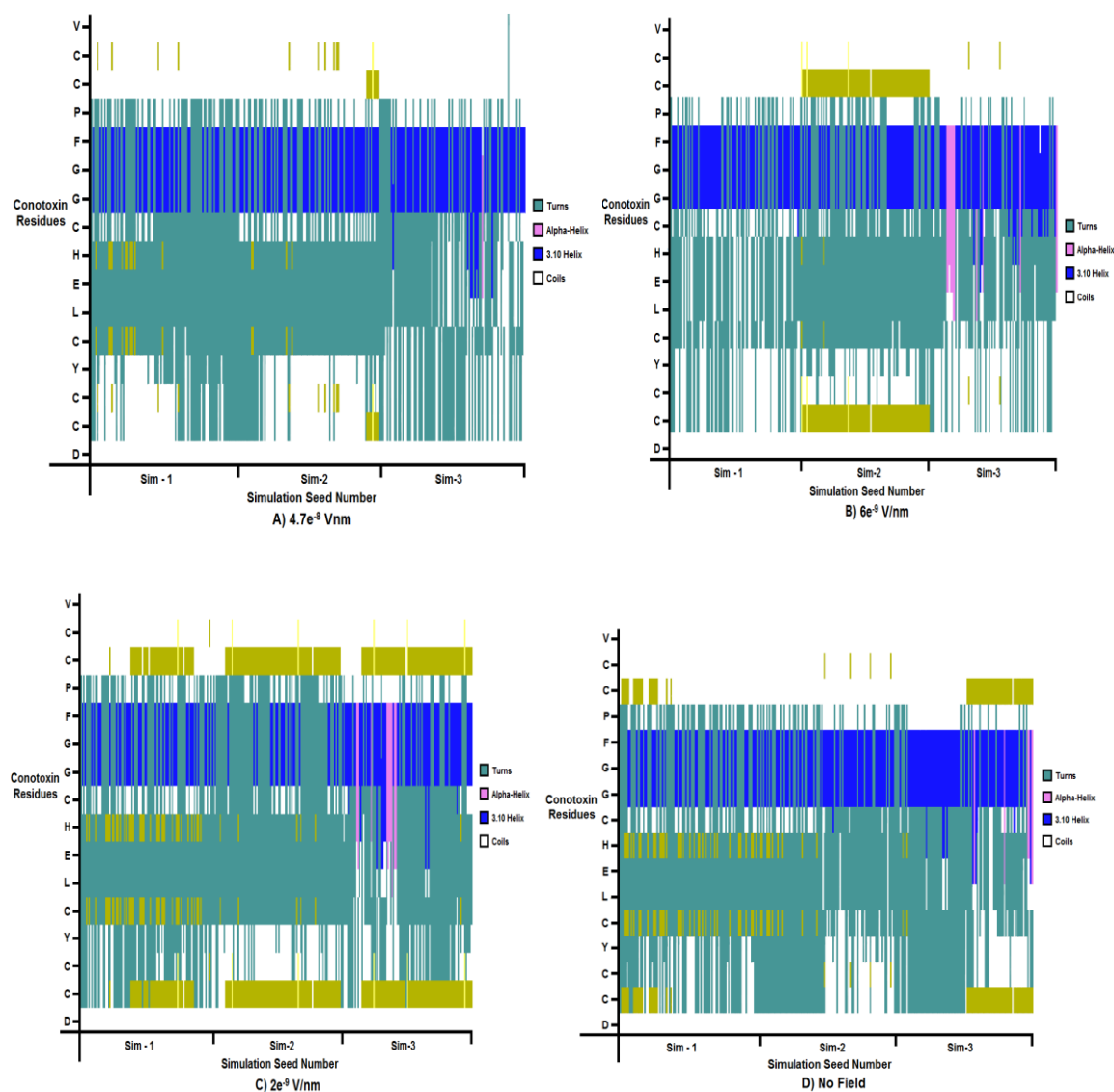


Figure 3.10: The secondary structure of lysozyme at different field strengths and “no-field” conditions. Distribution of secondary structure elements over the Conotoxin sequence at frequencies of 1.800 GHz and power of 4.7×10^{-8} V/nm (purple), 6×10^{-9} V/nm (blue), 2×10^{-9} V

The effect of the external oscillating electric fields on the secondary structure of Conotoxin was evaluated using the STRIDE algorithm. Figure 3.10 demonstrates that application of electric field with the strengths 6×10^{-9} V/nm and 2×10^{-9} V/nm had no significant effects on the helical region of Conotoxin, but minor changes can be observed on turns and coils, as compared to “no-field” condition. Application of the field 4.7×10^{-8} V/nm induces minor disruptions within the helical region of the peptide. However, these changes may not be significant enough to cause any major structural change that can lead to changes in the

functionality of Conotoxin.

Radial Distribution Functions (RDFs) and Conotoxin confirmation

Accumulation of water molecules around the peptide plays a significant role in peptide's final conformation and ultimately contributes to its function(s). It is critical to understand the peptide's interaction with water molecules when it is exposed to time-varying electric fields of different strengths. The interaction between Conotoxin and water molecules was evaluated by calculating the radial distribution functions (RDFs) presented in Figure 3.11.

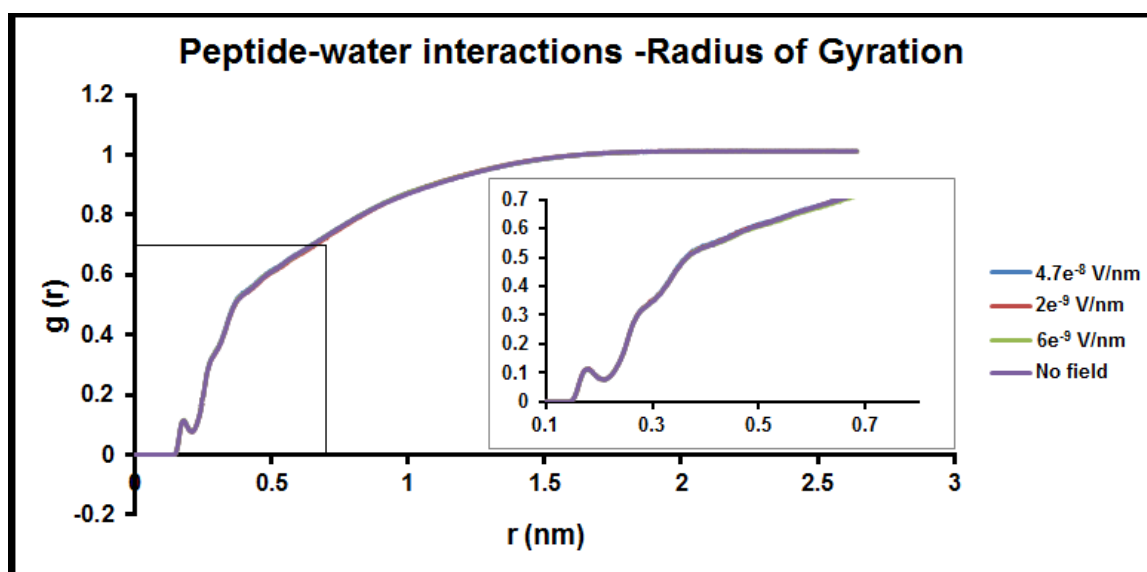


Figure 3.11: Peptide-water interactions represented by radial distribution functions The line colour is representative of the electric field strength: 4.7e-8 V/m (blue), 2e-9 V/m (red), 6e-9 V/m (blue), no-field (violet).

From Figure 3.11 the RDFs between Conotoxin peptide (16 aa) and water exhibit two separate peaks. The first sharp peak can be seen at ~0.19 and second less significant at ~0.4, indicating a formation of the hydrogen bond between Conotoxin and water molecules, which leads to the further formation of the hydration shell. The sharp water-peptide peak at 0.19 suggests the accumulation of water molecules around the peptide molecule, which interestingly remains the same at all powers of the applied field (Figure 3.11). This result implies that Conotoxin peptide does not show any effects under the selected range of electric field. This result also implies that the field at 1800 MHz and strengths of (-10 dBm, 0 dBm and 17 dBm) does not affect the peptide folding process. Hence, the applied fields produce no effect on the overall structure of the peptide.

3.3.5 Conotoxin Cluster analysis

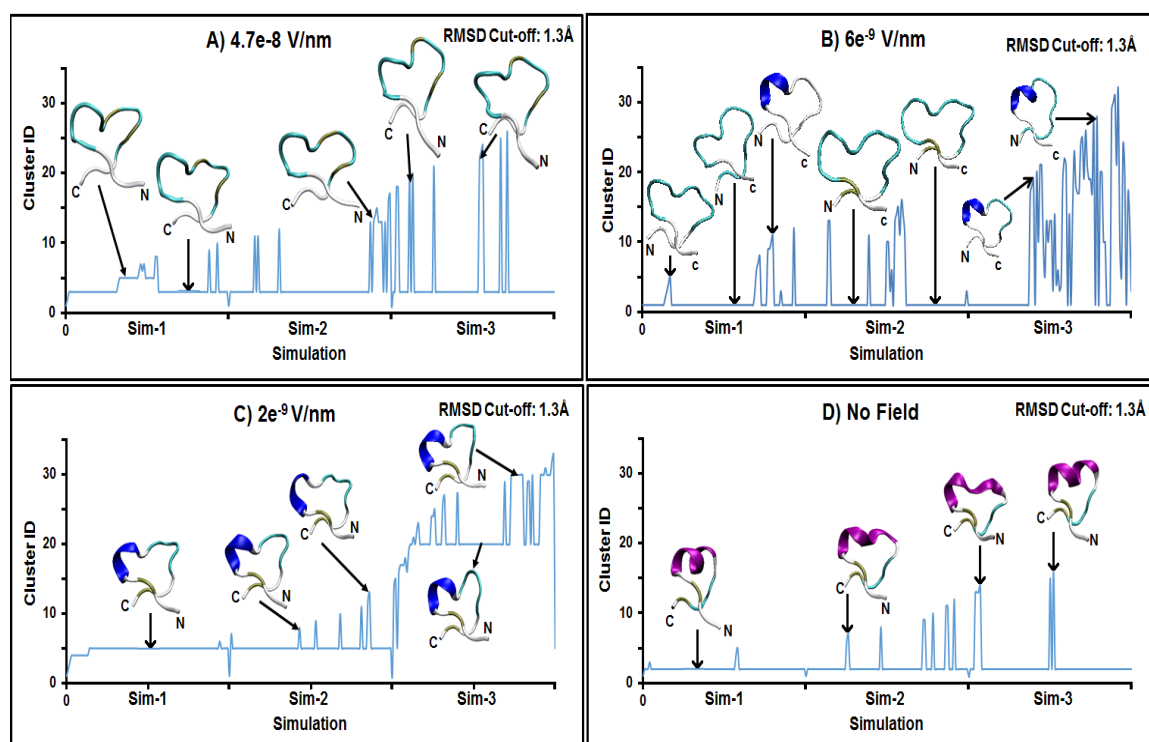


Figure 3.12: Schematic diagram showing the number of clusters sampled at the different field strengths during the simulation.

Cluster analysis was performed to identify the conformational changes in Conotoxin induced by the applied field of different strengths. Cluster analysis was performed using the respective simulation trajectories using the `g_cluster` function available in the Gromacs suite. The function `g_cluster` identifies the various conformations based on the C-alpha carbon atoms in Conotoxin. An RMSD cut-off of 1.3\AA was chosen after various trials. It was observed that lower cut-off produced too many unnecessary clusters and hence was uninformative. On the other hand, a cut-off higher than 1.3\AA produced very few clusters which also did not serve the purpose of this study. Figure 3.12 (A-D) shows the results of the cluster analysis, sampled by three simulations at the selected field strengths. For the sake of clarity, only prevalent structural conformations observed as the clusters are represented.

From Figures 3.12 (A-D), we observe that the overall conformation of the M-1 Conotoxin remains relatively intact in the presence/absence of the selected fields. At the field strength of $4.7e^{-8}$ V/nm, the cluster analysis conformations show a loss in the helicity of the peptide (Figure 3.12A). However, with the field strength reduction, the helicity of the peptide is recovered. Also, under another field of different strengths, the peptide does not show

significant fluctuations in its conformation. For example, at the field strength of $4.7e^{-8}$ V/nm. At “no-field” condition, the alpha-helix is visible in all clusters (Figure 3.12D). The structure also seems to be relatively more rigid and stable in comparison to that exhibited under the field strength of $4.7e^{-8}$ V/nm.

The peptide conformations of the most common clusters at all the respective trajectories were also compared and superimposed over each other. The clusters that were most prevalent at the field strength of $4.7e^{-8}$ V/nm again showed a loss of the helicity within the peptide, which was also seen in the peptide at “no-field” condition. In the absence of the external field, M1 showed flexibility at the C-terminal in addition to the flexibility at the N-terminal. This flexibility at the C-terminal of the peptide was not affected in the presence of the oscillating fields. These results suggest that the applied fields investigated in this study did not produce the immediate and significant changes in structural conformation of Conotoxin. On the other hand, the results also show that the oscillating fields are indeed ‘disturbing’ residues in the peptide, and over time, can result in loss or mutation of a residue or function of the peptide as a whole molecule. However, various biological and physical factors will also play a role in addition to the presence of the oscillating electric field for any structural disruption to take place.

Figure 3.13 shows the snapshots of Conotoxin for every last frame of each simulation run for 10ns. At the field strength of 4.7 V/nm, the peptide is losing its internal structure, whereas at other two studied field strengths Conotoxin retained its stable structure. The results of the above simulation also reveal that initially due to the effect of the applied oscillating field Conotoxin’s structure is being affected at the field of 4.7 V/nm. However, the structure soon self-stabilises and returns to its original form.

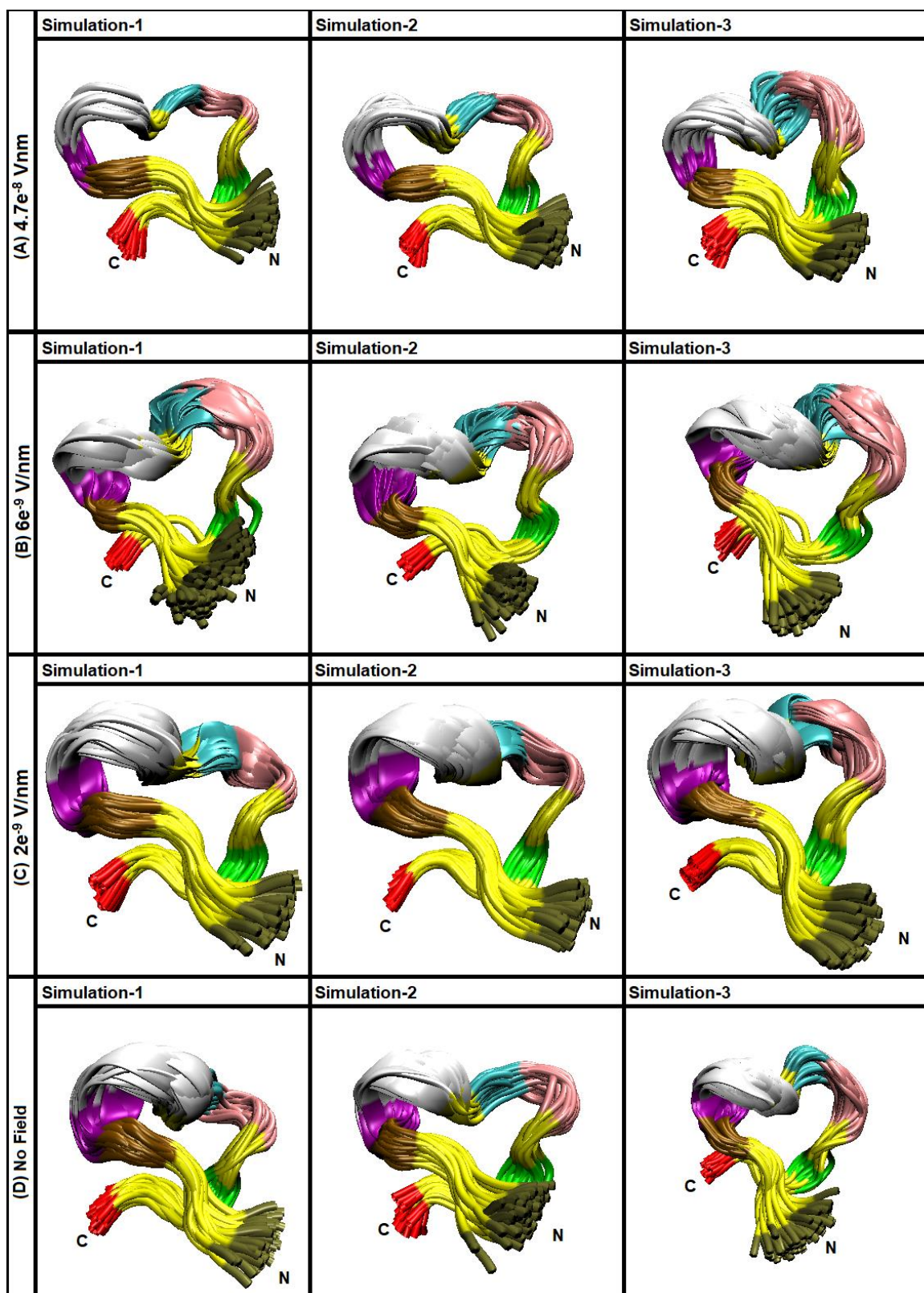


Figure 3.13: Snapshots of Conotoxin conformation at no-field condition (A, B), electric fields of 0.00123 V/m (C, D) and $1e+9$ V/m (E, F) at the last frame of each repeat.

3.4 Concluding Remarks

In this computational molecular study, a range of static and time-varying electric fields was applied to Conotoxin system to understand their effects on the peptide's conformation. Results show that at the higher strength external electric fields affect Conotoxin's structure. The findings are summarised and presented below.

3.4.1 The Conclusion from Study 1

To evaluate a magnitude/significance of the effects of applied static electric fields on Conotoxin's conformation, we analysed the distribution of Ramachandran torsion angles in the peptide backbones before and after the irradiation. As a measure of distance between the distributions of the torsion angles, we used the Dynamic Time Wrapping algorithm (DTW) for two-dimensional sequences. In Study 1, we explored the effects of the static electric fields of 0.01 V/nm, 0.001 V/nm and 0.0001 V/nm on the conformations of homologous Conotoxin peptides. In summary, the results obtained from this computational analysis reveal that applied static electric fields induce the conformational changes in the studied Conotoxin structure. Importantly, different strengths of exposures induce a different degree of changes in Conotoxin structures, ranging from no effect to statistically significant effect observed at electric field 0.01V/nm that may lead to changes in their biological activities. These findings thus imply that the effects are field-strength dependent.

3.4.2 The Conclusion from Study 2

This study was aimed to investigate the effects of external static electric fields $1\text{e}+9$ V/m, 0.00123 V/m and 0.000055 V/m on the structural stability of Conotoxin peptide. Results show that application of selected electric fields induced conformational changes in the peptide, particularly at $1\text{e}+9$ V/m and 0.00123 V/nm using the formation of hydrogen bonds between amino acid residues. It was also observed that the formation of hydrogen bonds between residues during simulation affected its RMSD and Rg values. The number of hydrogen bonds formed was increased with the increase in electric field strength, which has been shown by RDF analysis between the peptide and water molecules. Snapshots of Conotoxin at two selected time points, 500 and 1000 ps, indicate towards the unfolding of the peptide at the higher strengths of the electric field, which is the reason for the increase in the formation of hydrogen bonds between Conotoxin and water molecules.

The RMSD of C-alpha atoms and Rg was calculated to further assess the stability of Conotoxin under the static fields of the selected strengths. The findings showed that electric field 0.000055 V/m (the lowest strength) produced no effect on Conotoxin's conformation. The electric field 0.00123 V/m induced only minor changes in its structure; while the strongest field of 1e+9 V/m produced the major structural disruptions in Conotoxin peptide.

3.4.3 The conclusions from Study 3

This study explored the effect of oscillating (time-varying) electric fields of the strengths 2e-9 V/nm, 6e-9 V/nm and 4.7 V/nm on the structural stability of Conotoxin peptide. Results show that application of selected fields induced conformational changes in the peptide, mainly at 4.7 V/ m, whereas no significant effects were observed at other two strengths/powers at the frequency of 1800 MHz.

The results from Studies demonstrate that computational method such as MD simulations presents a useful tool in the analysis of effects of external electric fields (stressor) on peptide's structure and its functional properties. Knowledge gained through this computational study can aid in understanding the mechanistic aspects of change in conformation of a peptide to study the diseased condition under the effects of low strength static or varying electric fields. The use of MD simulation techniques can further be extended in exploring new applications of external static (or oscillating) electric fields such as explaining the effects of novel food processing techniques such as microwave, radiofrequency, pulsed electric fields and electro-hydrodynamic drying on the biochemical composition of food products.

CHAPTER 4: EFFECTS OF LOW POWER MICROWAVE RADIATION ON KINETICS OF L-LACTATE DEHYDROGENASE AND CATALASE ENZYMES

4.1 Introduction

In Chapter 3, the computational modelling approach, applied to understand the interaction between applied static and time-varying electric fields in the MWs range and selected Conotoxin protein at the nanoscale/ atomistic level, was presented in great details. In this chapter, the investigation into biological effects of MWs at the molecular level continues via experimental evaluation of particular MW exposures on the selected enzymes. This study was aimed to improve our understanding of the impact of low power MW radiation at the frequencies used in the 4G mobile networks on the kinetics of enzymatic reactions. L- Lactate dehydrogenase (LDH) and Catalase enzymes were selected as the model systems to evaluate the effects of MW at different frequencies and powers to understand further if the effects are frequency and power-dependent.

The selected enzymes play crucial roles in various biological processes occurring in a living system. For example, LDH is extensively present in blood cells and heart muscles and is a marker of common injuries and disease. Catalase enzyme can be found in all living organisms; it is essential for protecting a cell from oxidative damage by reactive oxygen species (ROS). The conducted *in vitro* study evaluated the effects of MW exposures at the frequencies of 1.8, 2.1, 2.3, and 2.6 GHz and powers -10dBm, 0dBm and 17dBm on the kinetics of LDH and Catalase enzymes irradiated using the commercial Transverse Electro-Magnetic (TEM) cell.

4.2 Experimental Evaluation *in vitro*

4.2.1 Transverse Electro-Magnetic (TEM) cell Exposure System

The commercial Transverse Electro-Magnetic (TEM) cell (No. TC-5062A UHF-TEM Cell) was used in this study to irradiate the selected enzymes. TEM cell is an enclosed box made of a conductor material, with its dimensions varied depending on the operating frequency used. One end of the box is connected to signal generator from which external signal was applied to generate a predictable field inside the TEM Cell. The absorption coefficients of the

analysed samples were measured using an Ocean Optics USB2000 spectrometer. All measurements performed using the TEM cell are very simple to perform and require minimum detection equipment, e.g. no additional antennas are required [159]. Figure 4.1 shows the experimental set up of the exposure system.

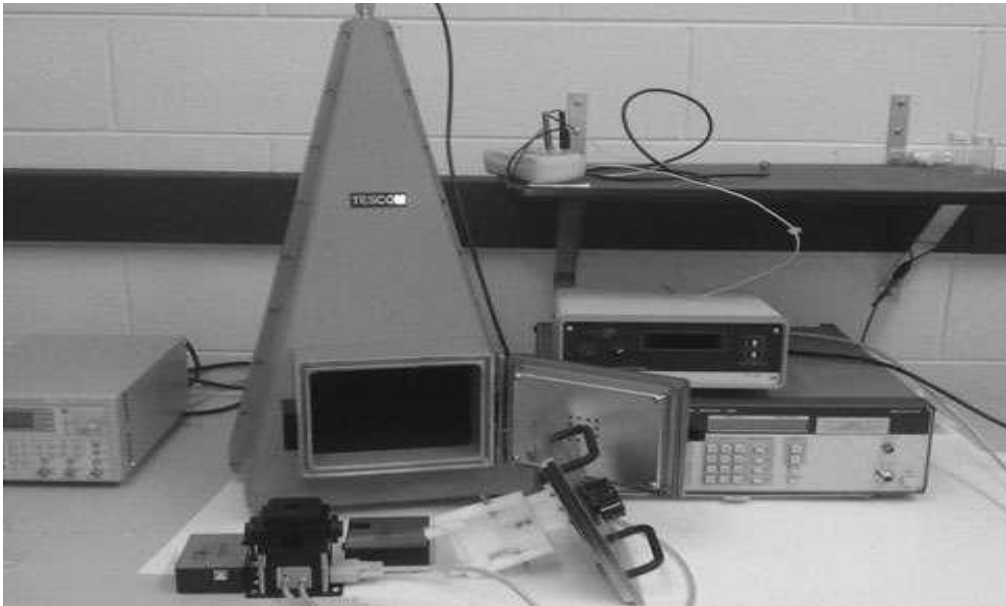


Figure 4.1: Experimental set up showing exposure camera, signal generator, controller, cuvette holder and spectrophotometer [20]

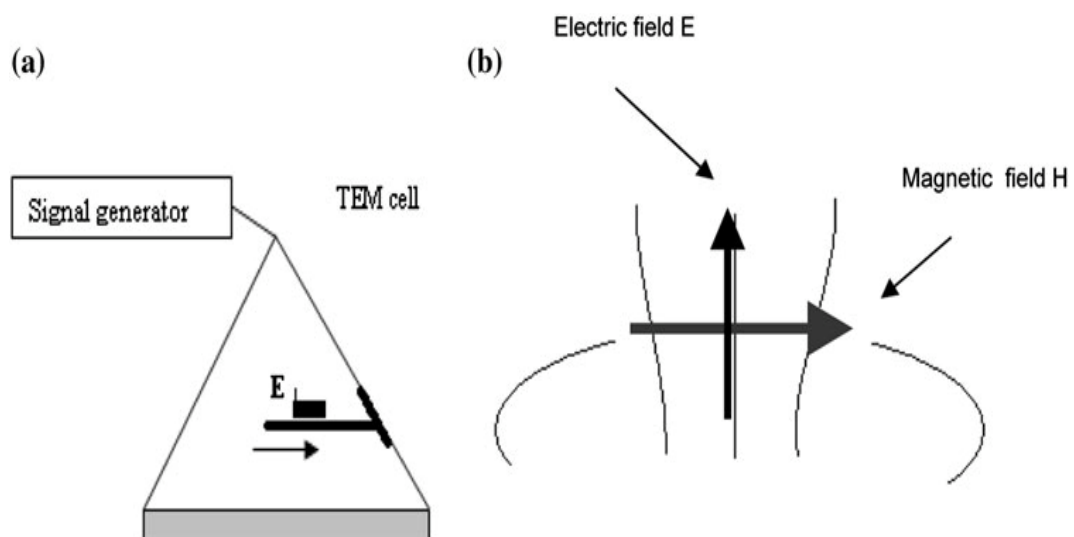


Figure 4.2: The position of the sample and the direction of the electric field inside the TEM cell; b. The vertical distance from the top of the cell to the sample is 22 cm. b Field pattern at the position of the sample (top view)[109]

A TC-5062AUHF TEM cell, operating range 100 kHz–3 GHz (TESCOM Ltd, Goyang, Korea) [20], was used to irradiate all model systems used to study in this project. A field, generated inside the TEM cell, was calibrated using a broadband electric field probe to determine the electric field produced at the sample position inside the camera for given input power (Figure 4.2). The calibration test showed the estimated uncertainty in the field is $\pm 1-3\%$, depending on the input signal frequency [88]. The RF voltage is applied to one port of the cell, while the other port is terminated with a 50Ω resistor, with a 50Ω characteristic impedance maintained along the cell.

The electrical field at the test point inside the TEM cell is calculated as follows:

$$E = \frac{\text{signal level [V]}}{\text{dis. from top [M]}} \quad \text{Equation 4.1}$$

The TC-5062 has a specific pyramidal geometry designed to extend the usable frequency range 100kHz – 3GHz [160]. Since the TEM cell produces the TEM waves, there is an orthogonal H-field (A/m) proportional to the E-field inside the TEM Cell. The relationship between the H- and E-fields is defined by the equation [161]:

$$H = \frac{E}{Z_{free}} \quad \text{Equation 4.2}$$

The electrical field inside the TEM cell can be calculated using the equation:

$$E = \frac{V}{L} \quad \text{Equation 4.3}$$

Where E is Electrical field in V/m,

$Z_{free} = 377\Omega$ represent free space wave impedance.

V is Voltage in [V]

L is the length of the camera in [m].

For the model TC-5062, the distance, L , between the top of the TEM cell and a sample holder is 0.22m [162]. The TEM cell is an accurate, broadband RF coupler with a high-quality shielding wall. The voltage standing wave ratio (VSWR) of the TEM cell was tested and

reported to have a maximal value of 1.7 for 3GHz. Therefore, the power propagating through the TEM cell can be calculated as follows [162]:

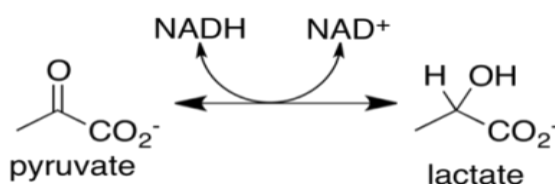
$$P_p = P_g \left(1 - \frac{VSWR - 1}{VSWR + 1}\right) \quad \text{Equation 4.4}$$

where P_p is the power propagating through the cell, and P_g is the generator power. For $VSWR = 1.7$, the ratio $P_p/P_g > 0.93$.

We used the signal generator Wiltron 68247B, operating range 10 MHz - 20 GHz. To measure changes in absorbance of studies samples, a spectrophotometer USB2000 (Ocean Optics) was used. The absorption coefficient was set at 600 nm. All experiments were conducted at 28°C, with the temperature being monitored continuously by a Temperature controller (Quantum Northwest) during experimentation.

4.2.2 Lactate dehydrogenase (LDH)

LDH enzyme plays a central role in metabolic pathways of almost every cell. It acts as a safety valve in our pipeline of energy production [163]. Our cells break down glucose completely and release carbon dioxide and water. This process requires a lot of oxygen. When the supply of oxygen is low and insufficient, however, the pipeline of energy production gets stopped up at the end of glycolysis. Lactate dehydrogenase is the way for cells to solve this problem. Lactate dehydrogenase catalyses the interconversion of pyruvate and lactate with concomitant interconversion of NADH and NAD⁺. It converts pyruvate, the final product of glycolysis, to lactate when oxygen is absent or in short supply and it performs the reverse reaction during the Cori cycle in the liver. At high concentrations of lactate, the enzyme exhibits feedback inhibition, and the rate of conversion of pyruvate to lactate is decreased. It also catalyses the dehydrogenation of 2-Hydroxybutyrate, but it is a much poorer substrate than lactate.



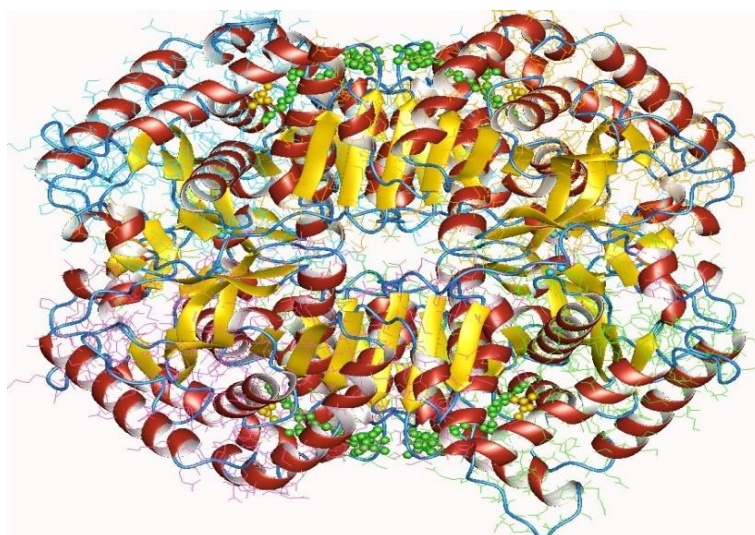


Figure 4.3: PDB structure of LDH M tetramer (LDH5) from human[164].

LDH catalyses the reversible reduction of Pyruvate to L-lactate using NADH as a co-enzyme. LDH activity is calculated from the rate of change in NADH absorbance at 340 nm. In this experiment, LDH enzyme was irradiated at frequencies of 2100 MHz, 2300 MHz and 2600 MHz at a power of 17 dBm and -10 dBm.

Measurement Procedure for LDH

In this sub-study, LDH [EC1.1.1.27] enzyme solutions were prepared according to the LDH enzyme Assay (Worthington Biochemical Corporation). Tris HCl, 0.2 M, pH 7.3, 2.8 ml + 6.6 mM NADH, 0.1 ml + 30 mM Sodium Pyruvate were mixed, and a final aliquot was prepared for each of the test and control samples. Amount of 0.1 ml of LDH solution was added to the cuvettes (external dimensions are h=50mm; d=25mm, V=20ml). The activity of LDH enzyme was measured by calculating a rate of change of absorption of enzyme substrate solution at 340nm, and immediately after the cuvettes was transferred to TEM cell for irradiation. Five repeats the same sample were irradiated inside TEM. An additional sample (pyruvate and same buffer but without LDH enzyme) was also exposed to MW radiation. As controls, we used five non-irradiated samples with enzyme and one without enzyme. The control samples were kept under the same experimental condition.

After irradiation, the cuvettes were removed from the TEM cell, and the absorbance was measured again at 340 nm. The spectrophotometer was set to record the absorbance at every 2 s. This procedure was repeated for both irradiated and control samples after every 5 minutes. The temperature was maintained at 25⁰C using Temperature Controller (Quantum Northwest, Inc.) shown in Figure 4.1.

4.2.3 Catalase enzyme

Catalase is found in almost all living organisms. Catalase (EC 1.11.1.6) is a very important enzyme, which helps to protect the cell from oxidative damage by reactive oxygen species, hence protect us from dangerous oxidizing molecules. Catalase helps to catalyze the decomposition of hydrogen peroxide into water and oxygen. Catalase activity is calculated by measuring a total amount of H₂O₂ decomposed to form O₂. The reaction catalysed by Catalase enzyme is comparatively different from other enzymes as the rate of decomposition of H₂O₂ is proportional to the amount of Catalase present. Unlike other enzymatic reaction, Catalase undergoes spontaneous decomposition during the reaction.

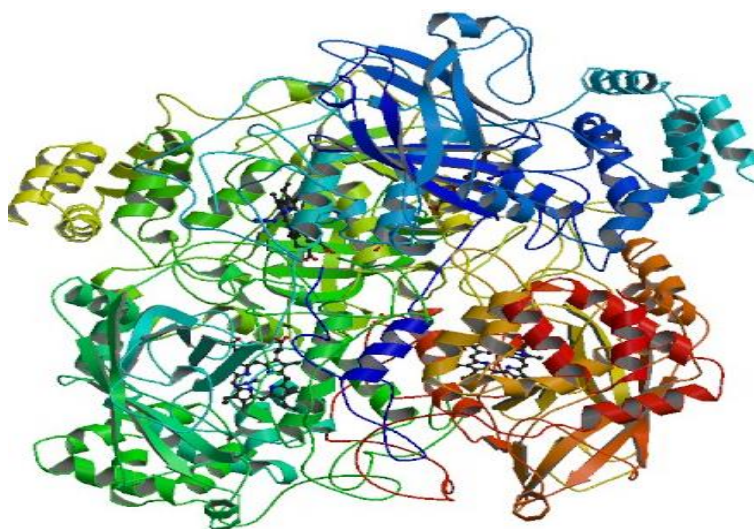
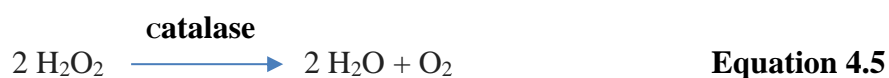


Figure 4.4: PDB structure of catalase from *Saccharomyces cerevisiae*[165].

Catalase can also accelerate the oxidation, by hydrogen peroxide, of various metabolites and toxins, including formaldehyde, formic acid, acetaldehyde and alcohols. It does so according to the following reaction:



Measurement Procedure for Catalase Reagents

A standard assay for Catalase (Sigma-Aldrich) was used to analyse the changes in the reaction catalysed by Catalase enzyme. Catalase [EC 1.11.1.6] was selected as a model system. Potassium phosphate, dibasic (Catalog Number P5504), Hydrogen Peroxide Solution (Catalog Number H1009) and Lyophilized powder of Catalase (Bovine) were purchased from Sigma-Aldrich. Phosphate buffer (50mM Potassium Phosphate Buffer, pH 7.0 at 25±C) was prepared

in ultrapure ionized water using potassium phosphate, dibasic, trihydrate (Catalog Number P5504). Hydrogen peroxide solution (0.036% (w/w)) was prepared in Phosphate buffer using Hydrogen peroxide (30% (w/w), catalogue number H1009). An initial Catalase solution of 10 mg/ml was prepared and immediately before use; it was diluted to 100 units/ml in cold Phosphate buffer. 1.45 ml of Hydrogen peroxide solution was pipetted into the test cuvettes, and 500 µl of previously prepared Catalase solution was added to the cuvette.

In this experiment, three Catalase enzyme samples were irradiated continuously for 5min, and the other three control Catalase samples were kept for the same time period under the standard conditions. The absorbance of each sample, i.e. three exposed and three non-exposed (control) samples were measured in the time interval of 30 seconds for 5 minutes.

The activity of Catalase was measured using a spectrophotometer, and the absorption coefficient values were recorded at 240nm before and after the MW irradiation. Absorption coefficients of Catalase enzyme were measured using Ocean Optics USB2000 spectrometer. Immediately after the recording of absorption coefficients, the cuvettes were placed inside the TEM cell for irradiation. The same procedure was repeated after 2 min, 7 minutes and 9 minutes and measurements were recorded. During the experiment, the temperature was maintained at 25 C° (as presented above).

In order to determine the rate of reaction, the dissociation constant of hydrogen peroxide, K , was calculated using the following formula:

$$K = \frac{1}{t} \log \left(\frac{A}{A-x} \right) \quad \text{Equation 4.6}$$

where t is the time interval of the second reading, A is the amount H_2O_2 absorbed at the end of reaction and x is the H_2O_2 absorbed at the time of the second reading.

In this experiment, Catalase enzyme solutions were exposed at the frequencies of 1800 MHz and 2100 MHz at powers of -10 dBm, 0 dBm and 17 dBm.

4.3 Results and Discussion

The experimental evaluation of changes in catalytic activities of LDH and Catalase enzymes, exposed to MW of different frequencies and powers, was conducted and the changes in the rate of absorption (rate of reaction) of irradiated samples were compared with the

absorption coefficient values of non-irradiated samples in order to understand the effects induced by applied MW exposures.

4.3.1 Changes in LDH Enzyme Catalytic Activity

Relative change in the rate of reaction of NADH was evaluated and compared to control samples (non-irradiated) LDH at the frequencies of 2100 MHz, 2300 MHz and 2600 MHz at powers of 17 dBm and -10 dBm.

Figure 4.5 shows the modulating effects of irradiation on LDH enzyme. Consistent decrease in the rate of reaction at 17 dBm was observed: a 21% increase at 2100 MHz and almost 50% decrease at 2600 MHz in comparison with the control samples. Further, at the power of (-) 10dBm under similar experimental conditions, a steep change in the rate of reaction was observed. At -10dBm and 2100 MHz reaction rate was increased by 75% and at 2600 MHz it decreased by 35% when compared to the control samples. Important to note, in both cases, the relative changes induce by exposures at -10dBm, and 2300 MHz are not significant. At 2600 MHz and power 17dBm the change in the rate of reaction was 25% compared to sample exposed to MW at (-) 10 dBm power. This suggests that MW at 17dBm adversely affect the enzymatic rate of reaction of LDH.

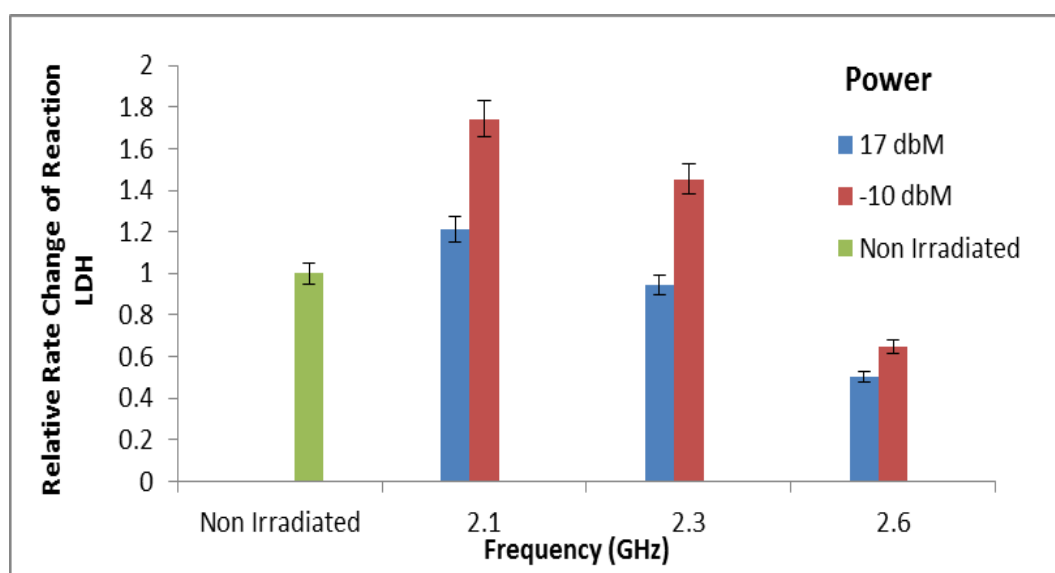


Figure 4.5: Relative change in the rate of reaction of NADH for irradiated vs non-irradiated LDH at different frequencies and powers

4.3.2 Changes in Catalase Enzyme

The experimental evaluation of catalytic activities in selected Catalase enzyme exposed to MW of different power and frequency range was conducted. The changes in the rate of absorption (rate of reaction) of irradiated samples were compared with non-irradiated samples. Test samples were exposed to MW at 2100 MHz, 2300 MHz and 2600 MHz and different powers. The objective of the experiments was to understand the modulating effects of MW at a different combination of frequency and power and to further evaluate the power-dependency of enzymatic reaction rate at the particular frequency of MW

The results are presented in Figures 4.6 and 4.7. Figure 4.6 shows a consistent modulating effect of irradiation on the dissociation constant, K , of H_2O_2 . At 17dBm 20% increase at 2100 MHz exposure and a 25% decrease at 2600 MHz exposure is recorded. At the power of -10dBm, the relative change in K value is inconsistent. As can be seen from Figure 4.6, at 2100 MHz and 2300 MHz relative change in K was increased by 20% as compared to non-irradiated sample, but at 2600 MHz it is reduced by 22%. However, exposure at 2100 MHz for both power levels induces maximum increase on the dissociation constant, K . At 2600 MHz and powers 17 and (-) 10dBm, a consistent 25% decrease in activity was observed.

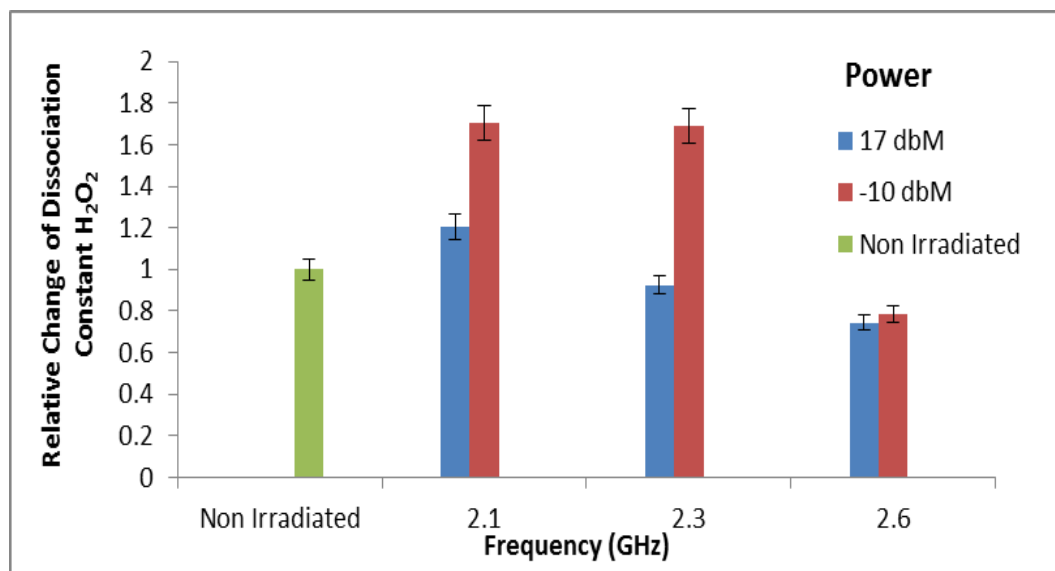


Figure 4.6: Relative change of Dissociation constant of H_2O_2 for irradiated vs non-irradiated Catalase samples at the frequencies of 2.1 GHz, 2.3 GHz, and 2.6 GHz at 17 dBm and -10 dBm

Modulating effects at 2600 MHz were further analysed by exposing Catalase enzyme test samples at 2600 MHz and different powers of 0 dBm, -20 dBm -30 dBm, -40 dBm and -50 dBm to elucidate power-dependence effect at the particular frequency. The effects induced

by exposures at 2600 MHz were studied because 2600 MHz is a carrier frequency for many telecom systems. The dissociation constant, K , was calculated using the same methodology as described above. The results are presented in Figures 4. 7.

An interesting pattern is observed in the relative change of dissociation constant (K) of H_2O_2 for irradiated vs non-irradiated samples. At 2600 MHz and 0 dBm power, the K value of the exposed sample was 32% higher than of non-irradiated sample. For -20dBm the increase of almost 20% is recorded. For -30dBm, an increase of 9% in K value is observed.

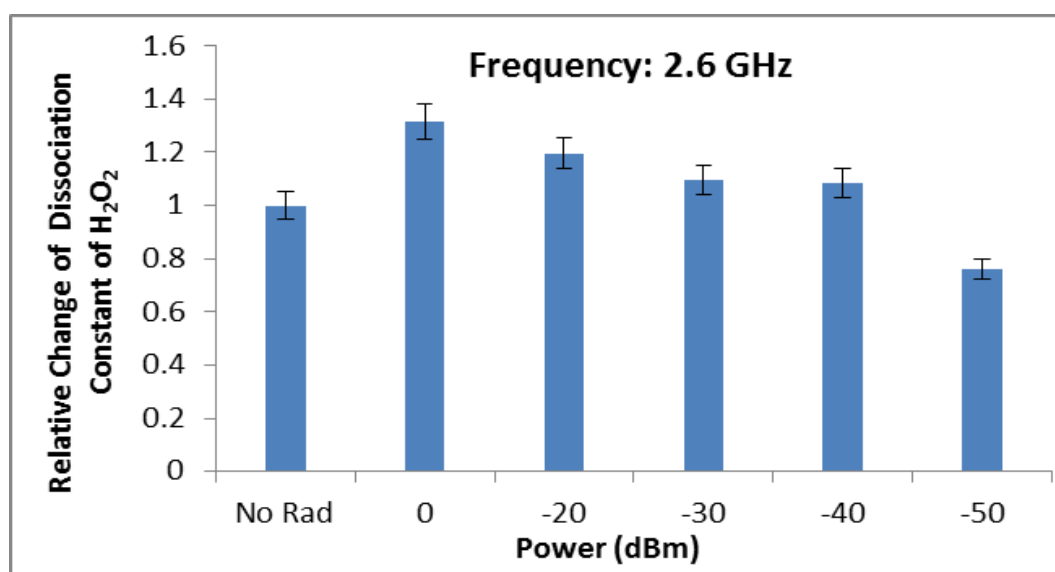


Figure 4.7: Relative change of dissociation constant of H_2O_2 for irradiated vs non-irradiated Catalase at 2600 MHz and five different powers of 0 dBm, -20 dBm, -30, -40, and -50 dBm

The less significant increase is observed for -40dBm. However, for -50 dBm, K was decreased by 25% compared to the non-irradiated sample. These findings confirmed our hypothesis that enzymatic activities could be changed by external exposures at low power MW irradiation, with the observed effects being power and frequency-dependent.

Figures 4.8 and 4.9 show the relative change in absorbance of Catalase enzyme samples irradiated by applied MWs for 5 min. At 1800 MHz/ -10dBm, the initial change in absorbance of Catalase was almost 30% compared to the non-irradiated sample. However, it increased steadily for the first 90 sec of irradiation and then became relatively consistent (92% - 97%) in comparison to non-irradiated sample (100%). At 1800 MHz/ 0dBm, a small relative increase (6% to 7%) in the absorbance during the first 30 sec of exposure compared to the non-irradiated sample was observed. Moreover, at 1800 MHz/ 17dBm the relative change in absorbance compared to the non-irradiated sample was negligible. Hence, the results imply that enzyme

kinetics of Catalase is not affected by MW at the frequency of 1800MHz and powers of 0 dBm and 17dBm.

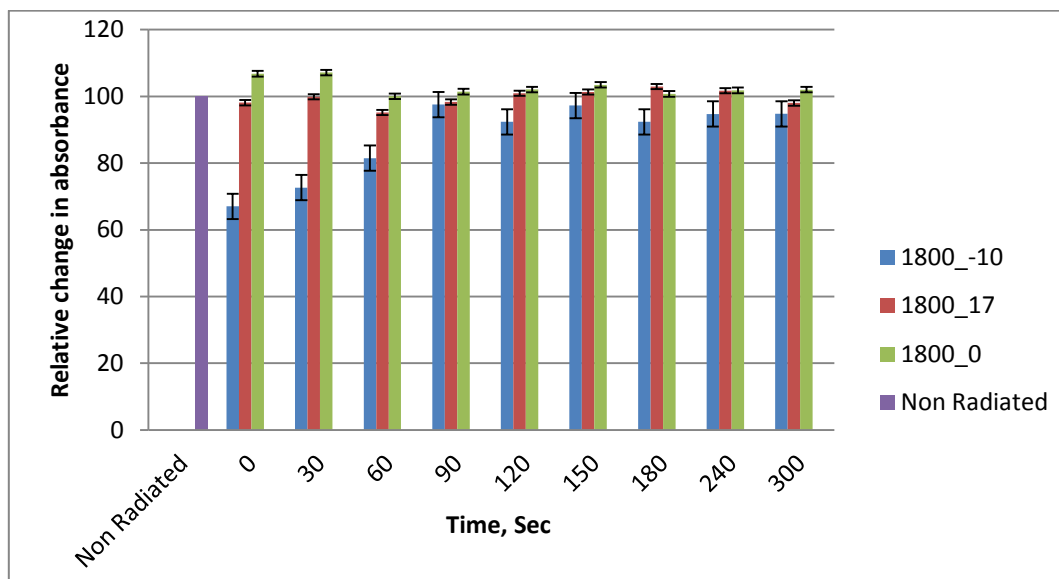


Figure 4.8: Relative change in absorption at 1800 MHz and power of 0, -10 and 17 dBm

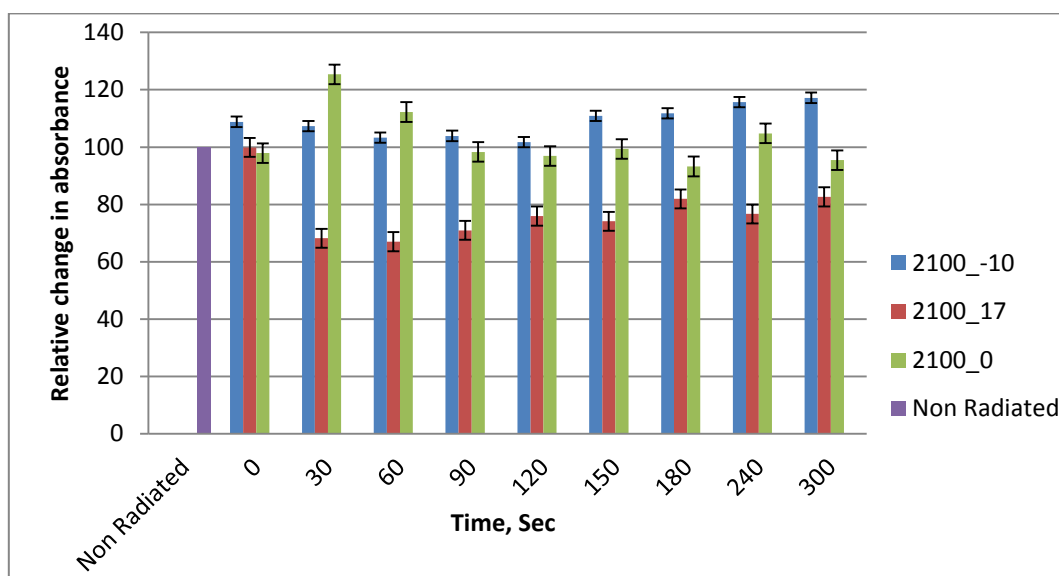


Figure 4.9: Relative change in absorption at 2100 MHz and power of 0, -10 and 17 dBm

The maximum effect of MW exposures on absorbance was observed when Catalase samples were irradiated at 2100 MHz and different powers. At 17 dBm the relative absorbance compared to the non-irradiated sample was decreased by more than 30% in the first 30 sec of reaction and remained at 80% for an entire reaction time of 300 sec. This indicates inhibitory effects of MW at 2100 MHz/ 17 dBm on enzyme kinetics of Catalase.

When Catalase samples were exposed to MW at 2100 MHz/ (-)10 dBm, an increase in

relative absorbance (compared to control sample) was observed for the reaction time of 300 seconds. At 2100 MHz/ 0 dBm, a sudden increase in absorbance was observed during the first 30 sec of exposure, and then the absorbance started to decrease and mostly stabilized as the reaction progresses. *This does not give any conclusive evidence in support of change in enzyme kinetics at 2100 MHz/ 0 dBm.* Figures 4.10 and 4.11 show the changes in absorbance of Catalase in time under MW exposures at the selected frequencies and powers. The results clearly show that the selected frequency and power induce significant effects on Catalase's absorbance, thus affecting the rate of reaction during the experiment. At the frequency 1800 MHz/ (-)10 dBm, we can see the apparent relative increase in absorbance of Catalase (the concentration of oxygen is maximum) compared to non-irradiated samples, especially during 120-180 sec of reaction.

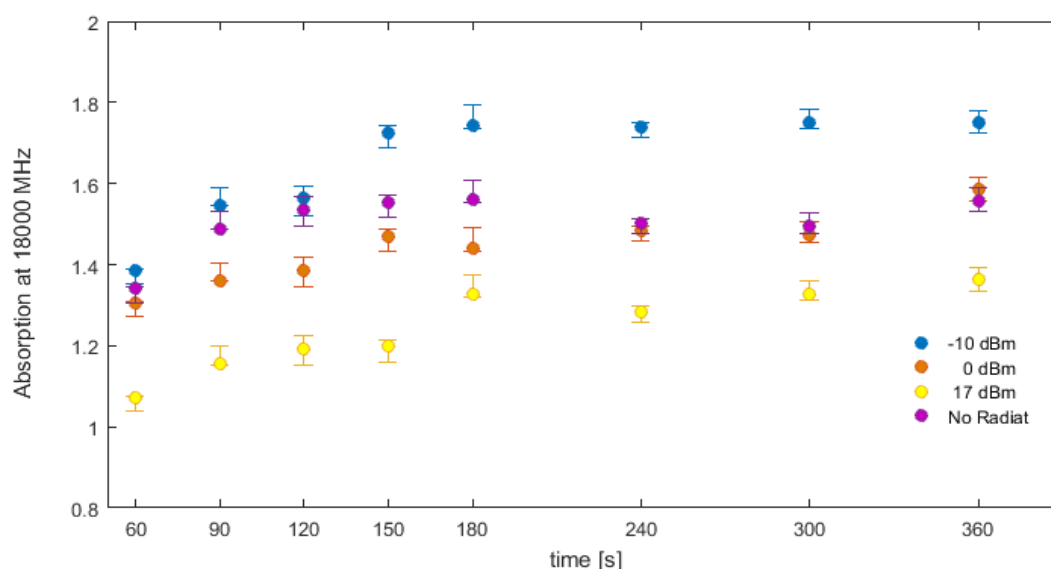


Figure 4.10: Changes in the absorption of Catalase at 1800 MHz and power of -10 dBm, 0 dBm and 17 dBm compared with Control (Non-irradiated) sample

MW exposures at the frequency 1800MHz and power 17 dBm reduces the absorbance of Catalase, which remains consistently low when compared to a non-irradiated sample. This implies that these particular exposure parameters induce the inhibitory effects on Catalase enzyme. However, at the frequency 1800MHz and power 0 dBm, no significant change in absorbance was observed.

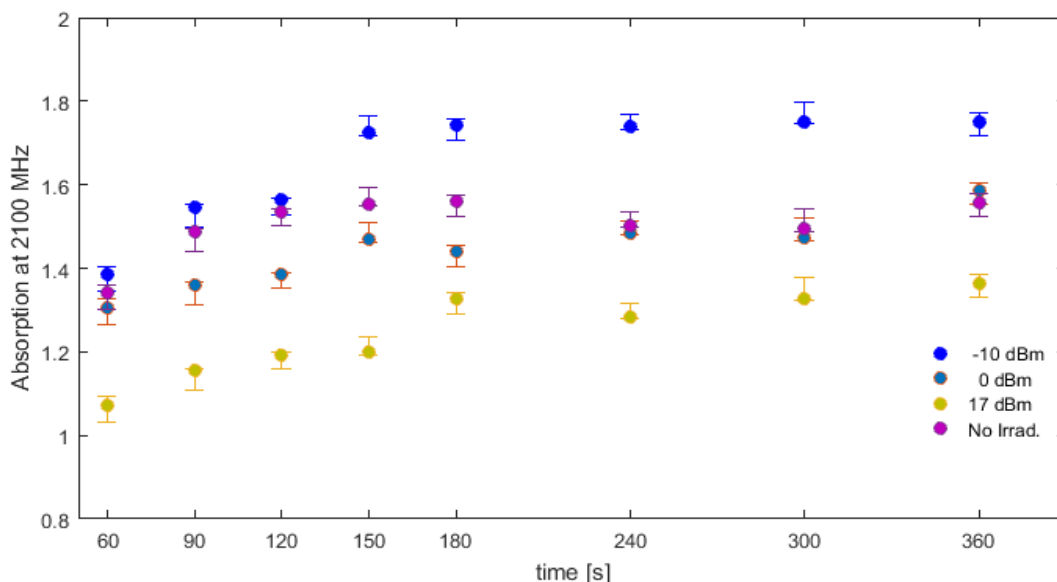


Figure 4.11: Changes in the absorption of Catalase at 2100 MHz and power of -10 dBm, 0 dBm and 17 dBm compared with control (non-irradiated) samples.

Interestingly, the consistent and similar results were observed in Catalase for MW exposures at the frequency 2100 MHz (Figure 4.11) and three selected powers. At 2100 MHz/ (-) 10dBm the increase in Catalase absorbance was evident. However, the significant decrease in absorbance (minimum concentration of oxygen) was recorded upon MW exposures at 2100 MHz/ 17 dBm. Exposure at 2100 MHz/ 0dBm induced no significant change in absorbance (oxygen concentration) when compared to non-irradiate sample. These findings indicate that MW irradiation at the selected frequencies and powers produce modulating effects on the dissociation constant of Catalase.

4.4 Concluding Remarks

In the previously reported study using L-Lactate dehydrogenase (LDH) and Glutathione Peroxidase enzymes [109], the effects of frequencies 1800 MHz, 2100 MHz and 2300 MHz and power of 10 dBm were evaluated on the selected enzyme reactions. The findings of this work reveal that MWs at the studied parameters induce changes in the enzyme's kinetics which lead to modulation of the rate of change in corresponding reactions these enzymes catalysed. The presented study was aimed to test further the hypothesis that the external low power MW radiation can affect the catalytic activity of LDH and Catalase enzymes by expanding the range of exposure parameters, especially the powers to investigate if the observed are effects are power-dependent. The results obtained and discussed above suggest that the *applied MW radiation at selected frequencies of 1800 MHz, 2100 MHz and 2300 MHz at a power of (-)10*

dBm can produce modulating effects on the catalytic activity of LDH and Catalase enzymes by either increasing or decreasing the reaction rates.

The study using LDH assay, was aimed to test the hypothesis that the external low power MW radiation can affect catalytic activity of LDH enzyme at frequencies of 2100 MHz, 2300 MHz and 2600 MHz at power of 17 dBm and -10 dBm can produce modulating effects on the catalytic activity of LDH by either increasing or decreasing the rate of reaction.

Kinetics of Catalase was studied under the MW exposures at the frequencies of 2100 MHz and 1800 MHz, and powers of 0dBm, -10dBm and 17dBm. The most significant effects were observed at 2100 MHz and powers of -10 dBm, 0 dBm and 17 dBm. The inhibitory and excitatory actions observed at the frequency of 2100 MHz indicate the dependence of chemical reaction on power and frequency of MW exposure. At 1800 MHz and different powers, no significant modulating effects were observed.

The results of the experiments suggest that both frequency and power parameters contribute separately to produce modulating effects on the catalytic activity of the selected enzyme. The experimental findings highlight the finding that even at low powers MW can induce modulating effects at the frequencies used in 4G mobile phone networks. However, it requires further detailed investigation on a wide range of combinations of frequency and power to establish safe limits of MW exposures.

CHAPTER 5: EFFECTS OF MICROWAVES AT 1800MHZ AND DIFFERENT LOW POWERS ON YEAST CELLS

5.1 Introduction

In Chapter 4, the author studied the effects of the selected frequencies and powers on the kinetics of LDH and Catalase enzymes. In this Chapter, the author was interested in studying whether microwave radiation affects the growth rate of *Saccharomyces cerevisiae* cells and their morphology. Initially, the effects of applied microwave exposures (6 h of irradiation) on yeast cells were studied using spectrophotometry. The obtained results showed that at the particular frequency and powers the rate of yeast cells growth was affected [27] [88]. To evaluate the dependence of yeast cell growth rate on MW exposures frequency and power, statistical analysis (Chi-square test of independence) was performed. The results showed that the MW radiation parameters (frequency and power) contribute independently to the observed modulating effects on yeast cell growth.

Furthermore, the effects of MW radiation at 1800 MHz and three powers, -10 dBm, 0 dBm and 17 dBm on the growth rate and morphology of *Saccharomyces cerevisiae* cells were investigated using TEM. TEM images showed structural disruptions in the exposed yeast samples. A significant increase in total cell count and changes in cell viability were observed at the powers of 0 dBm and -10 dBm respectively. However, corresponding changes in morphology and increased formation of budding cells were observed in samples exposed at -10 dBm and 17 dBm. The findings suggest that low power MW radiation can induce modulating effects on yeast cell growth and affect their internal structural organisation.

5.2 Experiments and Analysis

5.2.1 Model System: Yeast

Micro-organisms are the most accessible and most convenient objects to study the effects of various types of stress factors. Among different model organisms the yeast, *Saccharomyces cerevisiae*, is of most importance. Yeast type II (Sigma) was selected as the model system in this study. It is well documented that yeast cells are representative of eukaryotes, including human cells, in many aspects of fundamental cellular processes [166] [87]. The budding yeast,

Saccharomyces cerevisiae was selected as a model organism to study the effects of electromagnetic radiation (EMR) and conduct experiments under controlled conditions [167].

5.2.2 Yeast Growth Phases

As with most micro-organisms, when a yeast inoculum is added to a rich nutrient broth and allowed to grow under favourable conditions, there are three main growth phases (Fig. 1) [166]. Initially, cells enter into the lag Phase in which they are biochemically active, but conditioning themselves to the new surroundings, often coming from a limited nutrient environment into a rich one. During this phase, cells are actively metabolizing in order to prepare themselves for the cell division. The second phase of yeast growth is an exponential growth phase, in which cells divide exponentially resulting in the increase in the total cell count in a culture medium. The third phase of yeast cells growth is a stationary phase, in which the cells stop cell division; this condition is reached due to changes in the environmental condition caused by high cell density, such as a lack of a critical nutrient or the build-up of toxins.

In this study, we compared the normal exponential growth phase of yeast cells (control) with that of yeast cells irradiated by MW at the selected frequencies and powers. [166]. *Saccharomyces cerevisiae* type II (YSC2-Sigma) was selected on the basis of its fast growth rate (~120 min doubling time).

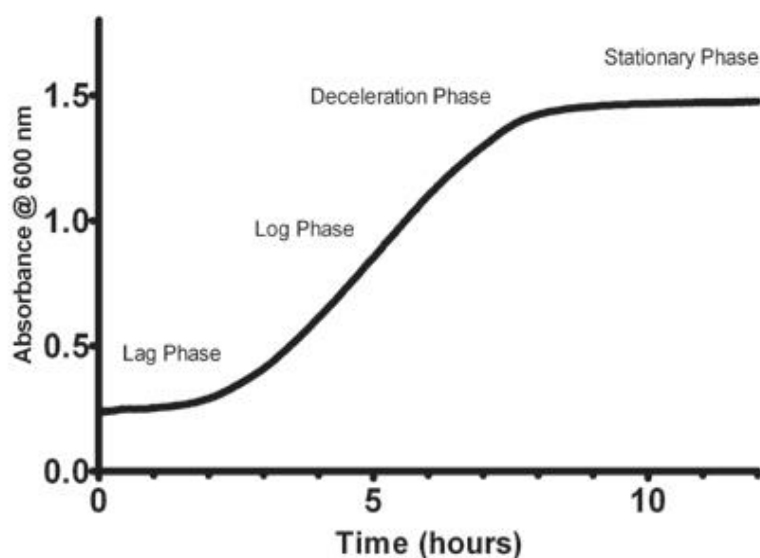


Figure 5.1: Typical Yeast Growth Curve of *Saccharomyces* [87]

5.2.3 Microwaves Exposure Parameters

Specific absorption rate (**SAR**) is a measure of the rate at which energy is absorbed by the human body when exposed to a radio frequency (RF) electromagnetic field. The SAR values of the MW exposures used in this study (Table 5.1) were below and above the standard safety limit, SAR of 2.0 W/kg, which is based on the International Commission on Non-Ionizing Radiation Protection (ICNIRP) limit. The safety limit for exposure to mobile phone emissions is set by determining the lowest level of exposure known to cause health hazards and then adding a safety margin. Our previous research using photo spectroscopy assessment showed that low power MW exposures (frequencies used in 3G and 4G networks) induce modulating effects on the studied biological models [27].

Table 5.1. Exposure System and Sample Preparation for Spectrophotometric Analysis

Power, dBm	Power density, mW/cm²	Electric field, V/m	SAR
-10	0.00121	2	0.0078
0	0.01210	6	0.0700
17	0.606	47	4.314

In order to measure the absorption coefficients of the yeast cell sample solution, an Ocean Optics USB2000 spectrometer was used. The exposure system consists of Transverse Electro-Magnetic (TEM) TC-5062AUHF cell (100 kHz–3 GHz) from TESCOM Ltd, and the signal generator (Wiltron 68247B), operating range 10 MHz to 20 GHz [160]. The exposure system is discussed in details in Chapter 4. The wavelength for measurement of absorption was set at 600 nm; a value commonly used to measure absorbance due to scattering and the molecular absorption of radiation, as a function of frequency. *S. cerevisiae* yeast powder was purchased from Sigma (Australia). The solution for the experiment was prepared as follows: 50 g/l of YPD broth (Sigma, Australia); 20 g/l of *S. cerevisiae* yeast and ionized water. The solution was incubated at 37°C for 48 h with shaking at 608 ppm. The yeast samples were prepared by diluting the experimental solution 100-fold using ionized water. The yeast samples were placed in 2 ml cuvettes for measuring the total transmittance. In this experiment, three replicates yeast cultures were irradiated for 6 hours, while another three control yeast cultures were kept for the same period without irradiation. The absorbance of each (3 exposed and 3 non-exposed) sample was measured every hour for 6 hours. Cell growth was monitored by spectrophotometric analysis using OD₆₀₀. All experiments were conducted at 28°C.

5.2.5 Yeast cell sample preparation for TEM

Samples for TEM assessment were prepared from yeast irradiated at -10 dBm and 17 dBm (the lowest and highest power values used in this study). Samples were centrifuged in a PCR tube to obtain concentrated cell pellets. The cells were suspended in fixative overnight. Cell pellets were washed with Karnovsky's fixative in 2% paraformaldehyde +2.5% Glutaraldehyde in 0.1 M Cacodylate buffer. The cells were then rinsed thrice in 0.1 M Cacodylate buffer. Following rinsing, the cells were post-fixed at room temperature in post-fixative solution [168]. The cells were then washed thrice with distilled water. After washing, the samples were dehydrated with increasing ethanol gradients from 50 to 90% followed by 100% ethanol for 30 mins. Following ethanol dehydration, the samples were completely dehydrated in acetone and infiltrated with 1:1, 1:2, 2:1 and 100% acetone: Spurr's resin mixture [169]; the samples were placed in the oven at 70°C for polymerization. Ultrathin sections (90 nm thicknesses) were cut with a diamond knife using an ultramicrotome (Leica Microsystems, Wetzlar, Germany). The sections were observed at 80 kV with a Jeol Jem 1010 (Japan) Transmission Electron Microscope (TEM), and images were examined using the Gatan Microscopy Suite software, version 2.3.

5.2.6 Cell Count and Viability

Total cells were determined hourly using a BioRad automated cell counter (TC20 automated cell counter) over 6 hours. Cell counts and viability of control samples and test samples were assessed immediately after the simultaneous exposure. Three technical replicates were taken to confirm the consistency of the test conditions and to identify any discrepancy/error during the experiment. Cell viability was determined using the equation:

$$\text{Viability [\%]} = \frac{(\text{total counted cells} - \text{total counted dead cells}) \times 100}{\text{total counted cells}} \quad \text{Equation 5.1}$$

5.2.7 Fluorescence Microscopy

Fluorescence-based (NIS-AR-version 4) apoptosis was determined by using Propidium Iodide (PI) staining method. Yeast cells (0.5 ml) were placed in 24-well plates at 28°C. Cells were washed separately with PBS and treated with PI (10 µg/ml). Cells were observed under a fluorescence microscope using a red dye filter, and images were taken.

Image Analysis

Image analysis was performed using *ImageJ software* (Version 1.45) [170]. Cell morphology was studied through analysis of area, circularity and elongation in selected live cells in control and test (irradiated) samples. Yeast morphological data was captured by thresholding. A description of a self-developed image analysis procedure for *S. cerevisiae* morphology evaluation is presented in [170]. Cells were selected manually to minimise the noise, and the images were focused on enhancing the cell counters. Figure 2a shows an initial microscope image and Figure 2b shows processed final image reflecting the improvement in image quality for further analysis. The images were focused on enhancing cell contours (Fig 2a). Morphological operations such as erosion (noise removal) and reconstruction produced the final image, which was used to study the morphological changes (Fig 2b).

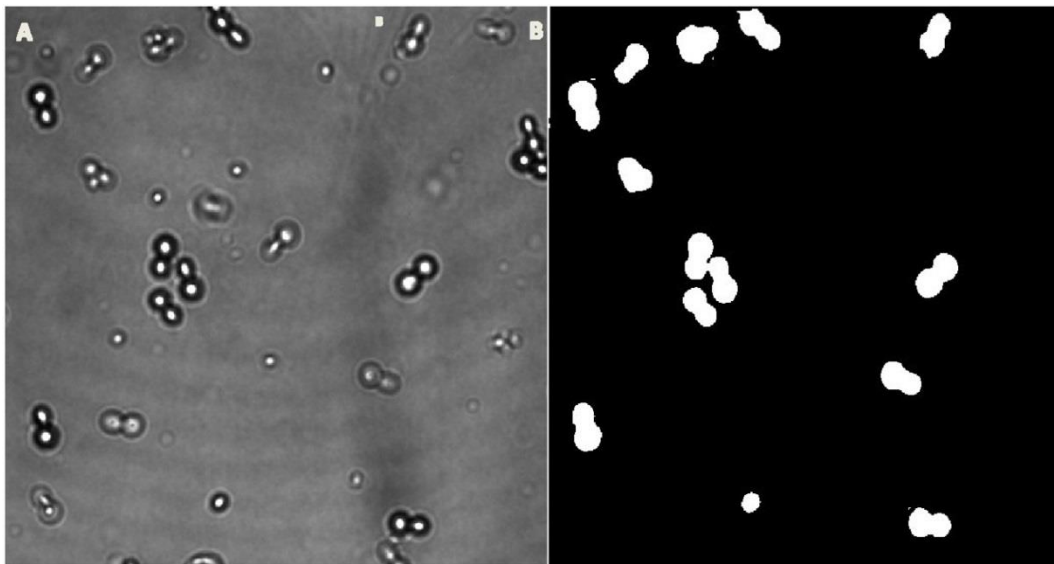


Figure 5.2 A) Initial image from the microscope B) Final image generated by ImageJ software

Yeast Cell Circularity

Circularity or isoperimetric quotient is a common shape factor. A measure of cell circularity is related to the compactness of a cell. It is determined as a function of the perimeter, P, and the area, A [171]

$$F_{circ} = \frac{4\pi A}{P^2} \qquad \text{Equation 5.2}$$

Cell circularity and elongation data were collected using image analysis techniques as described above and TEM.

Yeast Cell Elongation

Cell elongation is defined as the ratio between the major axis length and the minor axis length. Image analysis determines the cell size distribution at selected powers, thus allowing determining if the observed effects are power-dependent.

5.3 Results and Discussion

5.3.1 Spectrophotometric Analysis of Yeast Samples

Yeast cells were exposed to MWs at 1800 MHz and 2100 MHz and powers of -10 dBm, 0 dBm and 17 dBm. The cell growth of exposed yeast cells was observed for the period of 6 h and compared with a control group of non-irradiated (NR) yeast samples under the standard experimental conditions. The results are presented below.

Optical Density (OD) and Cell Viability

The experimental results show that OD₆₀₀ of all test samples increased throughout the course of the experiment except the 5th hour of exposure for the test sample exposed at 1800 MHz and -10 dBm (Fig. 3). However, at the 6th hour of exposure, cell count normalised and was almost equal to the total cell count, which indicates recovery of the irradiated cells. OD₆₀₀ measured at the exposure of 1800 MHz, and 0 dBm also showed the increase in the last 2 h of irradiation. At 1800 MHz and 17 dBm, the irradiated samples showed constant low OD₆₀₀ values, suggesting an inhibitory effect of the treatment.

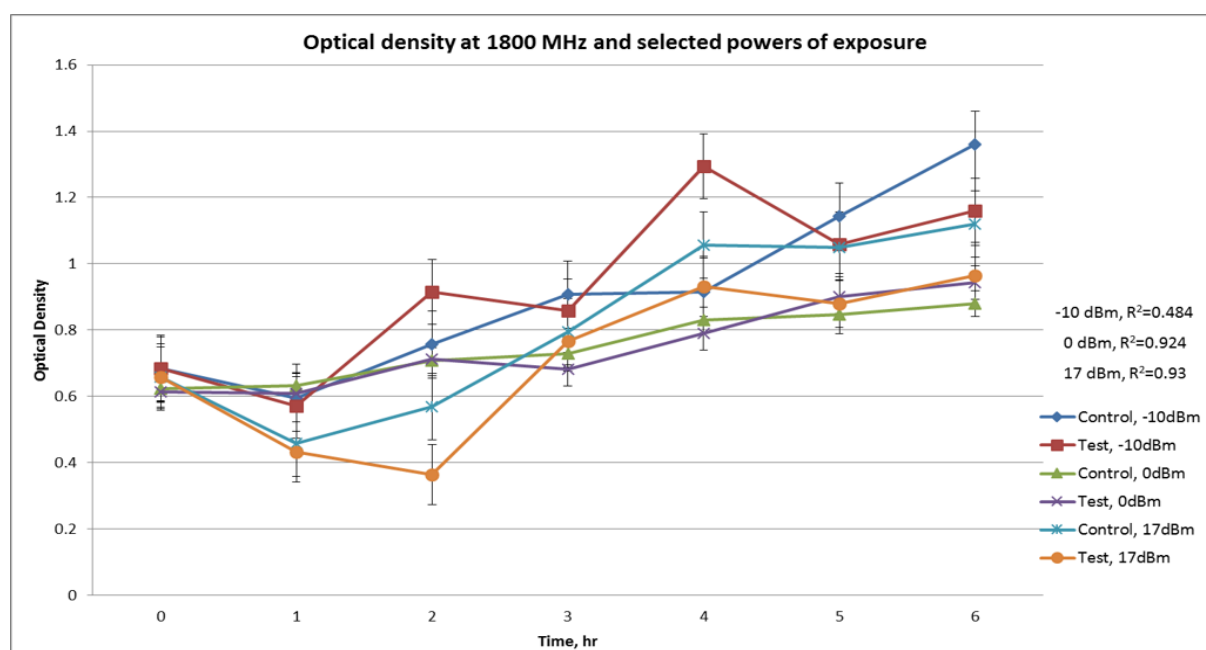


Figure Error! No text of specified style in document.3: OD₆₀₀ of control and a test sample of yeast cells irradiated at 1800MHz and selected power of 0, -10 and 17 dBm

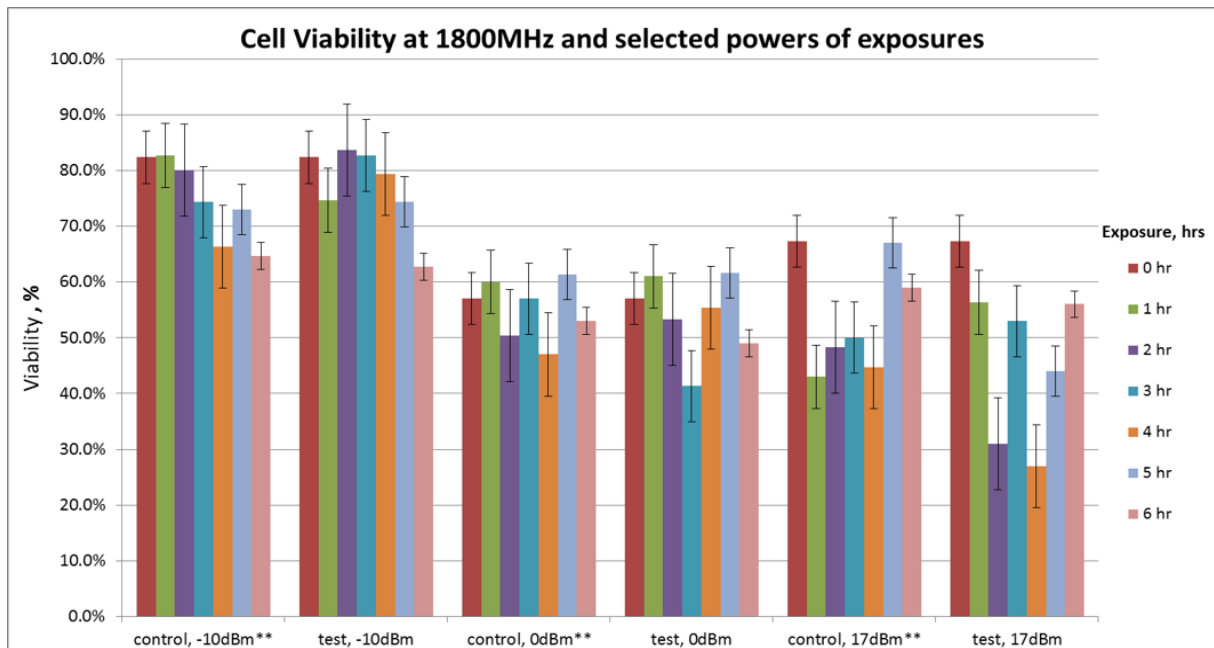


Figure 5.4: Cell viability of control yeast vs test yeast samples irradiated at 1800MHz and powers -10, 0, and 17 dBm

As shown in Figure 5.4, the cell viability of each set of control samples consistently showed a maximum increase of up to 15% in the 5th hour followed by 10% decrease in the 6th of yeast growth. The viability of control samples was over 50% but the average viability of samples exposed at -10dBm was 75%, at 0 dBm it reduces down to 55% and at 17dBm - viability is reduced further down to 45%. The decrease in cell viability of the exposed yeast samples with the increased powers of irradiation indicates an inhibitory effect of the applied exposure. The decrease in cell viability of test samples exposed at 1800 MHz and -10 dBm, after an initial increase (Figure 5.4), suggests possible DNA damage, which has been previously reported [5]. TEM images show that yeast cells lost their internal organisation after being exposed continuously at 1800 MHz and -10 dBm for 6 h. Also, cell wall disruption can be clearly seen in TEM images (Figure 5b-5d). MW exposures have also affected budding of new cells.

Cell viability of the control and test samples, exposed at 1800 MHz and 0 dBm, follows almost the same pattern except for the 3rd hour of the yeast growth (statistically insignificant effects). Hence, we suggest that MW exposure at 1800 MHz and 0 dBm has a negligible effect on yeast growth rate. As can be observed from Figure 2, as opposed to 0 dBm exposure, the irradiation at 1800 MHz and 17 dBm clearly affects yeast cell viability; the viability of exposed yeast cells decreases in the 2nd and 4th hours of irradiation and then increases in the 5th and 6th hour from 27% up to 56%. These results imply that MWs at 1800 MHz and 17 dBm induce

modulating effects in yeast cells ranging from inhibiting to proliferating (the last 2 h of the yeast growth).

Yeast Cell Growth Rate and Absorbance

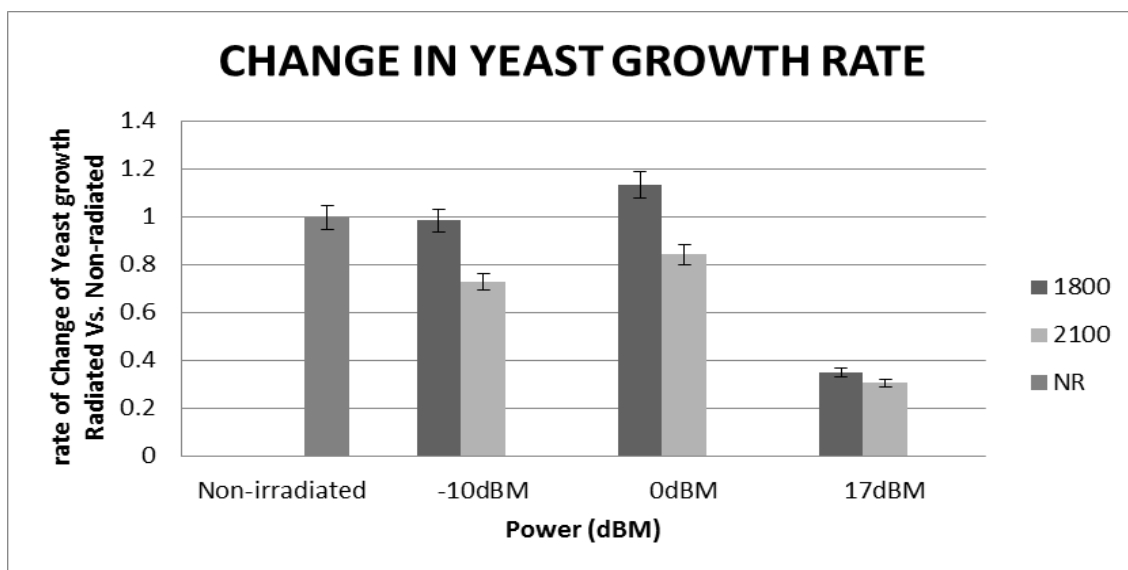


Figure 5.5: Change in yeast cells growth under MW exposures at the different frequency, and power

Figure 5.5 shows that in comparison with the control group of non-irradiated yeast cells (100%), the MW exposures at the frequencies 1800 MHz and 2100 MHz induce changes in yeast cell growth/proliferation. A consistent decrease in the rate of cell growth was observed at all combinations of frequency and power except at 1800 MHz and a power of 0 dBm, where an 13.5% increase in cell growth was observed. At 17 dBm the maximum decrease in yeast growth was observed (64% for 1800 MHz and 69% for 2100 MHz).

Absorption vs time curve (Fig. 5.6 and 5.7) was plotted to understand the changes in absorption coefficients of the irradiated vs non-irradiated yeast samples. The Figure 5.6 indicates that frequency and power have a significant influence on the absorption pattern, thus affecting the growth of the yeast cell during the experiment. At 1800 MHz/ 17 dBm, the rate of cell growth is maximum when compared to non-irradiated samples (Fig.5.4). Interestingly, more significant modulating effects were observed at 2100 MHz. As shown in Figure 5.5 and 5.7, at the 4th and 5th hours of irradiation at 2100 MHz and 0 dBm, a sudden decrease in absorbance is observed. A possible explanation for this change is cell death. At the power of -10 dBm, the cells initially show exponential growth and then stop growing towards the 4th hour of irradiation. Similarly, at the power of 17 dBm, yeast cells initially show the increased

cell growth, but during the 5th hour of irradiation, there is a sudden dip in their absorbance indicating the cells death. The absorbance vs time growth curve shows that there is a small effect on the growth of *S. cerevisiae* cells at the frequency of 1800 MHz at the corresponding powers of 17, 0, and -10 dBm. A significant modulation in the growth curve was observed at the frequency 2100 MHz and the selected powers of -10, 0, and 17 dBm (Fig. 5.7).

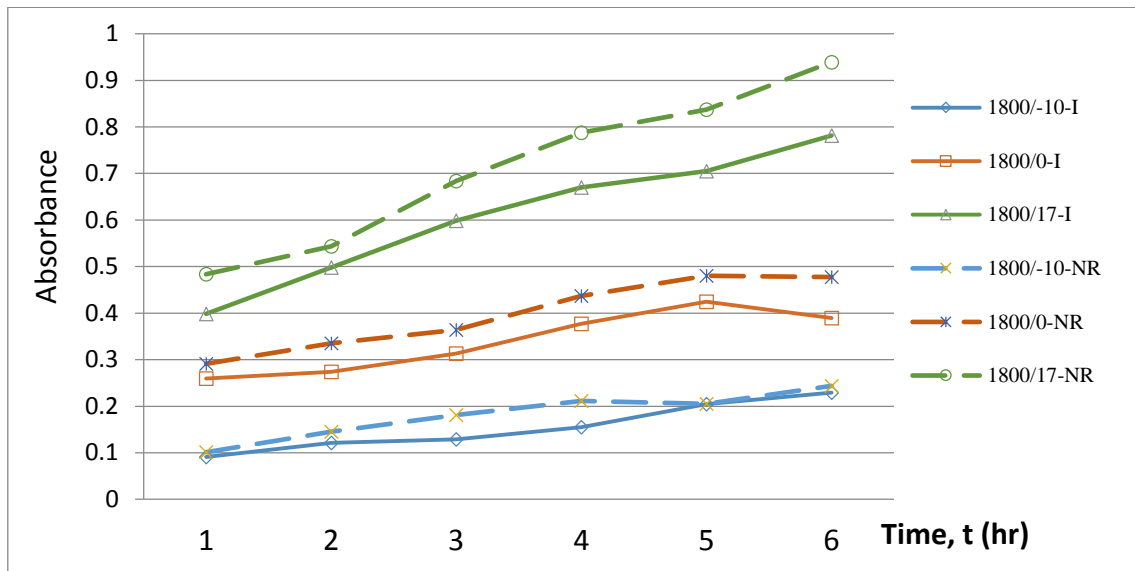


Figure 5.6: Changes in absorbance of yeast cells exposed to different frequencies of 1800 MHz and powers of 17 dBm, 0 dBm and -10 dBm.

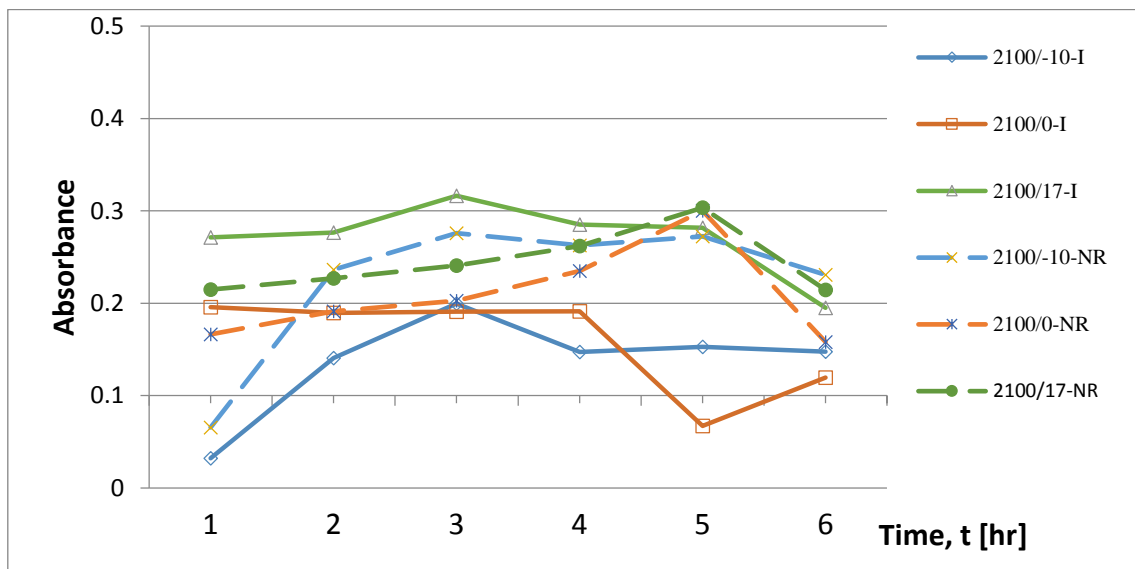


Figure 5.7: Changes in absorbance of yeast cells exposed to different frequencies of 2100 MHz and powers of 17 dBm, 0 dBm and -10 dBm. I : Irradiated samples, and NR :Non-irradiated

Figure 5.8 and 5.9 shows the relative change (%) in the concentration of yeast cells irradiated for 6 hours. At 1800 MHz and 10 dBm a change in concentration was observed, especially during the last two hours of irradiation when it increased from 70% to 100%. However, at 17 dBm, the relative change in concentration remained almost consistent.

Maximum effects of MW on cell growth were observed when the samples were irradiated at 2100 MHz and different powers. Especially at 0 dBm, the relative change was over 150% for the first hour, and it remained high compared to the relative changes at -10 dBm and 17 dBm. At the power of -10 dBm, the consistent increase in the concentration of yeast cells was observed for the first 3 hours of irradiation, which attained the study state in the following hours.

Similarly, with the frequency of 2100 MHz and power 17 dBm shown in figure 5.7 the consistent decrease in cell concentration was observed for almost 4 hours with the inhibitory effect in the 5th hour, followed by cell recovery during the last hour of irradiation. These results provide further evidence of cell death during the 5th hour of exposure. It is worth mentioning here that at 17 dBm the maximum inhibitory effects were observed at the frequency 2100 MHz.

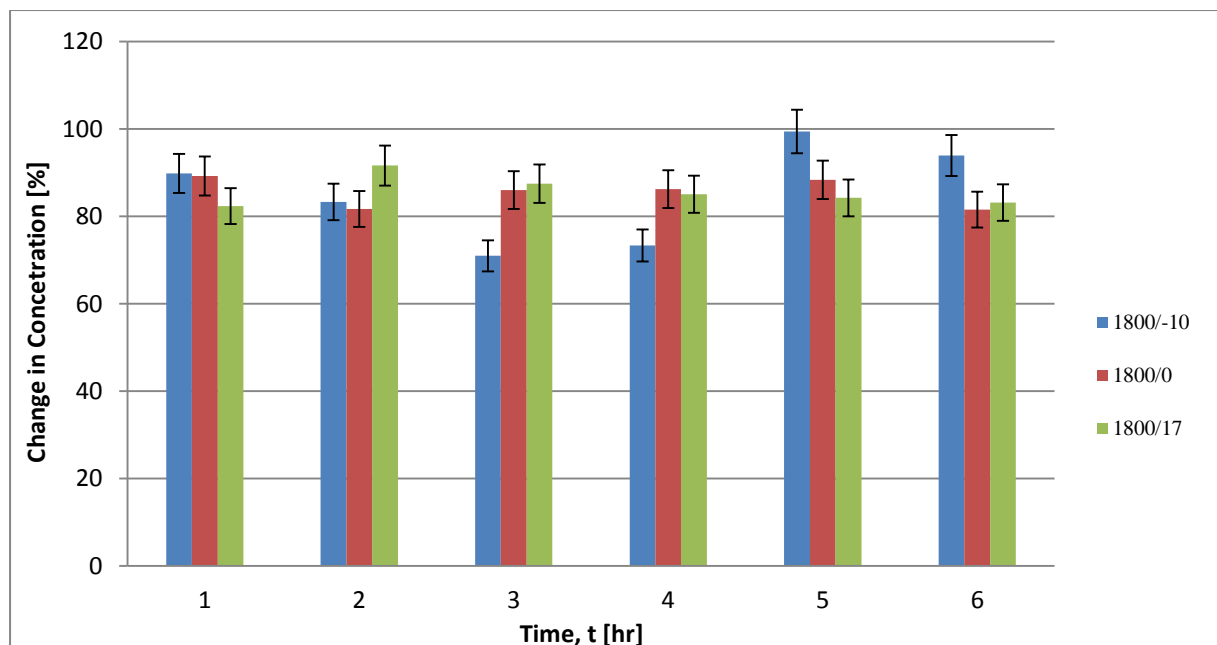


Figure 5.8: Change in concentration of yeast over the period of 6 hours; irradiated vs non-irradiated samples (%)

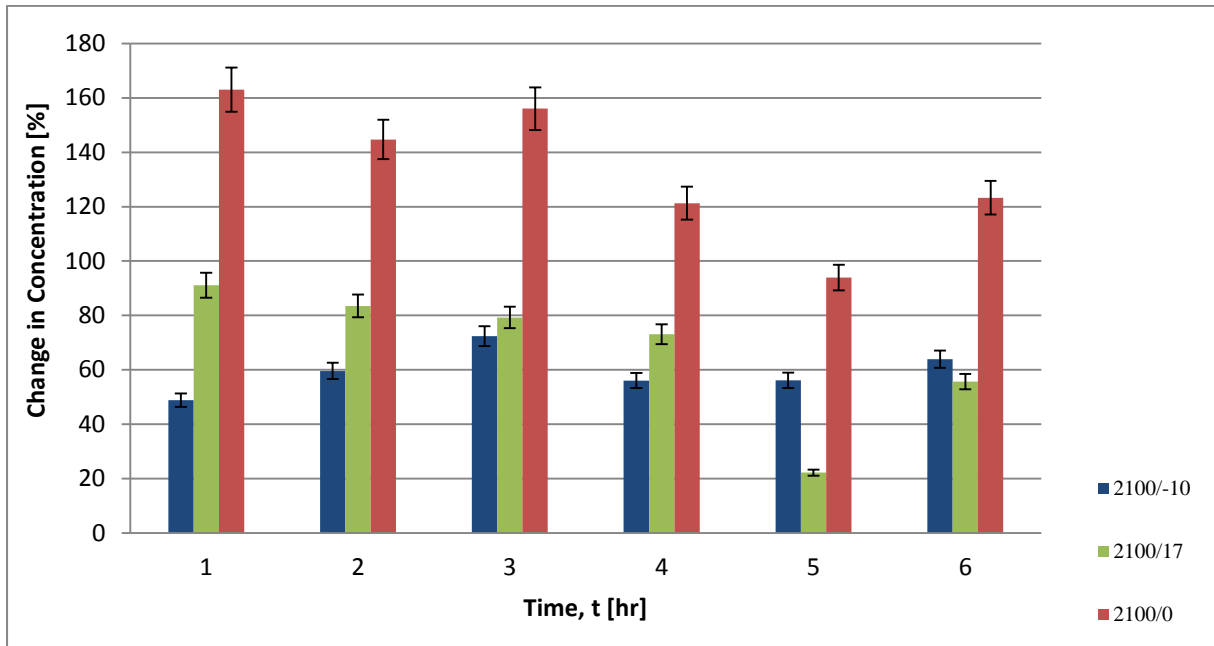


Figure 5.9: Change in concentration of yeast over the period of 6 hours; irradiated vs non-irradiated samples (%)

Chi-square test of independence (refer to Table 5.2) is usually applied to determine if there is a significant relationship between the variables used in the study. Chi-square test was performed here to evaluate the null hypothesis (H_0): whether two variable parameters, i.e. frequency and power, are inducing modulating effects (proliferating or inhibiting) on the rate of yeast cell growth in the independent manner. In the Chi-square test, if $p > 0.05$ (the probability of error is less than 5%), we accept the H_0 . The calculated p -value ($p=0.0577$) is higher than the significance level (O.OS), which supports our null hypothesis. Thus, we conclude that the frequency and power of the MW exposures independently affect the growth rate of the studied yeast samples.

Table 5.2: Chi-square test results

	-10 dBm	0 dBm	17 dBm	Non-Radiated
1800 MHz	0.383235	1.7644	0.316775	0.099276
2100 MHz	0.468297	2.156586	0.387187	0.121342

5.3.2 Image analysis of Yeast Cells

Cell morphology is intimately correlated with the ability of cells to perform a normal biochemical function. Yeast cell circularity and elongation were analysed to observe the

changes when exposed under different microwave exposure conditions. In this instance, image analysis was only performed on samples irradiated at 1800 MHz and the lowest, -10 dBm, and highest, 17 dBm, powers. The data from morphological analysis of three control and three test samples taken from the final 3 hours of the yeast growth phase were analysed.

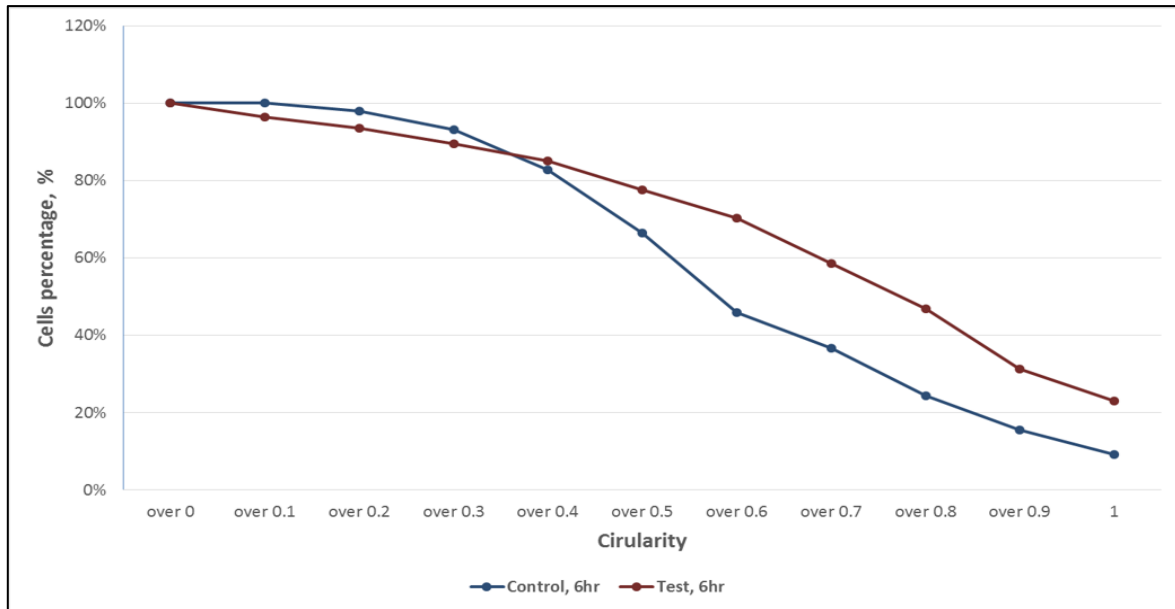


Figure 5.10: Effect of irradiation at 1800MHz and -10dBm on the circularity of yeast sample at the end of 6th hour of the growth phase

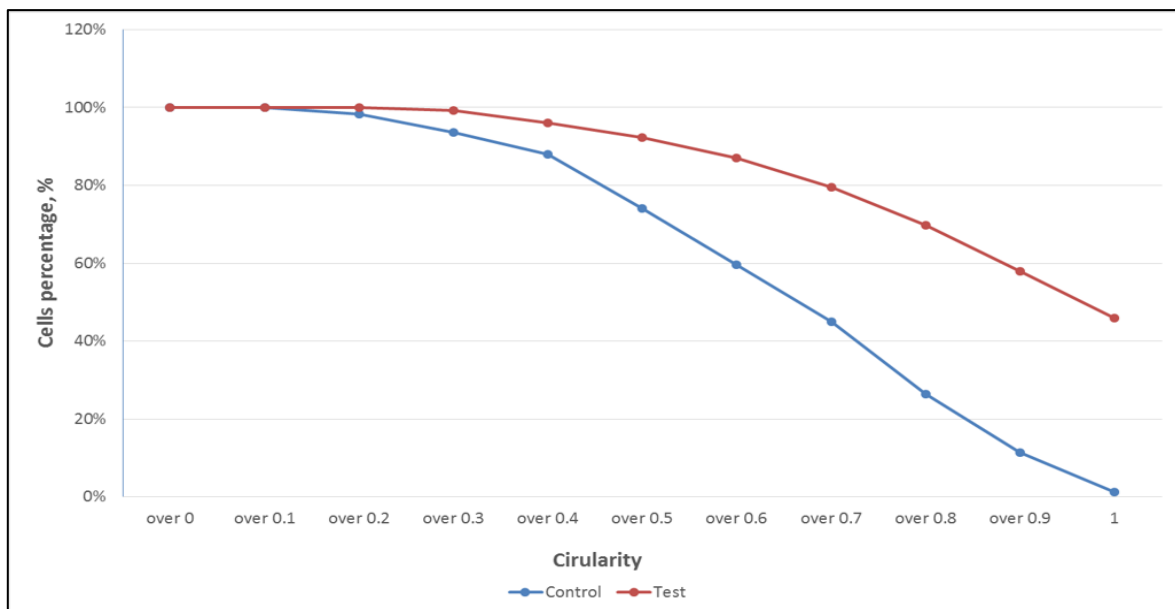


Figure 5.11: Effect of irradiation at 1800 MHz and 17dBm on the circularity of yeast sample at the end of 5th hour of the growth phase

Cell circularity represents a growth of the cell from a bud to cell division. Usually, new bud cells have a circularity of 1. Reduced circularity suggests that the cell is preparing for division [170]. Figure 10 shows circularity at the end of the 6th hour of the growth phase for control and test yeast cell samples exposed to microwaves at 1800 MHz and -10 dBm. Exposed yeast samples show a reduction in the change of circularity over the cell growth phase in the 6th hour of incubation. At the end of the 6th hour, only 45% of cells in the control sample has circularity over 0.6, whereas 71% cells in the test sample have circularity over 0.6.

These results suggest an inhibitory effect of the exposure on yeast cells growth. This may occur as a result of cell damage that can also lead to a decrease in the cell viability. The effects of irradiation at 1800 MHz and 17 dBm on the circularity of yeast cells is presented in Figure 11. As can be seen, 80% of the exposed cells have circularity over 0.7 during the 5th hour of incubation, whereas only 45% of cells in the control sample have circularity over 0.7. Also, only 7.5% of test samples have circularity between 0-0.5 at the end of the 5th hour. This result suggests the promotion of early cell proliferation due to the exposure at 17 dBm and explains the observed increase in cell viability in the final 2 hr of the yeast cells growth.

An average elongation factor of 1.5 for *S. cerevisiae* ATCC 32167 was used to discriminate bud cells from single cells [170]. Other authors have suggested an average elongation factor of 1.5 for single cells, including both non-budding and also budding mother cells, whose bud is not large enough to create a second sub-element [172]. Here, the same approach was used for analysis of the significance of the effects of three powers (-10, 0, 17 dBm) at the frequency of 1800 MHz on yeast cell division.

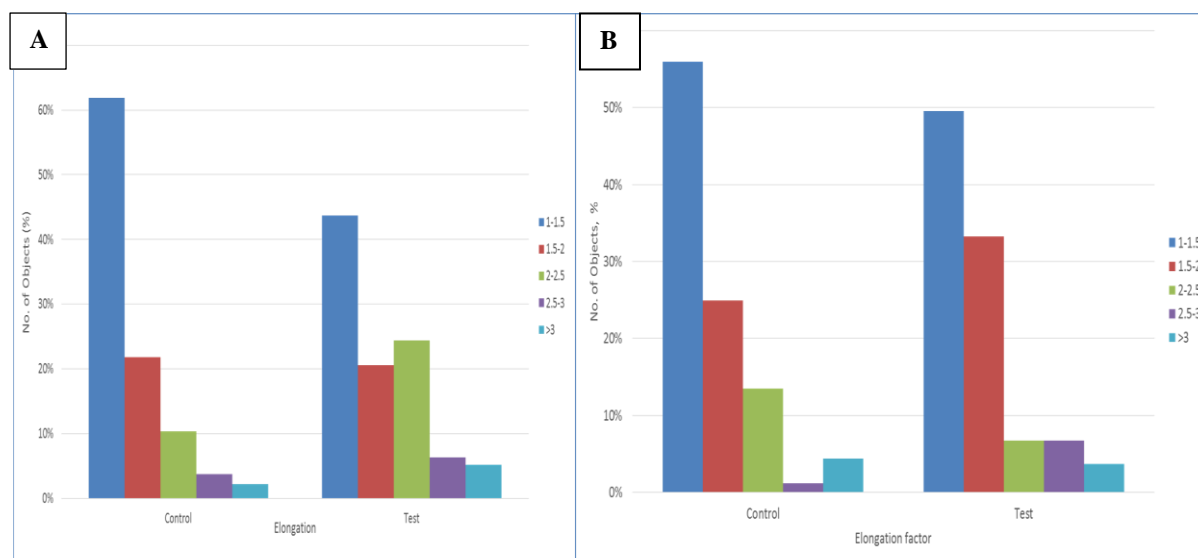


Figure 5.12: Elongation factor distribution among the irradiated vs non-irradiated yeast sample at the end of 6th hour of growth phase: [a] irradiated at 1800MHz and -10dBm; and [b] irradiated at 1800MHz and 17dBm

Figure 12a shows cell elongation of *S. cerevisiae* exposed at -10 dBm. The results suggest that by the end of the 6th hour of yeast growth, only 43% of cells in the test sample have elongation factor less than 1.5, while 25% of cells have elongation factors between 2 and 2.5, indicative of an increased number of budding cells. When compared with the control sample, exposed samples exhibited 30% more cells having elongation factor above 2. This confirms our observation of the cell recovery, as well as the inhibitory effect of exposure at 1800 MHz and -10 dBm. This finding highlights a phenomenon observed in yeast cell growth phase when they were exposed at 1800 MHz and the lowest power of -10 dBm – *the initial inhibition of yeast cell growth was followed by the cell recovery towards the end of yeast cells growth phase.*

Figure 12b shows the effects of 6 h exposure at 1800 MHz and 17 dBm on the percentage of *S. cerevisiae* having elongation factor between 1-1.5 and 1.5-2 cells respectively. Around 50% of cells irradiated at the highest power of 17 dBm have elongation factor above 1.5. That can further be correlated with the increased viability of exposed samples at 17dBm as discussed above.

5.3.3 TEM study of Yeast cells

TEM was used to see the changes in the internal organisation of yeast cells in control and irradiated test samples. The TEM images of control and test samples are shown in Figure 12. In control samples, cells were spherical or oval, with the majority of observed cells being in a budding phase. Their internal structure was intact, and no changes in the internal cellular organisation were observed, whereas the significant disruption in yeast cells was observed in the exposed samples (Figure 13).

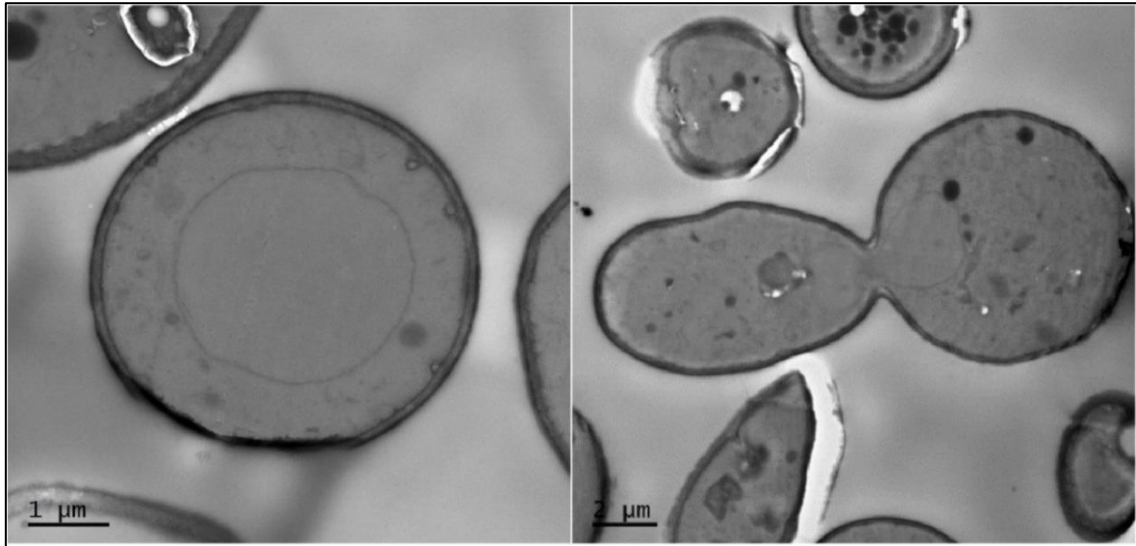


Figure 5.13: Transmission Electron Microscope (TEM) images of control yeast samples (unexposed after 6 hours) with a well-organised nucleus and cell membrane.

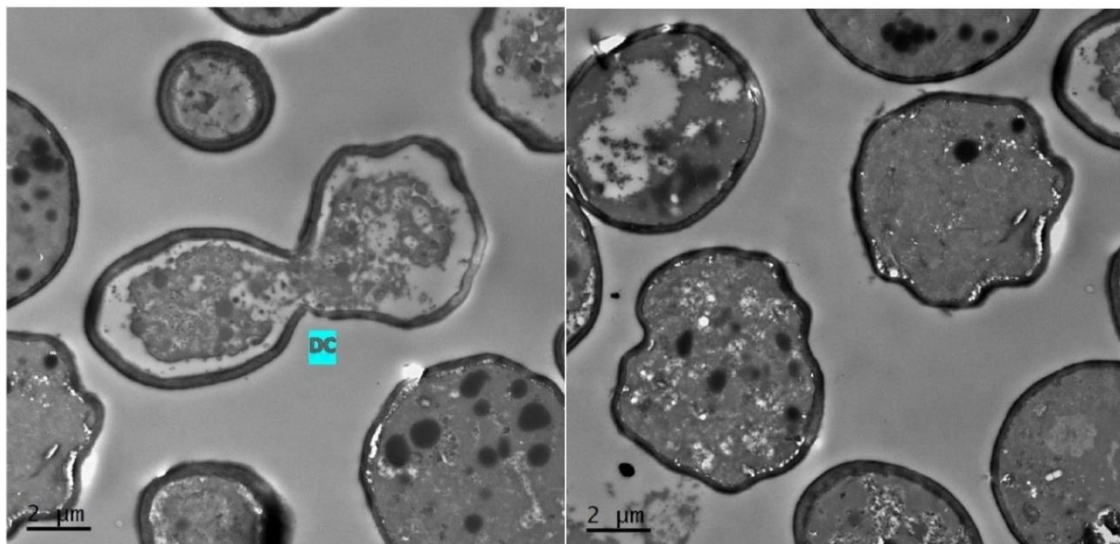


Figure 5.14: Transmission Electron Microscope (TEM) images of yeast cells irradiated at 1800 MHz at -10 dBm showing dividing cells (DC) after exposure and other cells.

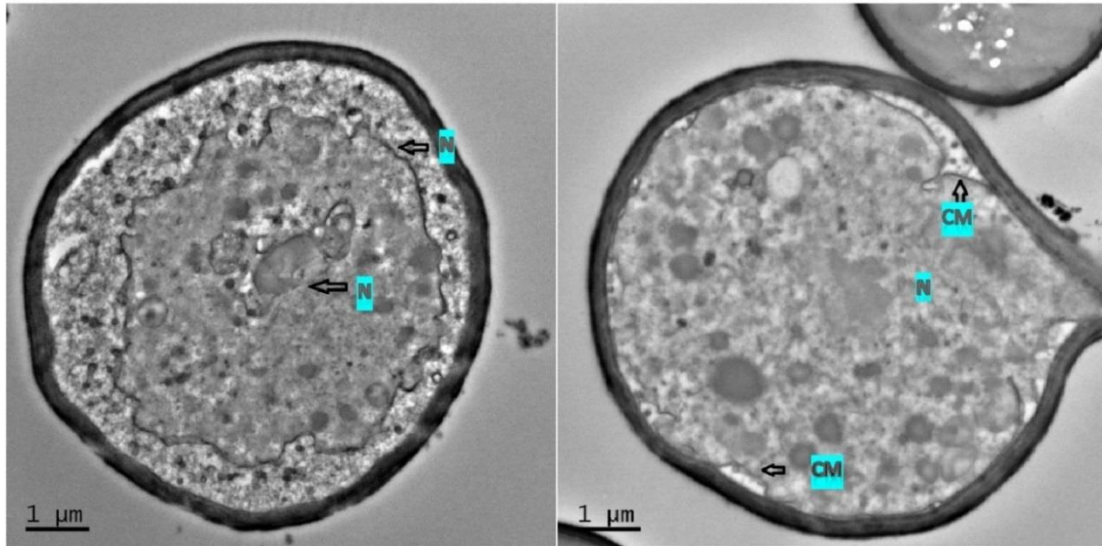


Figure 5.15: Transmission Electron Microscope (TEM) images of yeast cells irradiated at 1800 at 0 dBm. Loss of cell membrane (CM) and diffused nucleus(N)

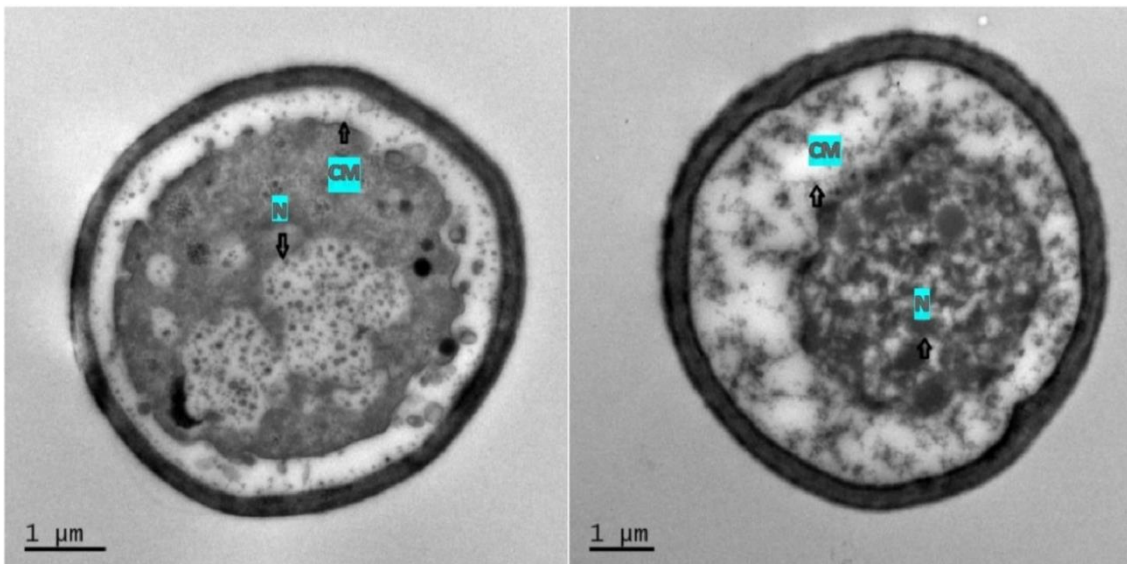


Figure 5.16: Transmission Electron Microscope (TEM) images of yeast cells irradiated at 1800 at 17 dBm. Arrows are showing affected nucleus (N) and cell membrane (CM) after exposure.

After 6 hours of irradiation at 1800 MHz and -10, 0, and 17 dBm, significant structural changes were observed. Most of the yeast cells in the irradiated samples showed raised vacuoles and also disruption of the cell membrane. As can be seen from Figure 14b, in yeast samples irradiated at 1800 MHz and -10 dBm, after 6 hours of exposure, budding cells were observed with highly scattered organelles; disruption of the cell wall was also evident. Similar results were obtained for yeast samples irradiated at 1800 MHz and 17 dBm after 6 hours of exposure a number of highly distorted budding cells can be seen (Figure 15). Again, similar

structural and functional changes were observed at 1800 MHz and 0 dBm (Figure 16). A disruption in the cell wall is evident in most of the irradiated yeast cells including dividing cells.

5.4 Concluding Remarks

This study was aimed to test the hypothesis that low power MW radiation at the selected frequencies and powers (1800 MHz and 2100 MHz; and -10, 0, 17 dBm) can affect the rate of growth of *S. Cerevisiae*. The yeast solutions used for the experiment were exposed under the controlled conditions with the changes in yeast cell growth pattern, and the temperature is continuously monitored. The results obtained show that the MW radiation at the selected frequencies and powers induces modulating effects in yeast cells. The findings reveal that MW at the particular frequency of 1800 MHz and power of 17 dBm, 0 dBm and -10 dBm can increase or inhibit the proliferation of *S. Cerevisiae* and these effects are not caused by an elevation in the temperature. Also, experimental results demonstrate that MW can induce yeast cell death followed by their recovery at 2100 MHz and 17dBm. The statistical analysis (Chi-square test of independence) was conducted to understand the influence and independence of frequency and power of MW exposures on the observed effects in the irradiated yeast cells. The outcome suggests that both frequency and power contribute independently towards the modulating effects in yeast cells growth.

Despite significant research efforts being directed towards investigating biological and health effects of mobile phone radiation, a limited number of studies were focused on non-thermal effects of MW radiation and these have reported conflicting results [173] [174] [91, 174] [78] [175] [55] [176]. Based on the current literature, it can be summarised that particular RF/MW exposures can change gene and/or protein expression in certain types of cells, even at intensities lower than the standard recommended exposure levels [177]. There have been a number of experiments conducted to study a growth pattern of yeast cells exposed to MW radiation [89] [178]. Yeast cells are frequently used as a model system in *in-vitro* studies as yeast is a simplest eukaryotic organism with a nucleus. Many essential cellular processes in yeast and human are the same, which makes yeast cells suitable to study basic molecular processes including a biological process in humans [87]. It was shown that the biological effects of mobile phone radiation depend on various parameters such as frequency, intensity (power), exposure duration, and power density [18]. Our previous studies with *S. cerevisiae* yeast cells demonstrated that their proliferation was significantly affected when exposed to

MW at the selected frequencies and powers [178]. In another study, we also showed that low power MW exposures induce yeast cell death followed by their recovery at 2100 MHz and 17dBm [27].

It was also aimed to study further power-dependent effects of MW exposures by testing the hypothesis that radiation at the frequency 1800 MHz and three different powers of -10 dBm, 0 dBm and 17 dBm can affect the rate of growth and viability of *S. cerevisiae* yeast cells. The morphological data clearly show that the applied exposures induce modulating effects in yeast cells. The findings reveal that MWs at 1800 MHz and -10 dBm stimulate the proliferation of *S. cerevisiae* cells which possibly change their cell growth phase. Interestingly, the results also showed that *S. cerevisiae* growth was inhibited at the beginning of the growth phase but recovered towards the end of the growth phase in cells exposed at 1800 MHz and -10 dBm. It should be noted that our results are in agreement with the findings reported by other research studies. For instance, in [179] [91], the authors evaluated the effects of low power MW radiation on bacteria and yeast strains and reported that yeast cell growth rate was affected by applied exposures. It was shown that microwave radiation induces frequency-specific effects on the yeast growth rate, i.e. increase up to 15% at the frequency 41.6 GHz and decrease up to 38% at 41.8 GHz.

The findings of our study show a significant interaction between viability and time point at 1800 MHz and -10dBm (f (F (2, 8) = 13.6, p=0.0027). Time point was observed to be significant at 1800 MHz exposures at both powers of 17 and 0 dBm (p=0.0033, p=0.0058 respectively). Our results are in accord with the study by Vrhovac [89], where three different strains of yeast were exposed to RF radiation at 905 MHz. Their findings revealed a statistically significant difference in colony growth at different time points of exposures. The results of our investigation also showed that 6 h exposures at -10 dBm and 0 dBm affected cell proliferation in *S. cerevisiae*. A significant increase in total cell count and changes in cell viability were observed at the powers of 0 dBm and -10 dBm respectively. This change is due to molecular transformations and alterations. Similar observations were reported by Lin et al. [167].

Further, yeast cell morphology was analysed particularly for circularity and elongation at 1800 MHz and two powers, highest power 17 dBm and the lowest power of -10 dBm to observe the changes produced by different microwave exposure conditions. The impact of the particular powers in selected MW exposures on *S. cerevisiae* was examined using TEM. TEM images revealed changes in the internal organisation of treated yeast samples exposed for 6

hours at 1800 MHz and selected powers. TEM images (Fig. 12b-12d) provide evidence of structural disruptions and disruption in the overall internal organisation in *S. cerevisiae* samples exposed at -10 dBm, 0dBm and 17 dBm. Assessment of morphological changes in yeast cells showed that exposures at -10 dBm and 17 dBm significantly affect the size and shape of the irradiated cells when compared to the control groups. TEM images showed visible changes in the internal organisation of the yeast cell for all the selected three powers at the frequency of 1800 MHz. At 0 dBm, although no significant changes were seen in yeast cell proliferation, TEM images show disruptions in their internal cellular organisation. These findings imply that studied MW exposures induce power-dependent effects on yeast cells. One possible explanation for these effects could be the change in the biochemical process of the treated cells as proposed by Lin et al. [167]. The obtained results clearly confirm our hypothesis that even at low powers of exposures which lead to no elevation in temperature MW radiation can affect the normal cellular processes in exposed *S. cerevisiae* cells. The findings imply that low power MW radiation can induce modulating effects on cell growth and internal structural organisation. Our findings also suggest that a further study is required to investigate the cause of the observed internal disruptions and surface changes in exposed yeast cells. Investigation of the effects of the same powers and different MW frequencies, used in mobile phone radiation, is also required.

CHAPTER 6: LOW POWER MICROWAVES INDUCE CHANGES IN FUNCTIONAL PROPERTIES OF TRPV4, A MECHANICALLY ACTIVATED ION CHANNEL

6.1 Introduction

RF radiation can alter the intracellular Calcium homeostasis and consequently target cell proliferation and differentiation as well as modify bioactivity of different enzymes [180]. Transient receptor potential vanilloid 4 (TRPV4) is a calcium-permeable ion channel protein encoded by the TRPV4 gene that is detectable in both sensory and non-sensory cells [2]. It is widely expressed in kidneys, lungs, heart, brain, endothelial cells, dorsal root and trigeminal sensory ganglia. It has a wide range of implications from osmoregulation to thermo-sensing. TRPV4 is a non-selective cation channel that is expressed in various tissues, including epithelial and endothelial cells, which can be activated by different stimuli such as heat, hypotonic stress, GSK1016790A, derivatives of arachidonic acids and shear stress [181] [182].

In this chapter, the PhD candidate reports on the study conducted to evaluate the effects of MW radiation at 1800 MHz and powers 17 dBm, 0 dBm and -10 dBm on TRPV4 channel function in HEK-293 cells stably expressing TRPV4, to improve understanding of thermal/non-thermal nature of RF-EMF interaction with normal epithelial cells.

The first series of experiments were performed at room temperature (25°C). At the second stage, the experiments were repeated at body temperature (37°C). The idea behind studying the effects of MW exposures at two different temperatures is to evaluate whether the induced effects/ cellular responses (if any) are caused by applied irradiation alone or are temperature dependent. The response of TRPV4-HEK293 to applied irradiation was studied at two different time points, i.e. two hours and four hours, to also evaluate whether the effects are time-dependent. The changes in the intracellular calcium levels ($[Ca^{+2}]_i$) of TRPV4-HEK293 cells were assessed using calcium-sensitive dye, Fluo-4AM and confocal microscopy. By employing these methods, we measured the effects of the MW exposures at 1800MHz and power of 17dBm on TRPV4 channel gating in response to its selective agonist GSK1016790A.

6.2 Materials and Methods

GSK1016790A Agonist

In this study, HEK293 cells stably expressing TRPV4 (TRPV4-HEK293 cells) [183] were exposed to MW radiation at 1800 MHz and powers 17 dBm (electric field 47 V/m, power density 0.606 mW/cm², SAR 4.314 W/kg), 0 dBm (electric field 47 V/m, power density 0.606 mW/cm², SAR 4.314 W/kg) and -10 dBm (electric field 47 V/m, power density 0.606 mW/cm², SAR 4.314 W/kg). The objective of the study was to elucidate whether the effects induced by applied low-power MW exposure on TRPV4 is non-thermal. GSK 101 (GSK 1016790A) is a novel and selective TRPV4 agonist, which has been shown to be a more specific and potent activator than some small molecule agonists such as Phorbol ester 4 α PDD (at nanomolar levels) [184]. GSK1016790A was used to observe the channel response at four different concentrations, 0.1, 1, 10 and 100 nM, diluted in HEPES buffer. For calcium imaging, the HEPES buffer consists of 140 mmol/L NaCl, 5mmol/L KCl, 10 mmol/L HEPES, 11mmol/L D-glucose, 1 mmol/L MgCl₂, 2 mmol/L, CaCl₂, and 2 mmol/L probenecid, adjusted to pH=7.4.

Cell culture and Ca²⁺ measurement protocol

Tetracycline-inducible TRPV4-HEK 293 cell line was generated as reported elsewhere [185]. Cells were cultured in Dulbecco's Modified Eagle's medium (Invitrogen) supplemented with 10% fetal bovine serum, hygromycin (50 mg/ml) and blasticidin (5 μ g/ml), under 5% CO₂ at 37^oC. For irradiation experiments, cells were seeded in a 24-well plate for 24 hours at the density of 2.5 \times 10⁵ cells per well [186], followed by 4 hours of exposure at 1800 MHz and powers of 17 dBm, 0 dBm and -10 dBm. After irradiation, TRPV4 expression was induced using 0.1 μ g/ml of tetracycline overnight. On the day of the experimental exposure, cells were loaded with Ca²⁺ sensitive dye (Fluo-4AM) for 30min in an imaging buffer. Cells then were washed with HEPES buffer and imaged immediately. Calcium imaging was performed using a Nikon A1 laser-scanning confocal microscope. The cell area was measured by acquiring region of interest (ROIs) around each cell automatically using a NIS element viewer (Nikon Instruments Inc). The average intensity of at least 100 ROIs has been measured and normalised to the time zero, presented as F1/F0 to evaluate the changes in intracellular Ca²⁺ level. The obtained data are shown as mean \pm SEM of at least three independent experiments.

Preparation of cells for Transmission Electron Microscopy

To perform TEM assessment, HEK-293 cells were grown on a coverslip inside the 6-well plate, followed by 4 hours of exposure at 1800 MHz and powers of 17 dBm, 0 dBm and -10 dBm. The cells were suspended in a Karnovsky's fixative overnight to fix and immobilise any cellular activity. Cells were scraped from the coverslip, and 1 pellets were washed thrice with cacodylate buffer. Following rinsing, the cells were post-fixed at room temperature (25°C) in the post-fixative solution following washes with distilled water [168]. After washing, the samples were dehydrated with increasing ethanol gradients from 50 to 90% followed by 100% ethanol for 30 mins. Following ethanol dehydration, the samples were completely dehydrated in acetone and infiltrated with Spurr's resin mixture [169]. After infiltration, the samples were polymerised at 70°C in the oven. Ultrathin sections (90nm thicknesses) were cut with a diamond knife using ultramicrotome (Leica Microsystems). The sections were observed at 80kV under a Jeol 1010 Transmission Electron microscope (TEM) using the Gatan Microscopy Suite software, version 2.3.

Statistical Analysis

All Ca^{2+} responses are presented as mean \pm SEM, and n represents the number of independent experiments, with > 50 cells analysed in each experiment. Statistical comparisons were made by student's t-test (Prism, GraphPad Software). Calcium response was observed to be significant for all the selected concentration of agonist GSK with $P < 0.05$.

Exposure System Setup

HEK-293 cells seeded on 24-well plate having 1 million cells in each of the selected 16-well plates. The exposure system consists of Transverse Electro-Magnetic (TEM) TC-5062AUHF TEM cell (100 kHz–3 GHz) from TESCOM Ltd, and the signal generator (Wiltron 68247B) operating range 10 MHz to 20 GHz. All experiments were conducted at room temperature of 25°C and body temperature of 37°, with the temperature being monitored continuously by a digital temperature controller (RS 206-3738) during experimentation to observe whether any effects induced in cells are due to the temperature change. Details of the exposure system set up, the position of the sample, and the direction of the electric field inside was discussed in detail in Chapter 4 and also published previously [27].

6.3 Results and Discussion

As mentioned above, the activity of TRPV4 channels was studied at two-time points and two temperatures to evaluate the channel's response when irradiated at 1800 MHz and three powers 17 dBm, 0 dBm and -10 dBm. The results are presented below.

6.3.1 Agonist (GSK1016790A) response of TRPV4 ion channel protein at room temperature when irradiated for 4 hrs and 2hrs at 1800 MHz and 17 dBm

Figures 6.1 and 6.2 show the dynamics of TRPV4 response to four different concentrations of GSK1016790A when exposed at 1800 MHz and 17 dBm, after 2 and 4 hrs irradiation. At 4 hrs of irradiation it was observed that, with the increase in the concentration of GSK1016790A from 0.1 to 100 nM, the cellular response time was reduced from 0.813 ± 0.1876 for 0.1nM ($p < 0.0216$, $N=6$), 1.166 ± 0.4072 ($p < 0.0191$, $N=6$) for 1nM, 2.502 ± 0.7096 ($p < 0.0106$, $N=6$) for 10nM and 2.851 ± 0.9264 ($p < 0.0186$, $N=6$) for 100nM. This suggests that the MW exposure at 1800 MHz and 17 dBm is sufficient enough to sensitise the TRPV4 channel response to its selective agonist.

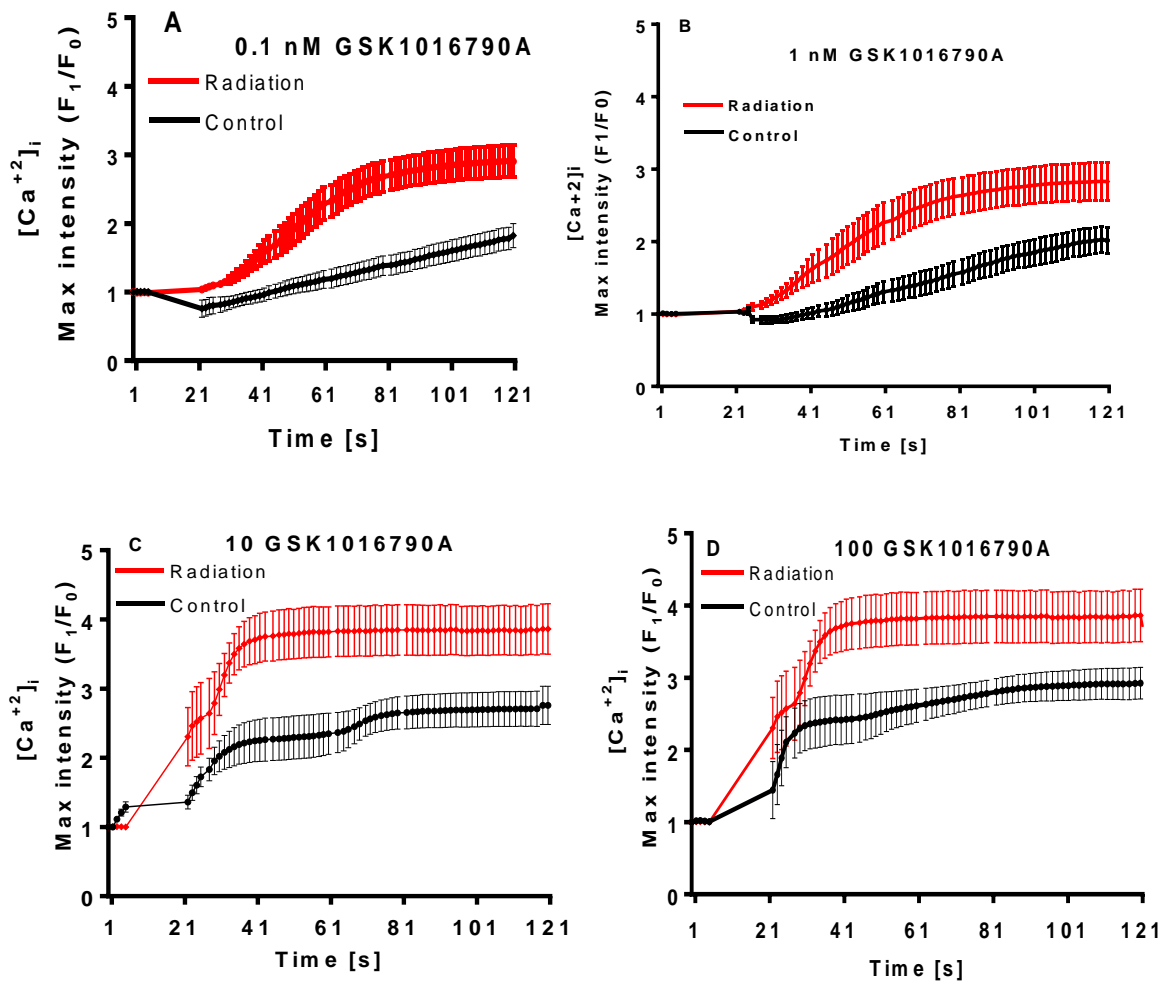


Figure 6.1: Agonist (GSK1016790A) response of TRPV4 ion channel protein at 25°C when irradiated for 4 hr at 1800 MHz and 17 dBm.

Figure 6.2 showed the ion channel response when TRPV4-HEK-293 cells were exposed for 2hrs. The results indicate that, at low concentration of 0.1 and 1nM, irradiation sensitises the response of TRPV4 by 0.461 ± 0.17 ($P= 0.0349$, value, $N=5$) for 0.1nM, 0.9773 ± 0.2949 ($p<0.0349$, $N=4$) for 1nM. However, at higher concentrations of 10nM and 100nM, no changes were observed. This could be because the response was already saturated.

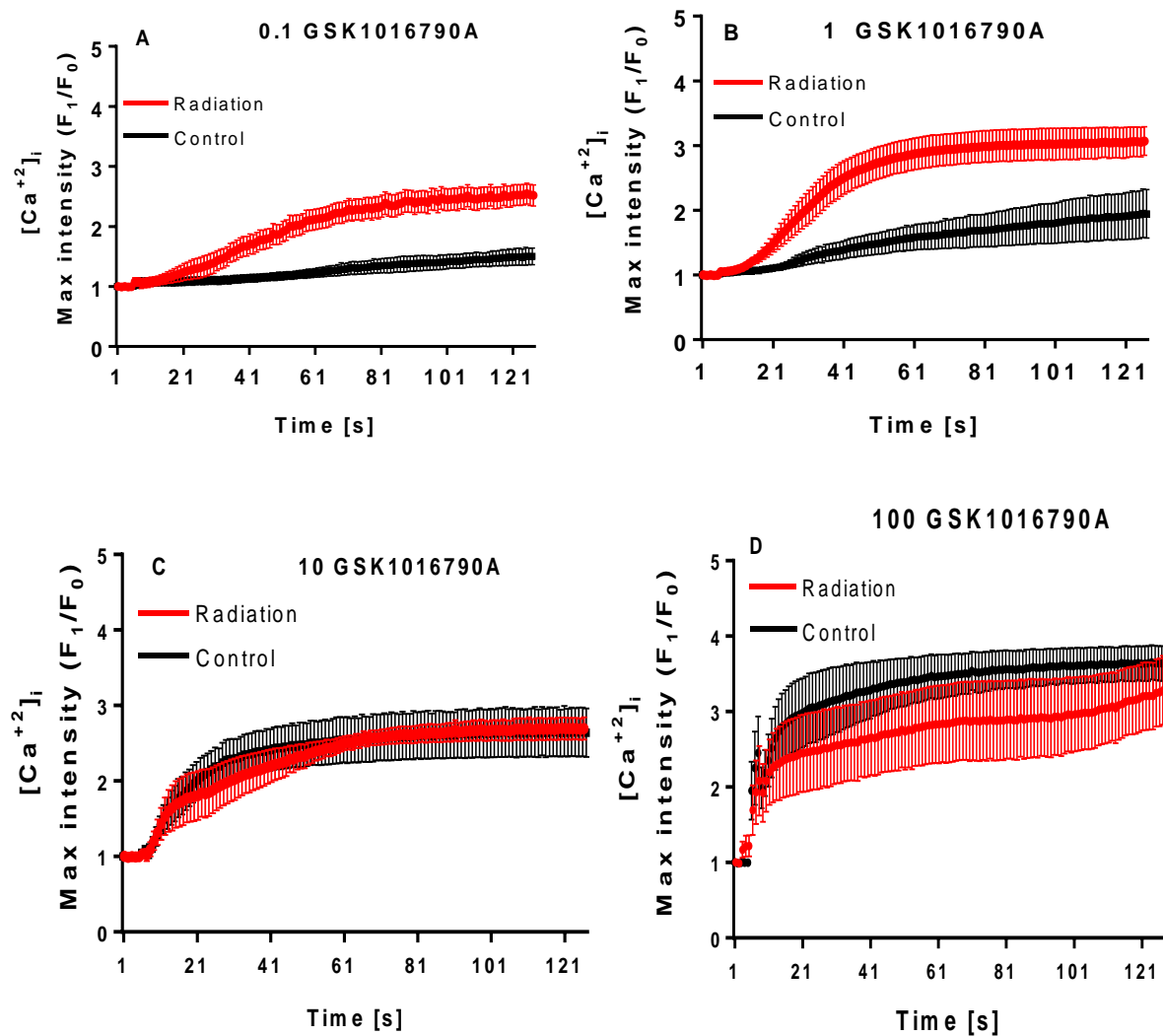


Figure 6.2: Agonist (GSK1016790A) response of TRPV4 ion channel protein at 25°C, when irradiated for 2 hr at 1800 MHz and 17 dBm.

6.3.2 Agonist GSK1016790A response of TRPV4 ion channel protein at 25°C after 2 and 4 hrs of exposure at 1800 MHz and 0 dBm

Figures 6.3 and 6.4 show changes in the dynamics of TRPV4 response to GSK1016790A when irradiated at 1800 MHz and 0 dBm for 2 and 4 hrs, respectively. At both exposure times, no significant difference in channel response was observed, suggesting that applied radiation does not affect the function of TRPV4-HEK293 cells.

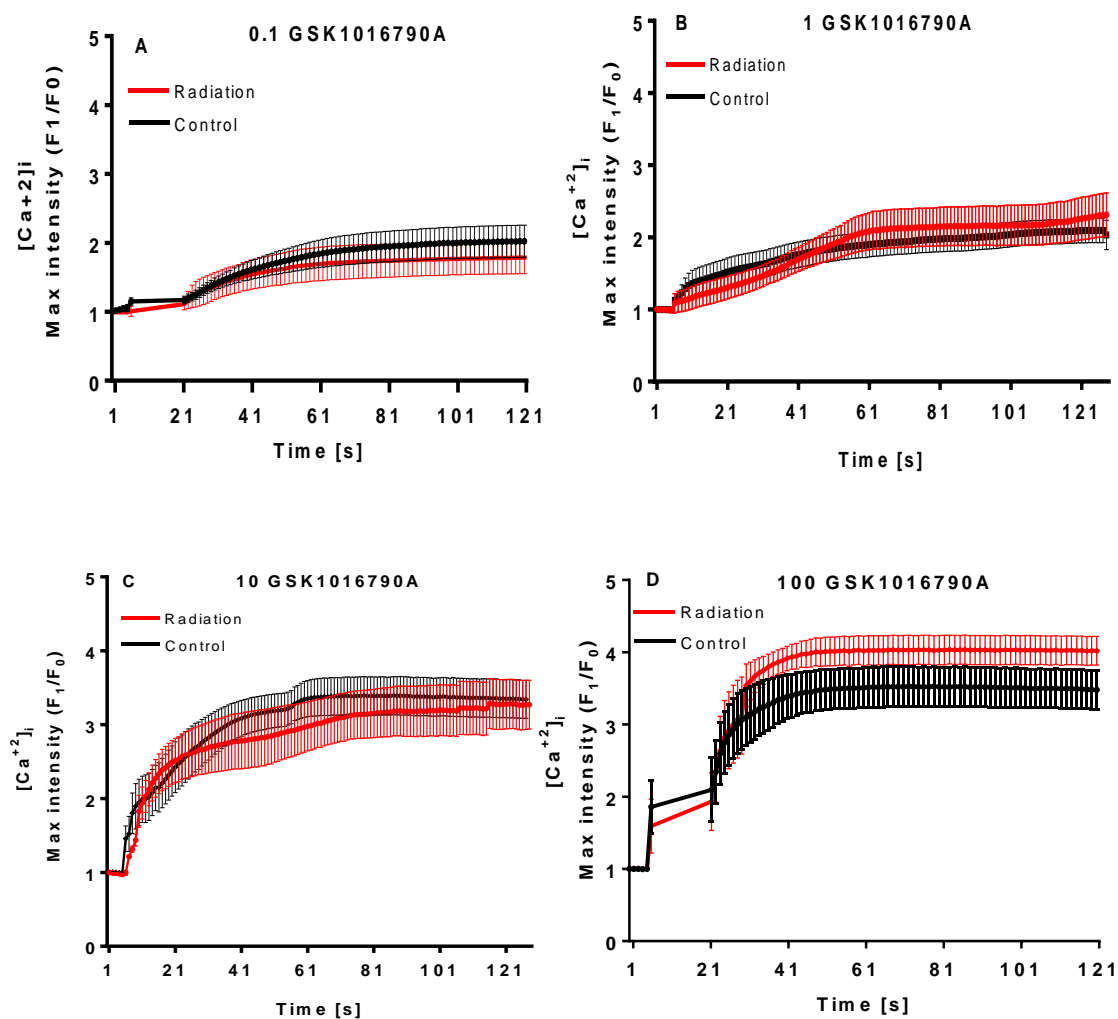


Figure 6.3: Agonist GSK1016790A response of TRPV4 ion channel protein at 25°C, when irradiated for 4hr at 1800 MHz and 0 dBm.

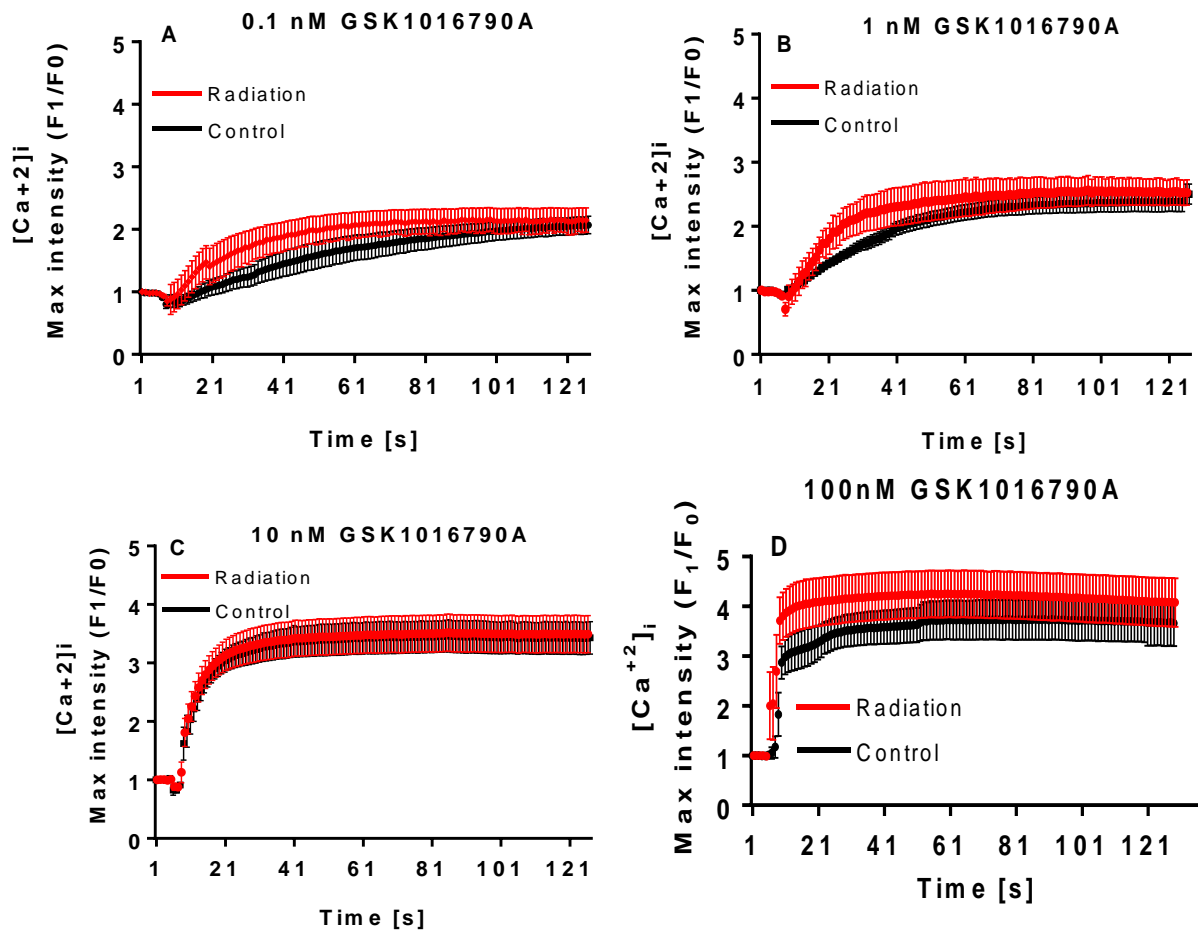


Figure 6.4: Agonist GSK1016790A response of TRPV4 ion channel pro attain 25°C when irradiated for 2 hr at 1800 MHz and 0 dBm.

6.3.3 The average maximum response of TRPV4 ion channel at 25°C irradiated for 4 and 2 hrs at 1800 MHz and -10 dBm.

Figures 6.5 and 6.6 show the response of the TRPV4 channel to its agonist. Irradiation of cells at 1800 MHz and -10 dBm at both time points, 2 and 4 hrs, did not induce any significant effect on the TRPV4 channel responses to its selective agonist.

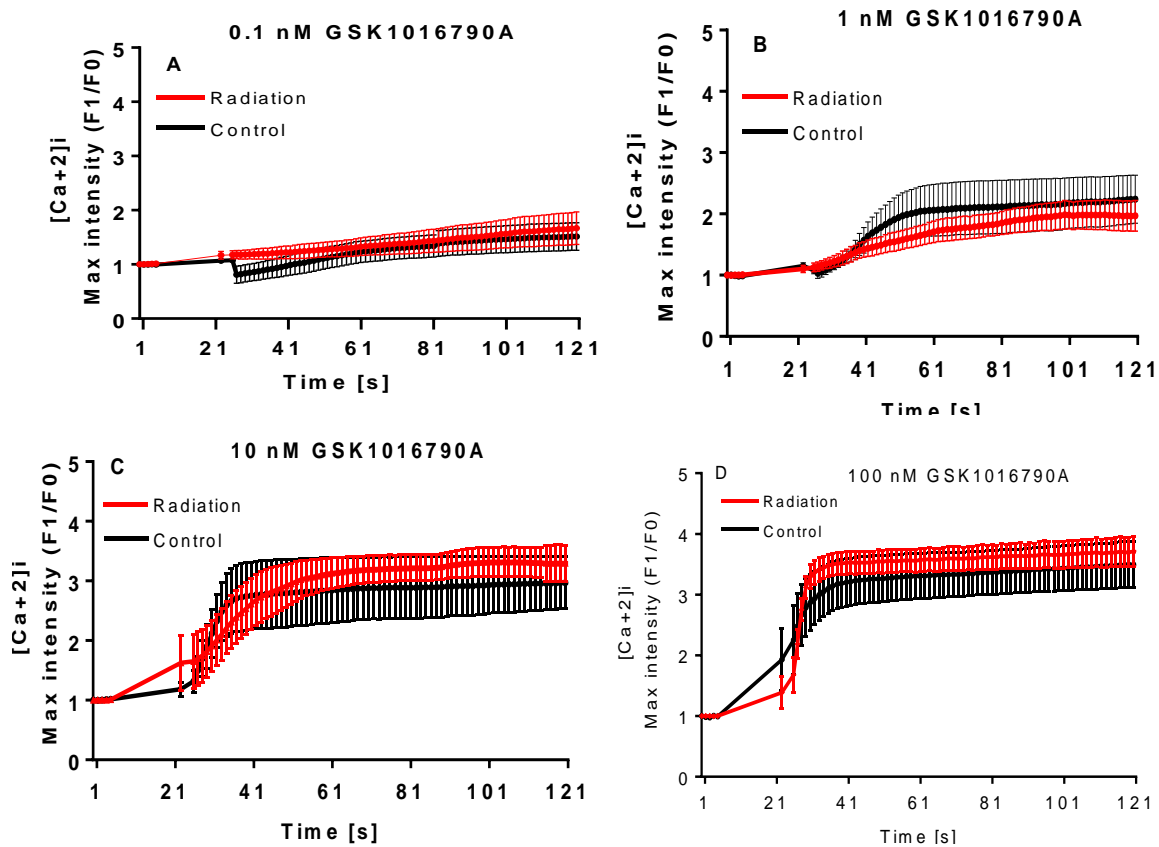


Figure 6.5: Agonist GSK1016790A response of TRPV4 ion channel protein at 25°C when irradiated for 4 hrs at 1800 MHz and -10 dBm. At all four concentrations of GSK1016790A, we do not find any changes in channel response.

The time dynamics graph of all experiments performed at 1800 MHz and powers 17 dBm, 0 dBm and -10 dBm clearly show that the power of 17 dBm significantly affect the TRPV4 ion channel response, whereas powers 0 dBm and -10 dBm produce no effects on channel's function.

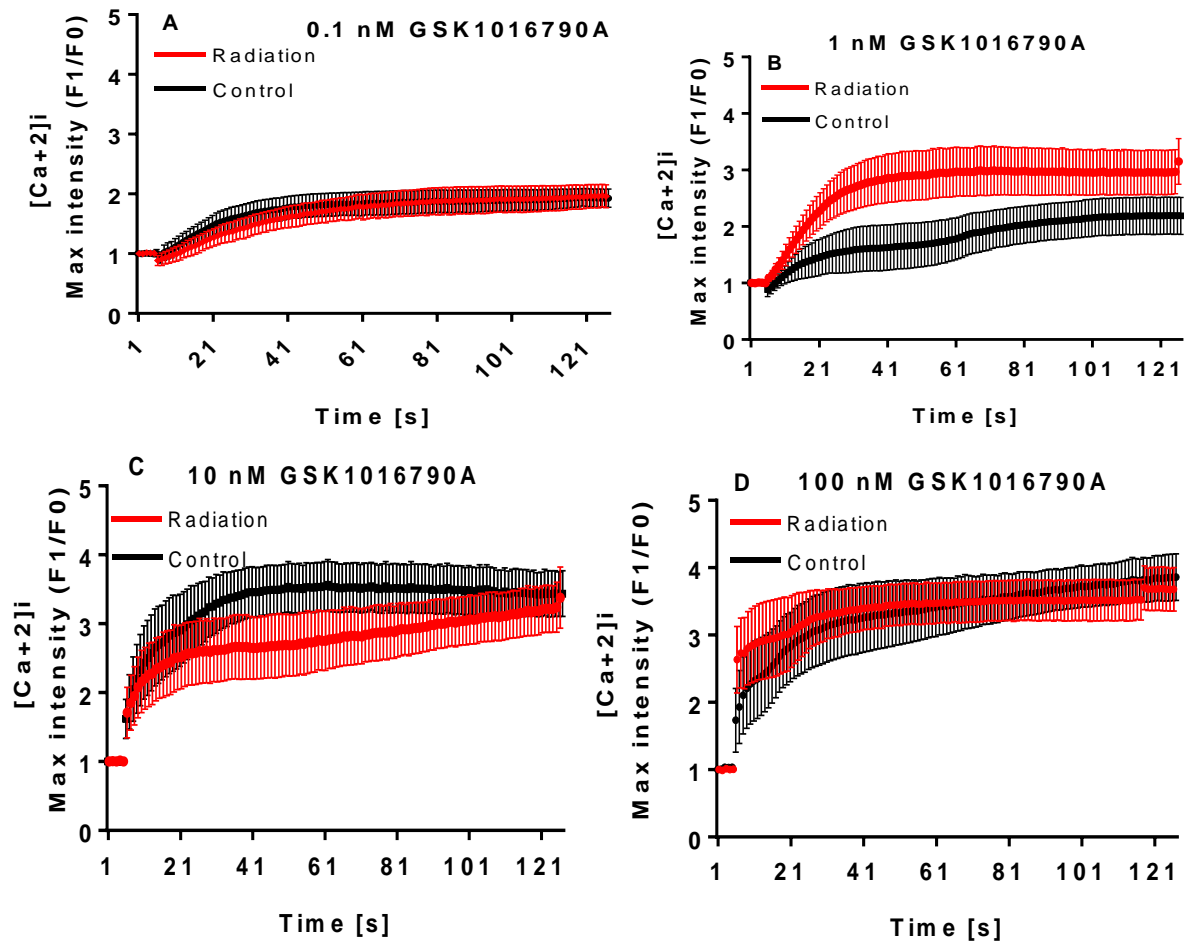


Figure 6.6: Agonist GSK1016790A response of TRPV4 ion channel protein at 25°C when irradiated for 2 hrs at 1800 MHz and -10 dBm. The black line corresponds to control and red line to irradiated sample.

6.3.4 The average maximum response of TRPV4 ion channel at room temperature (25°C ±2°C) when irradiated for 4 hrs and 2 hrs at 1800 MHz and 17 dBm.

As reported above, TRPV4-HEK-293 cells were exposed for 4 and 2 hr at the frequency 1800 MHz and three different powers (17 dBm, 0 dBm and -10 dBm) to investigate the influence of the exposure time on cellular responses at the different radiation powers. Average maximum response time was calculated for control and test (irradiated) groups. Figures 6.7A and B represent the average maximum response of TRPV4-HEK293 cells to different concentrations of GSK1016790A after exposure for 4 and 2 hrs at 1800 MHz and the highest power of 17 dBm.

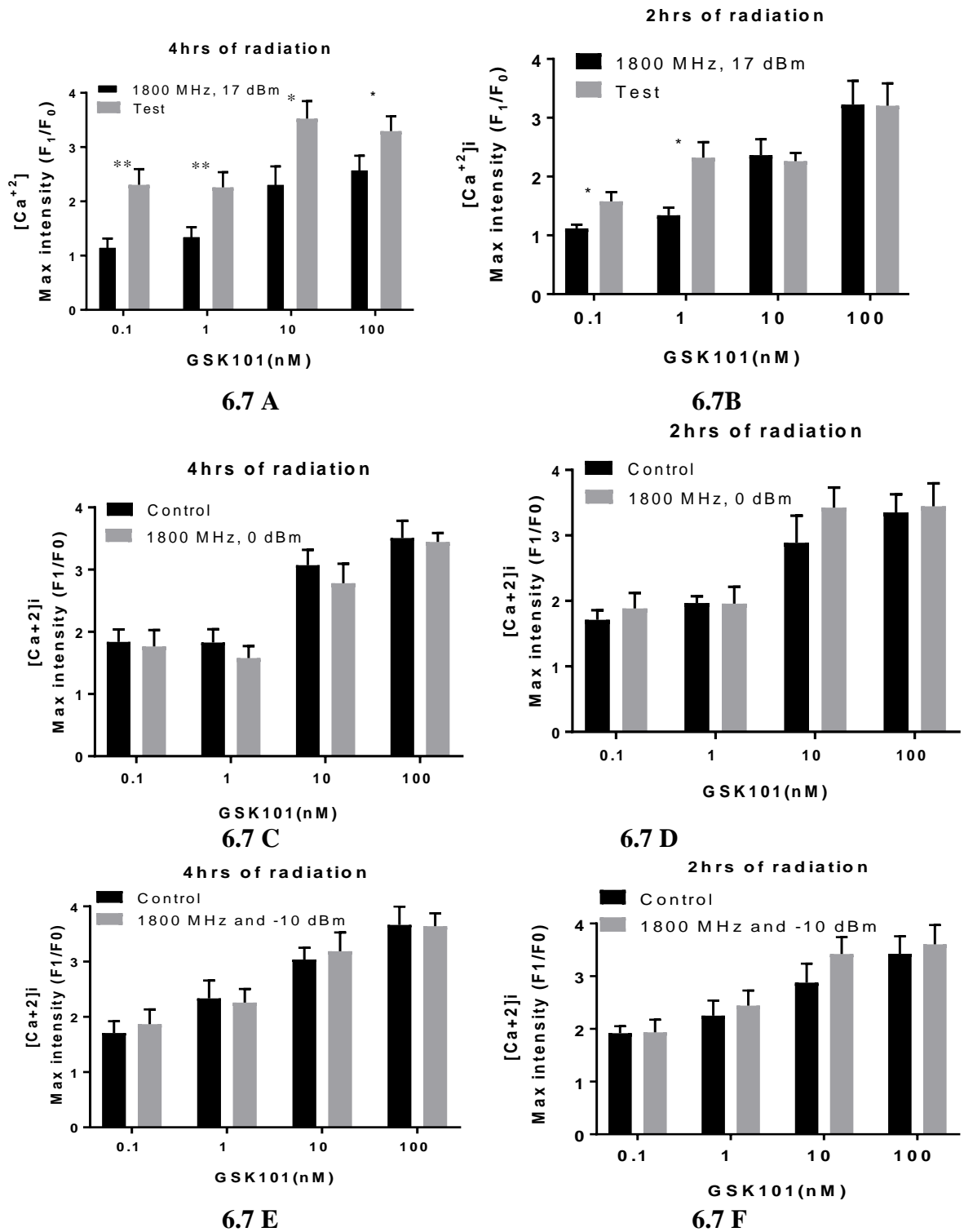
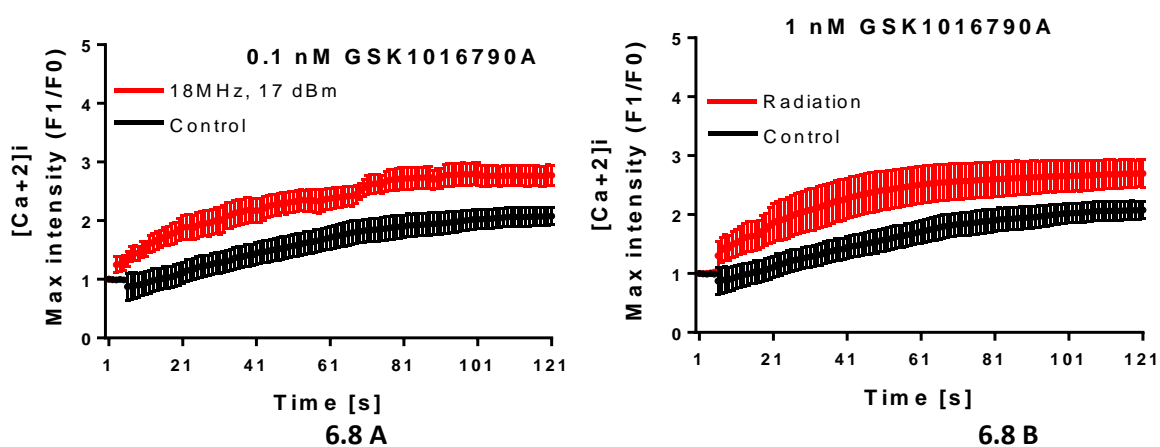


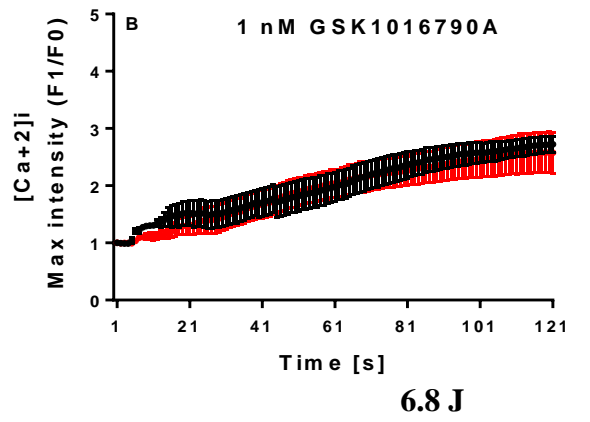
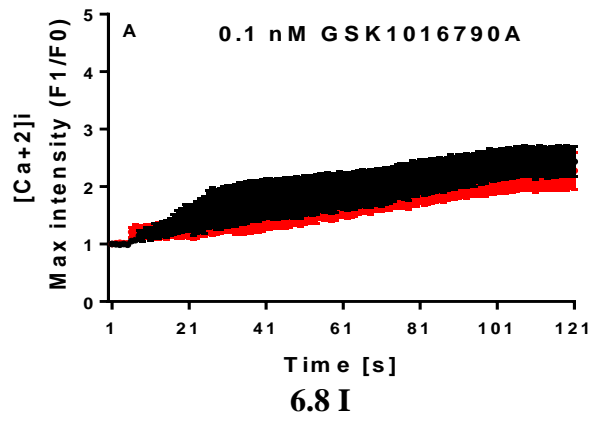
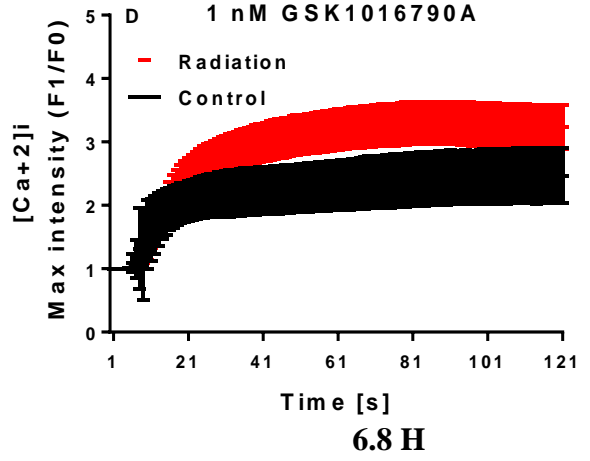
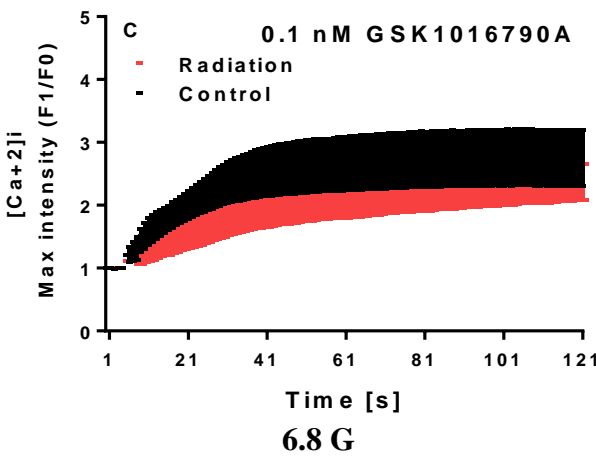
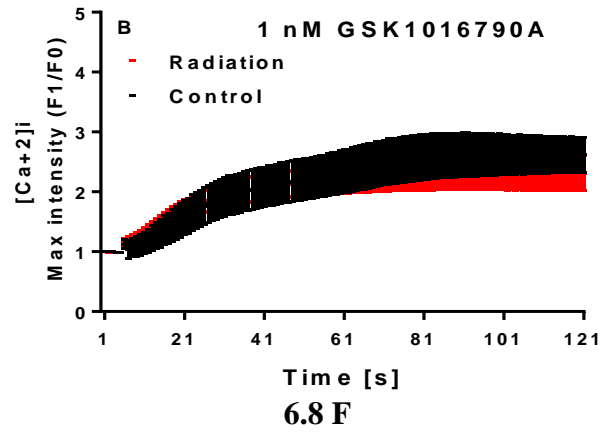
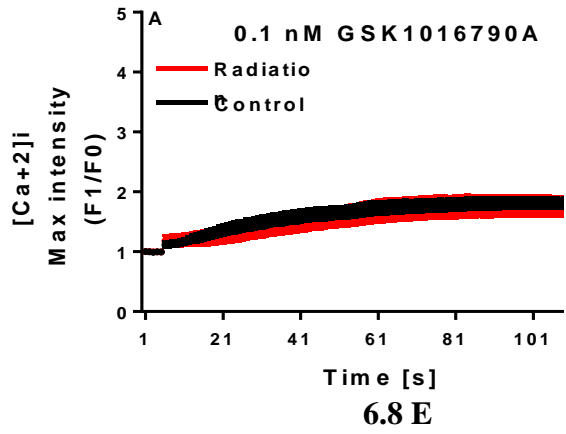
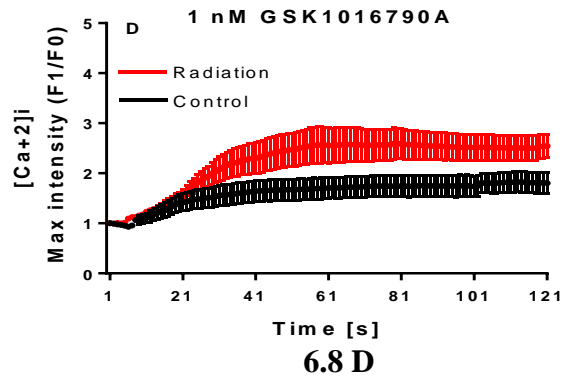
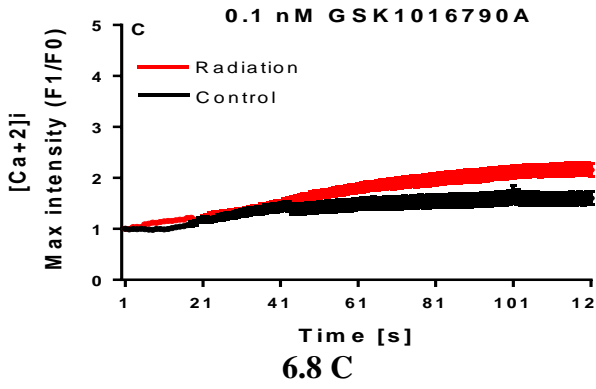
Figure 6.7: Effect of different radiation powers and times of exposure on TRPV4 responses to its selective agonist. (A&B) show the effect of 1800 MHz and 17 dBm radiation upon 4 hrs and 2 hrs respectively. (C&D) show the effect of 1800 MHz and 0 dBm radiation upon 4 hrs and 2 hrs respectively. (E&F) show the effect of 1800 MHz and -10 dBm of radiation upon 4 hrs and 2 hrs respectively.

The data show that 4 hrs radiation at 1800 MHz and 17 dBm sensitised the response of TRPV4 to its selective agonist by 1.12 ± 0.31 fold ($P < 0.005$, $N=6$) for 0.1nM, 0.87 ± 0.40 fold ($P < 0.01$, $N=6$) for 1nM, 1.17 ± 0.43 fold ($P < 0.023$, $N=6$) for 10nM; while 2 hrs exposure to the same power and frequency sensitised the cellular responses to only 0.46 ± 0.17 fold ($P < 0.05$, $N=6$) at 0.1nM GSK101 and 0.97 ± 0.29 fold ($P < 0.05$, $N=6$); and no difference in the cellular response was observed at other concentrations. Furthermore, irradiation at the powers 0 dBm and -10 dBm at both time points, 2 and 4 hrs, did not produce any effect on Max response time of TRPV4-HEK293 cells at any concentration of GSK1016790A, as shown in Figure 6.7C-D. Hence, the findings of this study demonstrate that applied non-thermal MW exposures affect TRPV4 channel response to its selective agonist in a dose- and time-dependent manner.

6.3.5 Agonist GSK1016790A response of TRPV4 ion channel protein at body temperature ($37^{\circ}\text{C} \pm 2.5^{\circ}\text{C}$) and 4hrs and 2 hrs of irradiation at 1800 MHz and 17 dBm.

To study the effect of temperature on TRPV4-HEK293 cells responses to low-power microwaves, the experiments were repeated at body temperature (37°C). Figures 6.8 and 6.9 show the dynamics of TRPV4 response to four different concentrations of GSK1016790A when exposed at 1800 MHz and 17 dBm, upon 2 and 4 hrs of irradiation. TRPV4 response after 2 hrs of irradiation at the same power and frequency sensitised the response by 0.1918 ± 0.2769 at 0.1 nM and -0.7014 ± 0.3263 . For 1 nM and 4hrs of irradiation at 1800 MHz and 17 dBm, the response was sensitised by 0.7682 ± 0.2954 for 0.1nM, 0.8274 ± 0.3774 for 1nM, 2.502 ± 0.7096 (Figure 6.8(A-D)).





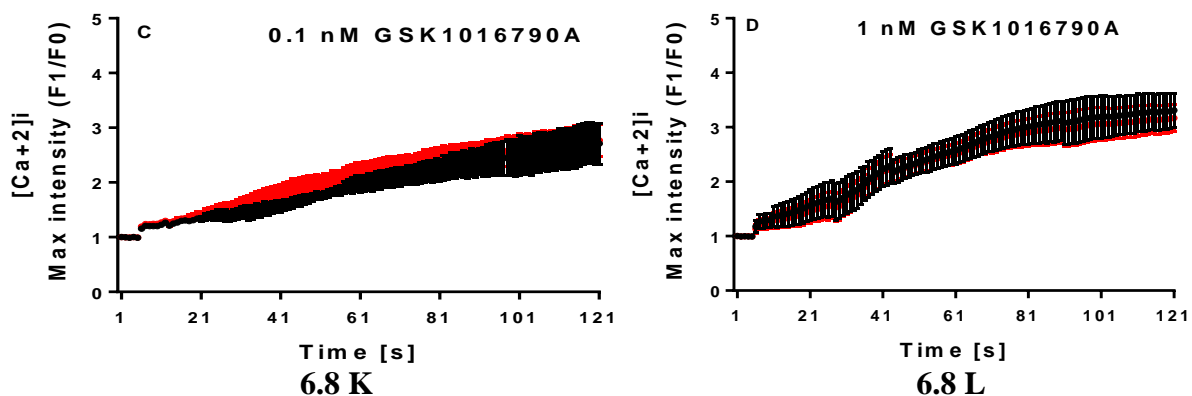


Figure 6.8: Agonist GSK1016790A response of TRPV4 ion channel protein at 37°C when irradiated for 4 hrs and 2hrs respectively at 1800 MHz and 17 dBm

Furthermore, exposure of cells for 4 and 2 hrs at 1800 MHz and 0 dBm did not induce any effect on TRPV4 channel’s response to its agonist, similar to the results obtained at 25°C. This suggests that low-power exposure does not affect TRPV4 channel’s function (Figure 6.8E-H).

Figure 6.8 (I-L) shows the response of TRPV4 to its agonist when irradiated at 1800 MHz and -10 dBm for four hr and 2hr. It can be seen that, for both times of exposure, the response of the ion channel is the same for control and irradiated samples, and no significant changes were observed.

The average maximum response of TRPV4 ion channel at body temperature (37°C± 2.0°C) when irradiated for 4 hrs and 2 hrs at 1800 MHz and 17 dBm.

In the study reported earlier in Section 6.3.4, we exposed TRPV4-HEK-293 cells for 4 hrs and 2hrs at room temperature 25°C to evaluate the effects of irradiation at 1800 MHz and powers of 17 dBm, 0 dBm and -10 dBm powers, and found that only exposure at the power of 17 dBm is sensitising the response of TRPV4 to its selective agonist independent of the temperature.

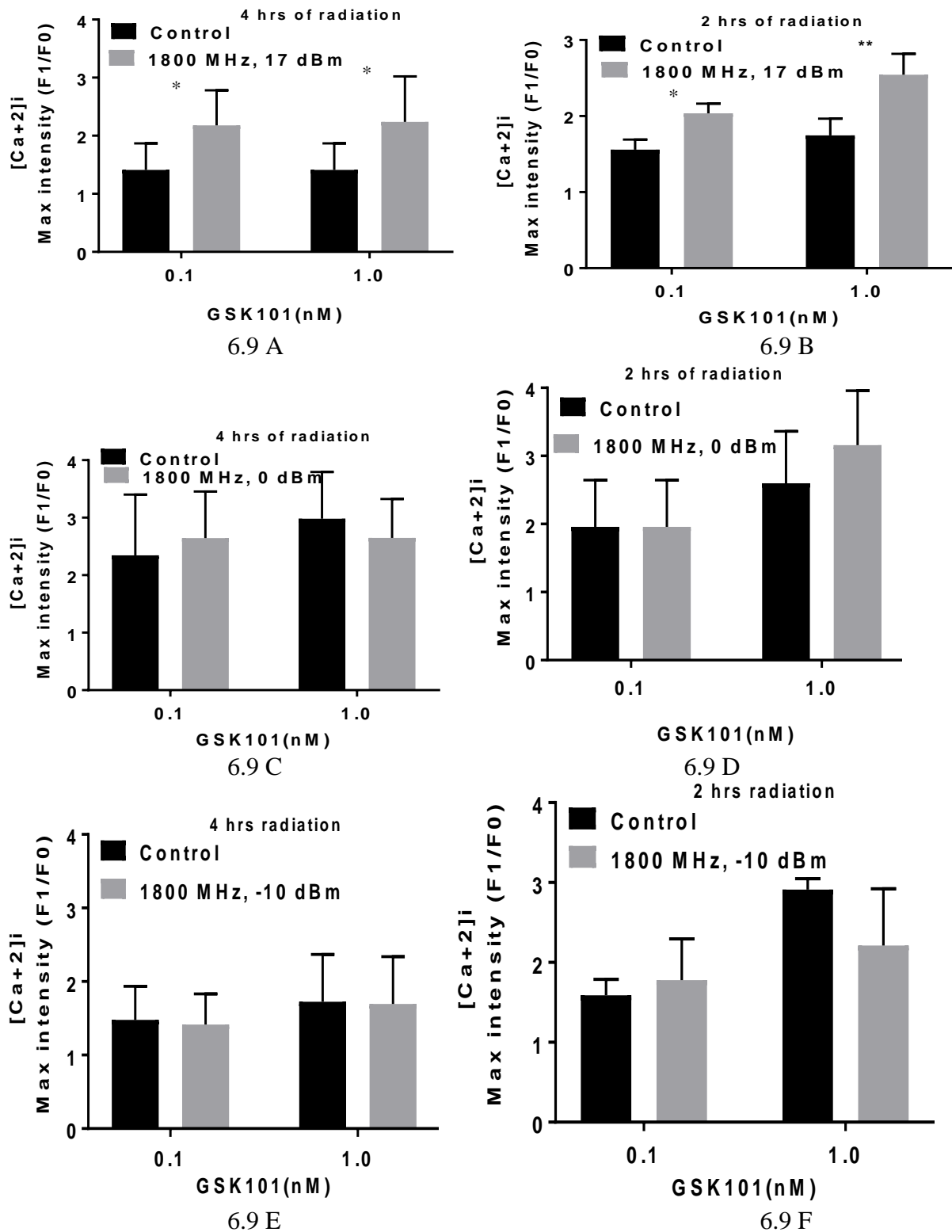


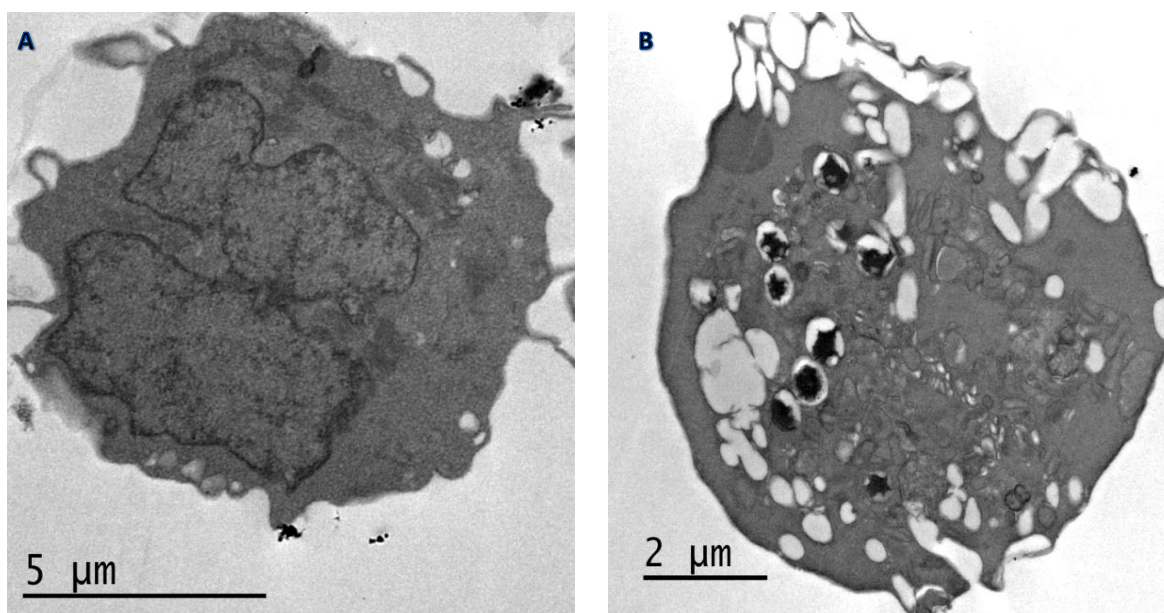
Figure 6.9: Effect of different radiation powers and times of exposure on TRPV4 responses to its selective agonist, (A&B) show the effect of 1800 MHz and 17 dBm radiation upon 4 hrs and 2 hrs respectively. (C&D) show the effect of 1800 MHz and 0 dBm radiation upon 4 hrs and 2 hrs respectively. (E&F) show the effect of 1800 MHz and -10 dBm of radiation upon 4 hrs and 2 hrs respectively.

By conducting similar experiments at body temperature of 37°C, Figure 6.9, it is found that irradiation at 4 hrs and 2 hrs at 1800 MHz and 17 dBm (Figures 6.9A and B) sensitises the response/bioactivity of TRPV4 ion channels, as follows: Exposure at 17 dBm (Figures 6.9A and B) for 4 hrs sensitised the response of TRPV4 to its selective agonist by 0.76 ± 0.29 for concentration 0.1nM, 0.82 ± 0.37 for 1nM; exposure at 0 dBm (Figures 6.9C and D) and at -10 dBm (Figures 6.9E and F) induced no significant effect of the ion channel response at peak response time.

6.4 TEM Analysis of HEK-293 Cells

To study the effect of selected frequency and power on the internal structure of HEK-293 cells, we used Transmission Electron Microscopy (TEM). Figure 6.10 (A-D) shows the TEM micrographs of the cells irradiated for 4 hrs at 1800 MHz and powers of 17 dBm, 0 dBm and -10 dBm at 37°C. TEM micrographs of cells exposed at 17 dBm for 4 hrs (Figure 6.10 B) show significant changes at the ultrastructural level, such as vesiculation in the cytoplasm, and the leaking of cellular contents compared to control cells (Figure 6.10A). However, exposure at 0 dBm (Figure 6.10C) and -10 dBm (Figure 6.10D) induces only minimum changes at the morphological level with visible leakage of contents in HEK-293 cells.

TEM images strongly indicate that irradiation at 17 dBm produces significant effects on the regular structural organisation of cells. In contrast, irradiation at other two powers 0 dBm and -10 dBm, produce no effect on cells - cell remains intact and well organised.



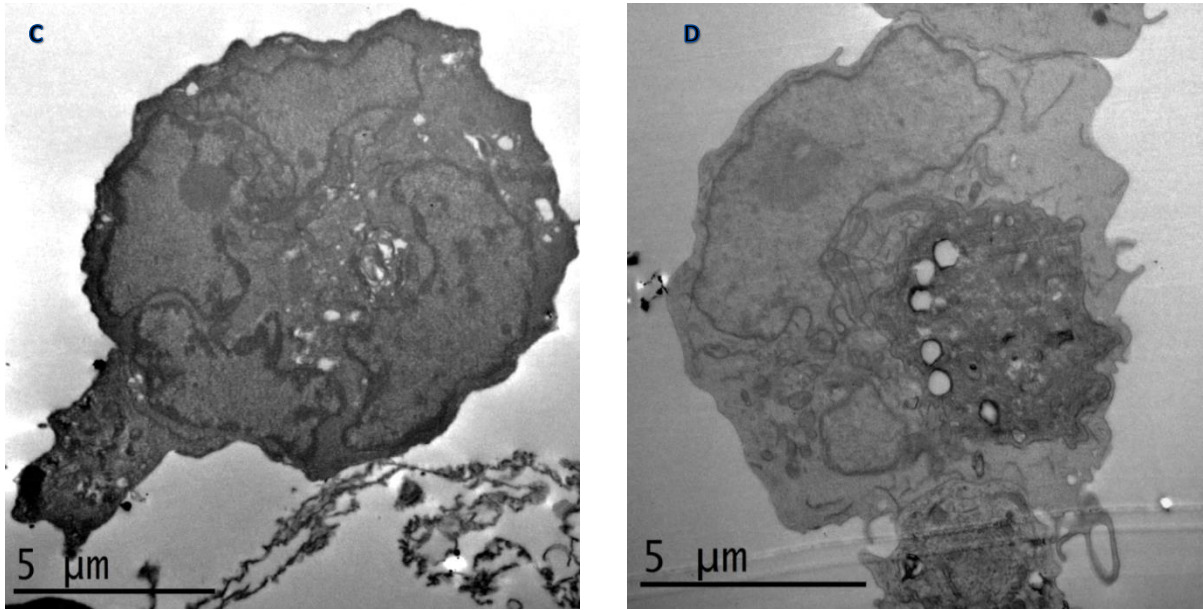
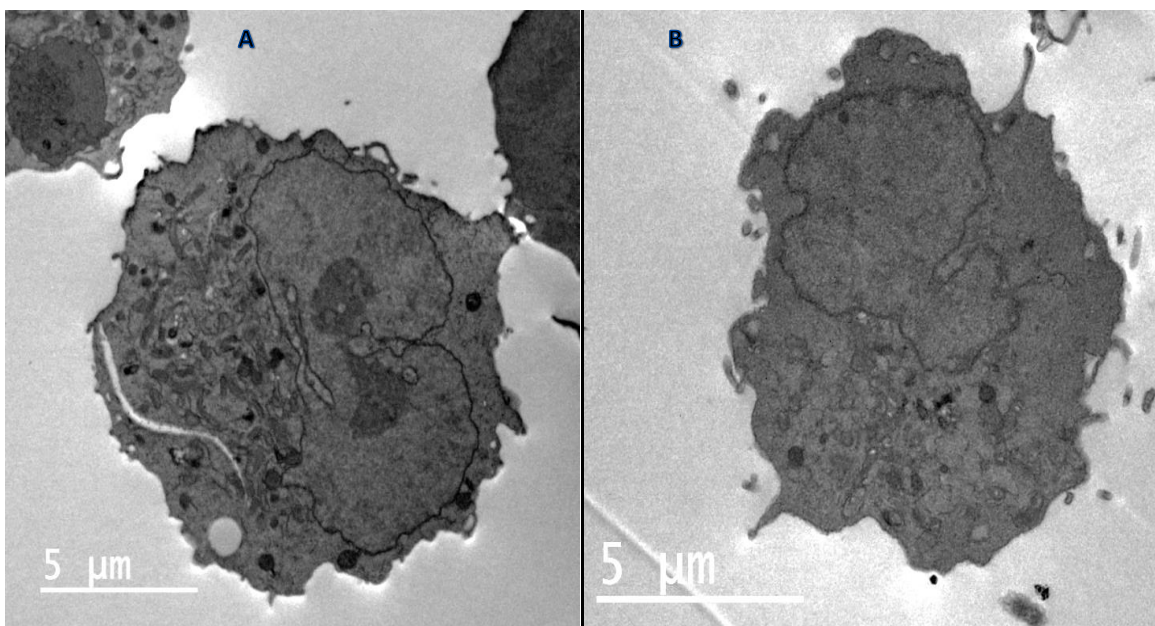


Figure 6.10: TEM micrographs show control and HEK-293 cells exposed at 1800 MHz and powers of 17 dBm, 0 dBm, -10 dBm exposed at 37 °C for 4 hrs. Figure a: shows control HEK-293 cells kept at 37 °C, Figure B: HEK-293 cells exposed at 1800 MHz and 17 dBm, Figure C: HEK-293 cells exposed at 1800 MHz and 0 dBm, Figure D: HEK-293 cells exposed at 1800 MHz and -10 dBm.

Figures 6.11(A-D) show the TEM micrographs of the cells irradiated for 2 hrs at 1800 MHz and powers of 17 dBm, 0 dBm and -10 dBm at 37°C. At 17 dBm, 0 dBm and -10 dBm (Figure 6.11B, C and D), no significant morphological changes were observed when compared to the control (Figure 6.11A).



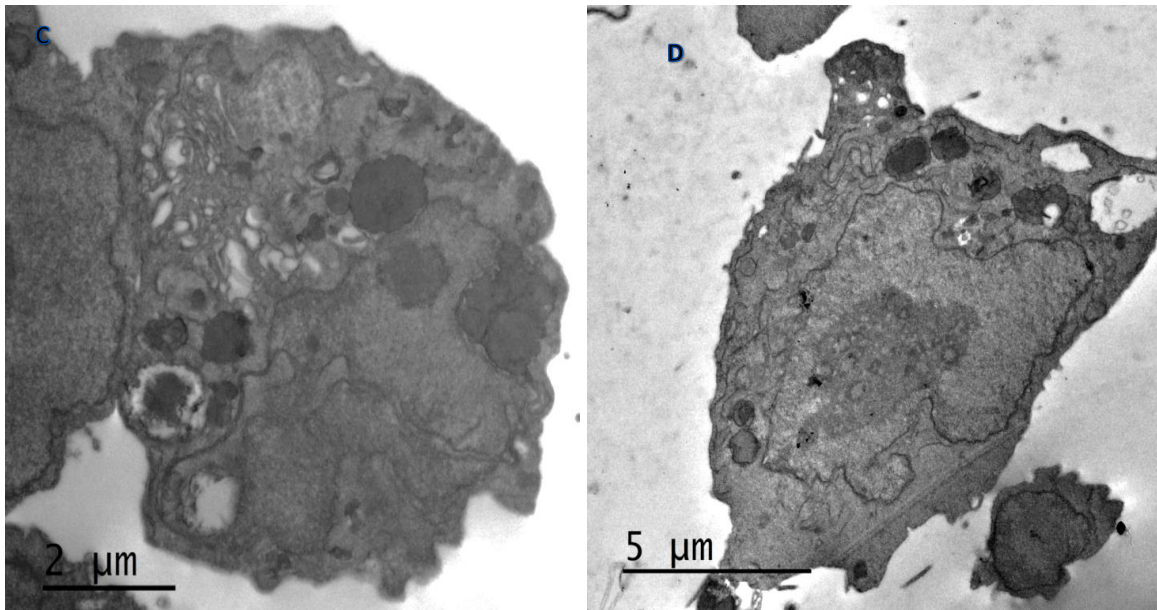


Figure 6.11: TEM micrographs show the control and HEK-293 cells exposed at 1800 MHz and powers of 17 dBm, 0 dBm, -10 dBm exposed at 37 °C for 2 hrs. Figure A: shows control HEK-293 cells kept at 37 °C, Figure B: HEK-293 cells exposed at 1800 MHz and 17 dBm, Figure C: HEK-293 cells exposed at 1800 MHz and 0 dBm, Figure D: HEK-293 cells exposed at 1800 MHz and -10 dBm

6.5 Concluding Remarks

Sub-study 1:

This study was aimed to investigate the hypothesis that low-power MW radiation can affect the bioactivity of TRPV4 channel proteins at room temperature (25°C). The hypothesis was tested at two different times of exposure, 4 hrs and 2 hrs. It is found that irradiation for 4 hrs and 2 hrs at 1800 MHz and 17 dBm sensitises the response/bioactivity of TRPV4 ion channels to its selective agonist GSK1016790A when compared to the control samples. This response is mainly due to the influx of Ca²⁺ through TRPV4 channel. Exposure at the powers of 0 dBm and -10 dBm produces no significant effect on ion channel's bio-activity when compared to control samples. The average maximum response was also studied. We observed that, at room temperature of 25°, irradiation at 0 dBm and -10 dBm induced no effect on ion channel, which is possibly due to saturation in channel response.

Sub-study 2:

Similar experiments were conducted at a body temperature of 37°C. In this sub-study, ion channel response to its agonist GSK-101 at two concentrations 0.1 nM and 1 nM was

studied. At the higher concentration, we could not see any difference in ion channel activity because the response was already saturated. It is interesting to note that the results obtained at 25°C and at 37°C were consistent, which indicates that the channel response was sensitised at 1800 MHz and 17 dBm because of the applied MW exposure, and that change in temperature does not affect the ion channel's response. We found that irradiation for 4 hrs and 2hrs at 1800 MHz and 17 dBm sensitises the response/bioactivity of TRPV4 ion channels to its selective agonist GSK1016790A when compared to the control samples. Irradiation at the powers 0 dBm and -10 dBm produces no significant difference between the control and test samples. The average maximum response was also studied at the peak response time, and it was observed that exposure for 4 hrs at 1800 MHz and 17 nM sensitised the response of TRPV4 to its selective agonist by 0.7682 ± 0.2954 for 0.1nM, 0.8274 ± 0.3774 for 1 nM; while at 10 dBm and 100 nM no significant response could be observed because of the saturation in GSK response; whereas at 0 dBm and -10 dBm, no significant changes in channel response were observed at the peak response time.

Sub-study 3:

TEM microscopy was performed on the HEK-293 cells exposed for 4 hrs and 2 hrs at body temperature of 37°C. TEM micrographs show significant changes in internal cellular organisation in HEK-293 cells exposed for 4 hrs at 1800 MHz and 17 dBm. There were significant leakage of cellular contents and blebbing observed. Minor disruptions were observed at 2 hrs of exposure; whereas irradiation at 0 dBm and -10 dBm induced minor internal changes in cells exposed for 4 hrs and 2 hrs.

These findings provide evidence that these particular non-thermal exposures induce changes in the gating function of TRPV4. Hence, long-term exposure at the power of 17dBm could lead to changes in the thermal sensation and thermoregulation, whereas the powers 0 dBm and -10 dBm do not produce any functional changes in the ion channel, despite minor structural changes being observed in TEM micrographs. Based on these results, we can conclude that these structural changes are not significant and do not affect the functional activity of TRPV4 ion channel proteins expressed in HEK-293 cells.

CHAPTER 7: CONCLUSION AND FUTURE DIRECTIONS

7.1 Conclusions

In the last five years, exposure to microwave (MW) radiation has dramatically increased due to advancements and penetration of communication technology, food-processing technology, and other industrial applications. The concept of non-thermal effects of MW radiation has received considerable attention in recent years and is the subject of intense debate in the scientific community. Non-thermal effects of MWs have been postulated to result from a direct interaction of the electric field with specific (polar) molecules in the reaction medium that is not related to a macroscopic temperature effect. Non-thermal biological effects of MWs depend on several physical parameters and biological variables [1]. Therefore, only results obtained under the same conditions of MW exposure should be compared in “replication” studies.

Essential features of non-thermal MW effects include the following [1, 2]:

- Effects of resonance type within specific frequency windows.
- Dependence on the type of signal, modulation, and polarisation.
- Decreasing Power Density (PD) by orders of magnitude can be compensated by an increase in exposure time. Therefore, duration of exposure may have a more significant role as compared to Power Density (PD).
- Cell density: radical scavengers/antioxidants have a potential to abolish MW effects.
- Genomic differences influence response to MWs [3].

This PhD research project was aimed at investigating the effects of low-power MW radiation on the selected cells and proteins, with a specific focus on the frequencies emitted by mobile phones. The frequencies selected for this investigation are used in 3G and 4G mobile networks. Following sub-studies were completed within the project.

[Effects of static and time-varying electric fields on the conformation of Conotoxin protein: a molecular modelling study \(Chapter 3\)](#)

In this computational molecular study, a range of static and time-varying electric fields was applied to the Conotoxin peptide to understand their effects on the peptide’s conformation.

Results show that, at the higher strength, external electric fields affect Conotoxin's structure. The findings are summarised and presented below.

In Sub-study 1, we explored the effects of the static electric fields of 0.01 V/nm, 0.001 V/nm and 0.0001 V/nm on the conformations of homologous Conotoxin peptides. Statistically significant effects were observed in the conformation of the peptide when Conotoxin has exposed to the electric field of the highest strength 0.01V/nm. These structural changes may lead to changes in its biological activity. These findings thus imply that the effects are field-strength dependent.

Sub-study 2 was aimed at investigating further the effects of static electric fields of much lower strengths (1e+9 V/m, 0.00123 V/m and 0.000055 V/m) on the structural stability of Conotoxin peptide. Results show that induced conformational changes in the peptide are directly affected by the strength of electric field. The electric field of 0.000055 V/m produced no effect on Conotoxin's structure. However, the strongest field of 1e+9 V/m produced major structural disruptions in the Conotoxin peptide. The number of hydrogen bonds formed was increased with the increase in electric field strength. Snapshots of Conotoxin at two selected time points, 500 and 1000 ps, indicate towards the unfolding of the peptide under the exposure at 1e+9 V/m electric field, which is the reason for the increase in the formation of hydrogen bonds between Conotoxin and water molecules.

Sub-study 3 explored the effects of oscillating (time-varying) electric fields of the strengths 2e-9 V/nm, 6e-9 V/nm and 4.7 V/nm on the structural stability of the Conotoxin peptide. Results show that selected fields induce conformational changes in the peptide, mainly at 4.7 V/ m, whereas no significant effects were observed at other two strengths/ powers at the frequency of 1800 MHz.

In essence, the above findings demonstrate that a computational method such as the Molecular Dynamics (MD) simulation presents a useful tool in the analysis of effects of external electric fields (stressor) on a peptide's structure and its functional properties. Knowledge gained through computational study can aid in understanding the mechanistic aspects of change in conformation of a peptide, to study the diseased condition under the effects of low strength static or varying electric fields. The use of MD simulation techniques can further be extended in exploring new applications of external static (or oscillating) electric fields, such as explaining the effects of novel food processing techniques, such as microwave,

radiofrequency, pulsed electric fields and electro-hydrodynamic drying, on the biochemical composition of food products.

Effects of Low Power Microwaves Radiation on Kinetics of L-Lactate Dehydrogenase (LDH) and Catalase Enzymes (Chapter 4)

The study using the LDH assay verified the hypothesis that the external low-power MW radiation could affect the catalytic activity of LDH enzyme at the frequencies of 2100 MHz, 2300 MHz and 2600 MHz, at the power of 17 dBm and -10 dBm, by either increasing or decreasing the rate of reaction. Kinetics of Catalase was studied under the MW exposure at the frequencies of 2100 MHz and 1800 MHz, and powers of 0dBm, -10dBm and 17dBm. The inhibitory and excitatory actions observed at the frequency of 2100 MHz indicate the dependence of chemical reactions on power and frequency of the applied MW exposure. At 1800 MHz and different powers (0dBm, -10dBm and 17dBm), no significant effects on the enzymatic activity were observed.

The results of these experiments suggest that both frequency and power of MW radiation contribute separately to modulating effects on the catalytic activity of LDH and Catalase enzymes. The experimental findings highlight that, even at the low powers, MW radiation can induce modulating effects at the frequencies used in 4G mobile phone networks. However, this requires further detailed investigation of a wide range of combinations of frequency and power to establish safe limits of MW exposures.

Effects of Microwaves at 1800 MHz and Different Low Powers on Yeast Cells (Chapter 5)

This study was aimed at testing the hypothesis that low-power MW radiation at the selected frequencies (1800 MHz and 2100 MHz) and powers (-10 dBm, 0 dBm, 17 dBm) can affect the growth rate of *S. Cerevisiae*. The findings reveal that MWs at 1800 MHz and power of 17 dBm, 0 dBm and -10 dBm could modulate (increase or inhibit) the proliferation of *S. Cerevisiae*, with no elevation in the temperature being observed during the experimentation. The spectrophotometric and morphological assessment data clearly show that the applied exposure induces modulating effects in yeast cells. In addition, the results demonstrate that MW at 2100 MHz and 17dBm can induce yeast cell death followed by their recovery. The statistical analysis (Chi-square test of independence) suggests that both frequency and power contribute independently towards the modulating effects observed in yeast cells growth. A significant increase in total cell count and changes in cell viability were seen upon exposure at

the powers of 0 dBm and -10 dBm, respectively. TEM images of the exposed samples show the disruptions in their internal cellular organisation, suggesting that MW exposure induces power-dependent effects in yeast cells.

In summary, the results of this study confirm the hypothesis that, even at the low powers of exposure (with no elevation in temperature), MW radiation can affect the standard cellular processes in the exposed *S. cerevisiae* cells. The findings imply that low-power MW radiation can induce modulating effects on cell growth and internal structural organisation. A further study is required to investigate the cause of the observed internal disruptions and surface changes in exposed yeast cells. Investigation of the effects of the same powers and different MW frequencies, used in mobile phone radiation, is also recommended.

Low Power Microwaves Induce Changes in Functional Properties of TRPV4, a Mechanically Activated Ion Channel (Chapter 6)

This study was aimed at investigating the hypothesis that low-power MW radiation can affect the bioactivity of TRPV4 channel proteins at room temperature of 25 °C. We tested this hypothesis at two different time points, i.e. at two hr and four hr of applied irradiation. Results suggest that MW exposure at 1800 MHz and the highest power of 17 dBm sensitises the response/bioactivity of TRPV4 ion channels to its selective agonist GSK1016790A, for both lengths of time exposure, when compared to the control samples. At the powers of 0 dBm and -10 dBm, no significant difference in the average maximum response was observed between the control and test samples.

Similar experiments were repeated at a body temperature of 37°C. In this sub-study, ion channel protein was given only two concentrations of its agonist GSK-101, 0.1 nM and 1 nM. It was interesting to note that the results obtained at 25°C and 37°C were consistent. This indicates that the ion channel response was sensitised at 1800 MHz and 17 dBm because of the applied MW exposure and that a change in the temperature does not affect its response. The average maximum response was also studied at the peak response time. It was observed that, for the MW exposure for 4 hr at 1800MHz and 17 dBm, the response of TRPV4 ion channel to its selective agonist GSK-101 varied as follows: 0.7682 ± 0.2954 (concentration 0.1nM), 0.8274 ± 0.3774 (concentration 1nM); whereas, at 0 dBm and -10 dBm, no significant change in response was observed at the peak response time.

In addition, TEM assessment was performed on the HEK-293 cells exposed for 4 hrs and 2 hrs at body temperature ($37^{\circ}\text{C} \pm 2^{\circ}\text{C}$). TEM micrographs show the significant changes in internal cellular organisation, particularly at 1800 MHz and 17 dBm, when cells were exposed to 4 hrs. There was significant leakage of cellular contents and blebbing observed. Only minor disruptions were observed at two hr of exposure; whereas, at 0 dBm and -10 dBm, minor internal changes were observed for both four hr and two hr of irradiation.

These findings provide evidence that these particular non-thermal forms of exposure induced changes in the gating function of TRPV4. Hence, long-term exposure at the power of 17dBm could lead to changes in the thermal sensation and thermoregulation, whereas exposure at the powers of 0 dBm and -10 dBm does not induce any change in the functional activity of TRPV4 expressed in HEK-293 cells, despite the fact that minor structural changes were seen in TEM micrographs.

In conclusion, this research project has successfully brought new knowledge to the field of bio-electromagnetics in general. As such, the outcomes of this PhD research have been published in peer-reviewed conferences, and three journal articles are under preparation. A complete list of publications by the author since the beginning of this PhD research project is presented as follows.

7.2 Future Work

Despite continuing research efforts aiming to understand the biological and health effects of low-power radiation on different biological media, the exact mechanisms behind non-thermal effects of MWs have not been fully elucidated. When discussing the biological and health effects of the radiation emitted by wireless communication devices, it is necessary to re-evaluate the meaning of terms, “thermal” and “non-thermal” effects. The following recommendations can be suggested:

1. The majority of published studies evaluating the effects of low-power MW radiation show conflicting results. It is apparent that the important parameters of MW radiation (frequency, intensity/power, exposure duration, and pulse modulation) are not properly controlled in “replication studies” on non-thermal effects of MWs, and therefore the data cannot be compared with the original results.

2. The mechanisms behind the observed non-thermal effects are not yet elucidated. There is a need to establish a national program via collaborative inter-institutional research involving biochemists, molecular biologists, engineers and physicists, to conduct interdisciplinary mechanistic studies on non-thermal effects of MWs (from mobile phones and base stations).
3. Based on the mounting evidence of biological non-thermal effects, new *in vivo* animal and human studies should be conducted. For public safety in the changed scenario, currently accepted industry standards for mobile phone exposure should be scrutinised. The frequency bands and power thresholds for mobile communication which do not affect human health should be identified.
4. Published *in vitro* studies indicate that the duration of exposure can be more critical for non-thermal effects than the intensity, and therefore effects of MWs from base stations on *primary human cells* should be studied [187-189]
5. There is a lack of studies performed on human volunteers to evaluate changes in biochemical reactions due to the applied electromagnetic radiation.
6. The minimal number of research studies conducted on human volunteers is a primary reason for our limited understanding of the effects of exposure of humans to MW radiation emitted by wireless communication devices on the physiology of cells/tissues/organs in the human body.

PUBLICATIONS

Conference Proceedings

- 1] Jain S., Vojisavljevic V., Pirogova E. (2015). Study of change in the enzymatic reaction under radiowaves/microwaves on lactic acid dehydrogenase and catalase at 2.1, 2.3 and 2.6 GHz: *Progress In Electromagnetics Research Symposium Proceedings*, Prague, Czech Republic, 6-9 July 2015.
- 2] Jain S., Vojisavljevic V., Pirogova E. (2016). “The Effects of Low Power Microwaves at 1.8GHz and 2.1GHz on Yeast Cells Growth” IEEE-APMC 2016, IIT Delhi, India.
- 3] Jain S., Vojisavljevic V., Pirogova E. (2016). “Low Power Microwaves at 1.8GHz and 2.1 GHz Induce Changes in Catalase Enzyme Kinetics.” IEEE-APMC 2016, IIT Delhi, India.
- 4] Jain S., Vojisavljevic V., Pirogova E. (2016). “Conformational Changes in Conotoxin Exposed to Static Electric Fields: A Molecular Modeling Study.” WIECON- IEEE 2016, Pune, India.
- 5] Jain S., Pirogova E. (2017). “Static electric field induces conformational changes in Alpha Conotoxin: A molecular simulation study” PIERS, 2017, NTU Singapore.
- 6] Jain S., Baratchi S., Pirogova E. (2017). “Low Power Microwaves Induce Changes in Gating Function of Trpv4 Ion Channel Proteins.” PIERS, 2017, NTU Singapore.

Journal Publications

- 1] **Jain S.**, Haleyur N., Dekiwadia C., Ball A.S., Pirogova E. “Effects of Low-Level Mobile Phone Radiation at 1800MHz on Yeast Cells” (submitted, under review).
- 2] **Jain S.**, Suresh A., Pirogova E., “Time-Dependent Electric Field Effects on Conotoxin Conformation: A molecular dynamics simulation study”. (Manuscript in preparation).
- 3] **Jain S.**, Dekiwadia C., Pirogova E. Baratchi S. “Low Power Microwaves Induce Changes in Gating Function of Trpv4 Ion Channel Proteins” (Manuscript in preparation).

REFERENCES

- [1] Gaestel, M., "Biological monitoring of non-thermal effects of mobile phone radiation: recent approaches and challenges," *Biological Reviews*, Review vol. 85, no. 3, p. 12, August 2010 2009.
- [2] (2015). *Number of mobile phone users worldwide from 2013 to 2019*. Available: <https://www.statista.com/statistics/274774/forecast-of-mobile-phone-users-worldwide/>
- [3] Lai, H. and Singh, N. P., "Single-and double-strand DNA breaks in rat brain cells after acute exposure to radiofrequency electromagnetic radiation," *International Journal of Radiation Biology*, vol. 69, no. 4, p. 9, 1996.
- [4] Liu, C. *et al.*, "Mobile phone radiation induces mode-dependent DNA damage in a mouse spermatocyte-derived cell line: A protective role of melatonin," *International Journal of Radiation Biology*, vol. 89, no. 11, p. 9, 2013.
- [5] M, T., B, O., OG, D., and S, K., "The role of electromagnetic fields in neurological disorders," *Journal of Chemical Neuroanatomy*, vol. 75, no. Pt B, p. 8, 2016.
- [6] Areti K. Manta *et al.*, "Mobile-phone radiation-induced perturbation of gene-expression profiling, redox equilibrium and sporadic-apoptosis control in the ovary of *Drosophila melanogaster*," *FLY*, vol. 11, no. 2, p. 11, 2016.
- [7] Arnold Kuzniar *et al.*, "Semi-quantitative proteomics of mammalian cells upon short-term exposure to nonionizingelectromagnetic fields," *PLOSone*, pp. 1-25, 2017.
- [8] Kwon MS, V. V., Kännälä S, Laine M, Rinne JO, Toivonen T, Johansson J, Teras M, Lindholm H, Alanko T, Hamalainen H., " Effects of cell phone radiofrequency signal exposure on brain glucose metabolism.," *JAMA*, vol. 305, no. 8, p. 6, 2011.
- [9] Kwon MS, V. V., Kännälä S, Laine M, Rinne JO, Toivonen T, Johansson J, Teras M, Lindholm H, Alanko T, Hamalainen H., "No effects of short-term GSM mobile phone radiation on cerebral blood flow measured using positron emission tomography.," *Bioelectromagnetics* vol. 33, no. 3, p. 9, 2012.
- [10] L., V., "Evaluations of international expert group reports on the biological effects of radiofrequency fields.," *Wireless communications and networks Recent advances. Rijeka, Croatia: Intech*, pp. 523-546, 2012.
- [11] ARPANSA, "Radiofrequency Electromagnetic Energy and Health: Research Needs," Australian Radiation Protection and Nuclear Safety Agency (ARPANSA), Victoria, Australia2017.
- [12] *Maximum Exposure Levels to Radiofrequency Fields - 3 kHz to 300 GHz*, 2002.
- [13] ARPANSA, "Analysis of EMR Health Complaints Register Data 2015–2016," ARPANSA2016.
- [14] Gromozova, E., Voychuk, S., Zelen, L., and Gretsky, I., "Microorganisms as a Model System for Studying the Biological Effects of Electromagnetic Non-ionizing Radiation," presented at the First International Conference on Radiation and Dosimetry in Various Fields of Research, Serbia, 25-27 April 2012, 2011.
- [15] "IEEE Standard for Safety Levels with Respect to Human Exposure to Radio Frequency Electromagnetic Fields, 3 kHz to 300 GHz," *IEEE Std C95.1-2005 (Revision of IEEE Std C95.1-1991)*, p. 238, 2006.
- [16] ICNIRP, "ICNIRP Statement on the "Guidelines for limiting exposure to time-varying electric, magnetic and electromagnetic fields (up to 300 GHz)", " *Health Physics*, vol. 97, no. 3, p. 2, 2009.

- [17] ICNIRP, "ICNIRP Guidelines For Limiting Exposure to Time-varying electric, magnetic and electromagnetic fields (up to 300 GHz)," *Health Physics*, vol. 74, no. 4, p. 31, 1998.
- [18] Sage, C., "Bioinitiative 2012: Summary for the Public (2014 Supplement)," BioInitiative Working Group, CA, USA 2014.
- [19] Loughran, S. P. *et al.*, "Bioelectromagnetics Research within an Australian Context: The Australian Centre for Electromagnetic Bioeffects Research (ACEBR)." *International Journal of Environmental Research and Public Health*, Review vol. 13, no. 10, p. 14, 29 September 2016 2016.
- [20] Alshaim, H. S., Vojisavljevic, V., and Pirogova, E., "Effects of low power microwaves at 1.8, 2.1, and 2.3 GHz on l-Lactic dehydrogenase and Glutathione peroxidase enzymes," *Journal of Electromagnetic Waves and Applications*, vol. 28, no. 14, p. 10, 2014.
- [21] Shamis, Y., Traub, A., Croft, R. J., Crawford, R., and Ivanova, E., "Influence of 18GHz microwave radiation on the enzymatic activity of Escherichia coli lactate dehydrogenase and cytochrome c oxidase," *Journal of Physical Science and Application*, vol. 2, no. 6, p. 9, 15.06.2012 2012.
- [22] Maroto, R., Raso, A., Wood, T. G., Kurosky, A., Martinac, B., and Hamill, O. P., "TRPC1 forms the stretch-activated cation channel in vertebrate cells," *Nature Cell Biology*, vol. 7, no. 2, p. 179, 01/23/online 2005.
- [23] Spassova, M. A., Hewavitharana, T., Xu, W., Soboloff, J., and Gill, D. L., "A common mechanism underlies stretch activation and receptor activation of TRPC6 channels," *Proceedings of National Academy of Science of the United States of America*, vol. 103, no. 44, p. 6, 2006.
- [24] Kunert-Keil, C., Bisping, F., Krüger, J., and Brinkmeier, H., "Tissue-specific expression of TRP channel genes in the mouse and its variation in three different mouse strains," *BMC Genomics*, vol. 7, no. 159, p. 14, 2006/06/20 2006.
- [25] Rafia, M., Sajjad, K., Mohammad, A. K., Wilson, C. M., and Zeenat, M., "Conotoxins: Structure, Therapeutic Potential and Pharmacological Applications," *Current Pharmaceutical Design*, vol. 22, no. 5, p. 8, 2016.
- [26] Nguyen, T. P. *et al.*, "The Bioeffects Resulting from Prokaryotic Cells and Yeast Being Exposed to an 18 GHz Electromagnetic Field," *PLoS/One*, vol. 7, no. 11, p. 19, 2016.
- [27] Jain, S., Vojisaveljevic, V., and Pirogova, E., "The Effects of Low Power Microwaves at 1800 MHz and 2100 MHz on Yeast Cells Growth," presented at the IEEE International Microwave and RF Conference (IMarC), New Delhi, 2016.
- [28] NL, D. and DJ, C., "Structural studies of conotoxins," *IUBMB Life*, Critical Review vol. 61, no. 2, p. 7, 2009.
- [29] NASA. (2013). *The Electromagnetic Spectrum*. Available: <https://imagine.gsfc.nasa.gov/science/toolbox/emspectrum1.html>
- [30] <http://www.arpana.gov.au>, A. A. R. P. a. N. S. A. A.
- [31] Domenech, H., "Biological Effects of Ionizing Radiation," in *Radiation Safety XV* ed.: Springer, Cham, 2017, p. 14.
- [32] (WHO), W. H. O., "Electromagnetic fields and public health: mobile telephones and their base stations," in "FS N 193," World Health Organization (WHO) 2014.
- [33] . *Radio wave*. Available: https://en.wikipedia.org/wiki/Radio_wave
- [34] Mohankumar, D. (2016). *Mobile Phone Communication. How it works?*
- [35] Al-Serori, H. *et al.*, "Evaluation of the potential of mobile phone specific electromagnetic fields (UMTS) to produce micronuclei in human glioblastoma cell lines," *Toxicology in Vitro*, vol. 40, p. 8, 2017.

- [36] (2018). *ACMA consults on 5G spectrum auction arrangements*. Available: <https://www.acma.gov.au/theACMA/acma-consults-on-5g-spectrum-auction-arrangements>
- [37] Megha, K., Deshmukh, P. S., Ravi, A. K., Tripathi, A. K., Abegaonkar, M. P., and Banerjee, B. D., "Effect of Low-Intensity Microwave Radiation on Monoamine Neurotransmitters and Their Key Regulating Enzymes in Rat Brain," *Cell Biochemistry and Biophysics*, vol. 73, no. 1, p. 8, 2015.
- [38] Sahin, D. *et al.*, "The 2100 MHz radiofrequency radiation of a 3G-mobile phone and the DNA oxidative damage in the brain," *Journal of Chemical Neuroanatomy*, vol. 75, p. 5, 2016.
- [39] "Maximum Exposure Levels to Radiofrequency Fields – 3 kHz to 300 GHz, Annex 3: Epidemiological studies of exposure to radio frequencies and human health," Australian Radiation Protection and Nuclear Safety Agency Sydney 2008.
- [40] (2018). *Electromagnetic Fields and Public Health: Mobile Phones and Health*. Available: <https://www.medikalnotes.com/2018/04/electromagnetic-fields-public-health-mobile-phones.html>
- [41] "Interphone study reports on mobile phone use and brain cancer risk," I. A. o. R. o. Cancer, Ed., ed: World Health Organisation, 2010, p. 3.
- [42] Panagopoulos, D. J. and Margaritis, L. H., "Mobile Telephony Radiation Effects on Living Organism," in *Mobile Telephones: Networks, Applications, and Performance*, A. C. Harper and R. V. Buress, Eds.: Nova Science Publishers, 2008, p. 43.
- [43] "Review of Radiofrequency Health Effects Research – Scientific Literature 2000 – 2012," in "ARPANSA Technical Report No. 164," Australian Radiation Protective and Nuclear Safety Agency, Yallambie, Vic 2014.
- [44] Ng, K.-H., "Non-Ionizing Radiations – Sources, Biological Effects, Emissions and Exposures," in *International conference on Non-Ionising Radiations (ICNIR)*, Kuala Lumpur - Malaysia, 2003, p. 16.
- [45] "New study: direct link to 4,924 cancer deaths from cellular antennas radiation.," ed. Brazil, 2011.
- [46] "Electromagnetic fields and public health: mobile telephones and their base stations," in "WHO: Electromagnetic fields and public health," World Health Organization (WHO) 2010, Available: <http://www.who.int/mediacentre/factsheets/fs193/en>.
- [47] Paulraj, R. and Behari, J., "Single strand DNA breaks in rat brain cells exposed to microwave radiation," *Mutation Research/Fundamental and Molecular Mechanisms of Mutagenesis*, vol. 596, no. 1-2, p. 5, 2006.
- [48] ND, V. *et al.*, "Effects of cell phone radiofrequency signal exposure on brain glucose metabolism.," *Journal of American Medical Association*, vol. 305, no. 8, p. 6, 2011.
- [49] Prasad, M., Kathuria, P., Nair, P., Kumar, A., and Prasad, K., "Mobile phone use and risk of brain tumours: a systematic review of association between study quality, source of funding, and research outcomes," *Neurological Sciences*, p. 14, 2017.
- [50] "WHO Research Agenda For Radiofrequency Fields," World Health Organisation, Geneva, Switzerland 2010.
- [51] Group, T. I. S., "Brain tumour risk in relation to mobile telephone use: results of the INTERPHONE international case-control study," *International Journal of Epidemiology*, vol. 39, no. 3, p. 20, 2010.
- [52] AF, F., P, M., A, S., F, S., SL, K., and LH., M., "Whole body exposure with GSM 900 MHz affects spatial memory in mice," *Pathophysiology*, vol. 17, no. 3, p. 9, 2010.
- [53] Leszczynski, D., Joenväärä, S., Reivinen, J., and Kuokka, R., "Non-thermal activation of the hsp27/p38MAPK stress pathway by mobile phone radiation in human

- endothelial cells: Molecular mechanism for cancer- and blood-brain barrier-related effects," *Differentiation*, vol. 70, no. 2-3, p. 10, 2002.
- [54] Racuciu, M., Miclaus, S., and Creanga, D., "On the thermal effect induced in tissue samples exposed to the extremely low-frequency electromagnetic field," vol. 13, no. 85, p. 12, 2015.
- [55] Ghanbari, M., Mortazavi, S. B., Khavanin, A., and Khazaei, M., "The Effects of Cell Phone Waves (900 MHz-GSM Band) on Sperm Parameters and Total Antioxidant Capacity in Rats," *International Journal of Fertility and Sterility*, vol. 7, no. 1, p. 6, 2013.
- [56] Aydogan, F. *et al.*, "The effect of 2100 MHz radiofrequency radiation of a3G mobile phone on the parotid gland of rats," *American Journal of Otolaryngology-Head and Neck Medicine and Surgery*, vol. 36, no. 1, p. 8, 2015.
- [57] Chen, C. *et al.*, "Exposure to 1800 MHz radiofrequency radiation impairs neurite outgrowth of embryonic neural stem cells," *Scientific Reports*, vol. 4, no. 5103, p. 10, 2014.
- [58] Barnes, F. S. and Greenebaum, B., *Handbook of Biological Effects of Electromagnetic Fields*, 3 ed. CRC Press, 2006, p. 960.
- [59] Vander Vorst, A., Rosen, A., and Kotsuka, Y., *RF/Microwave Interaction with Biological Tissue*. Wiley-Interscience, 2006, p. 330.
- [60] (2016). *Electromagnetic Radiation Health Complaints Register: Analysis of EMR Health Complaints Register Data 2015–2016*.
- [61] E Neumann, M Schaefer-Ridder, Y Wang, and Hofschneider, P. H., "Gene transfer into mouse lyoma cells by electroporation in high electric fields.," *The EMBO Journal*, vol. 1, no. 7, p. 5, 1982.
- [62] Kruse AC, Hu J, Pan AC, Arlow DH, Rosenbaum DM, and E, R., "Structure and dynamics of the M3 muscarinic acetylcholine receptor," *Nature*, no. 482, p. 5, 2012.
- [63] Astrakas, L., Gousias, C., and Tzaphlidou, M., "Electric field effects on chignolin conformation," *Journal of Applied Physics*, vol. 109, no. 9, p. 5, 2011.
- [64] Bekard, I. and Dunstan, D. E., "Electric field induced changes in protein conformation.," *Soft Matter*, vol. 10, no. 3, p. 7, 2014 Jan 21; 2014.
- [65] Budi, A., Legge, F. S., Treutlein, H., and Yarovsky, I., "Electric field effects on insulin chain-B conformation," *Journal of Physical Chemistry*, vol. 109, no. 47, p. 8, 2005.
- [66] Marracino, P., Apollonio, F., Liberti, M., d'Inzeo, G., and Amadei, A., "Effect of high exogenous electric pulses on protein conformation: myoglobin as a case study," *The Journal of Physical Chemistry* vol. 117, no. 8, p. 7, 2013.
- [67] Singh, A., Orsat, V., and Raghavan, V., "Soybean Hydrophobic Protein Response to External Electric Field: A Molecular Modeling Approach," *Biomolecules*, vol. 3, no. 1, p. 12, 2013.
- [68] Edwin Lok, Van Hua, and Eric T. Wong, "Computed modelling of alternating electric fields therapy for recurrent glioblastoma," *Cancer Medicine*, vol. 4, no. 11, pp. 1697–1699, 2015.
- [69] Singh, A., Munshi, S., and Vijaya, R., "Effect of External Electric Field Stress on Gliadin Protein Conformation," *Proteomes* vol. 1, no. 2, p. 15, 04.07.2013 2013.
- [70] Prithwish K. Nandi, Zdenek Futera, and English, N. J., "Perturbation of hydration layer in solvated proteins by external electric and electromagnetic fields: Insights from non-equilibrium molecular dynamics," *The Journal of Chemical Physics*, vol. 145, pp. 205101-205110, 2016.
- [71] Ojeda-May, P. and E. Garcia, M., "Electric Field-Driven Disruption of a Native β -Sheet Protein Conformation and Generation of a Helix-Structure," *Biophysical Journal* vol. 99, no. 2, p. 5, 2010.

- [72] Fallah, Z., Jamali, Y., and Rafii-Tabar, H., "Structural and Functional Effect of an Oscillating Electric Field on the Dopamine-D3 Receptor: A Molecular Dynamics Simulation Study," *PLoS/ONE*, vol. 11, no. 11, p. 15, November 10, 2016 2016.
- [73] Astrakas, L., Gousias, C., and Tzaphlidou, M., "Electric field effects on alanine tripeptide in sodium halide solutions," *Electromagnetic Biology and Medicine*, vol. 34, no. 4, p. 9, 2015.
- [74] Hess, B., Kutzner, C., van der Spoel, D., and Erik, L., "GROMACS 4: Algorithms for Highly Efficient, Load-Balanced, and Scalable Molecular Simulation.," *Journal of Chemical Theory Computation*, vol. 4, no. 3, p. 13, 2008.
- [75] MacKerell, A. D. J., Banavali, N., and Foloppe, N., "Development and current status of the CHARMM force field for nucleic acids.," *Biopolymers*, vol. 56, no. 4, p. 9, 2001.
- [76] Du, W.-H., Han, Y.-H., Huang, F.-j., Li, J., Chi, C.-W., and Fang, W.-H., "Solution structure of an M-1 conotoxin with a novel disulfide linkage," *The FEBS Journal*, vol. 274, no. 10, p. 7, 2007.
- [77] Diema, E., Schwarza, C., Adlkoferb, F., Jahna, O., and Rüdiger, H., "Non-thermal DNA breakage by mobile-phone radiation (1800 MHz) in human fibroblasts and in transformed GFSH-R17 rat granulosa cells in vitro," *Mutat Res*, vol. 583, no. 2, p. 6, 2005.
- [78] Fernandes, G. H. C. *et al.*, "The Effect of low-Level Laser Irradiation on Sperm Motility, and Integrity of the Plasma Membrane and Acrosome in Cryopreserved Bovine Sperm," *PLoS/ONE*, vol. 10, no. 3, p. 11, March 17, 2015 2015.
- [79] Manna, D. and Ghosh, R., "Effect of radiofrequency radiation in cultured mammalian cells: A review.," *Electromagnetic Biology and Medicine Review Article* vol. 35, no. 3, p. 37, 2016.
- [80] Editor, "Electromagnetic fields and public health: mobile phones, W.H.O. (WHO)," 2014.
- [81] Wang, X., Li, Y., He, X., Chen, S., and Zhang, J. Z. H., "Effect of Strong Electric Field on the Conformational Integrity of Insulin," *The Journal of Physical Chemistry*, vol. 118, no. 39, p. 11, 2014.
- [82] Joa, D. J. *et al.*, "Biomolecular structure manipulation using tailored electromagnetic radiation: a proof of concept on a simplified model of the active site of bacterial DNA topoisomerase," *Physical Chemistry Chemical Physics*, vol. 16, no. 39, p. 10, 2014.
- [83] Spoel, D. V. D., Lindahl, E., Hess, B., Groenhof, G., Mark, A. E., and Berendsen, H. J. C., "GROMACS: fast, flexible, and free.," *Journal of Computational Chemistry*, vol. 26, no. 16, p. 18, 6 October 2005 2005.
- [84] Zeni, O. *et al.*, "Evaluation of genotoxic effects in human peripheral blood leukocytes following an acute in vitro exposure to 900 MHz radiofrequency fields," *Bioelectromagnetics*, vol. 26, no. 4, p. 8, 2005.
- [85] Peinnequina, A. *et al.*, "Non-thermal effects of continuous 2.45 GHz microwave on Fas-induced apoptosis in human T-cell line," *Bioelectrochemistry*, vol. 51, no. 2, p. 5, 2000.
- [86] Dutta, S. K., Das, K., Ghosh, B., and Blackman, C., "Dose dependence of acetylcholinesterase activity in neuroblastoma cells exposed to modulated radio-frequency electromagnetic radiation," *Bioelectromagnetics*, vol. 13, no. 4, p. 6, 1992.
- [87] Botstein, D. and Fink, G. R., "Yeast: An Experimental Organism for 21st Century Biology," *Genetics*, vol. 189, no. 3, p. 10, 2011.
- [88] Alshaim, H. S., Vojisavljevic, V., and Pirogova, E., "The Effects of Low Power Microwaves at 500MHz and 900MHz on Yeast Cells Growth," in *Progress In Electromagnetics Research Symposium Proceedings*, Taipei, 2013, p. 4: IEEE.

- [89] Vrhovac, I., Hrascan, R., and Franekic, J., "Effect of 905 MHz microwave radiation on colony growth of the yeast *Saccharomyces cerevisiae* strains FF18733, FF1481 and D7," *Radiology and Oncology*, Research Article vol. 44, no. 2, p. 4, 2010.
- [90] Grundler, W. and Kaiser, F., "Experimental evidence for coherent excitations correlated with cell growth," *Nanobiology*, vol. 1, p. 14, 1992.
- [91] Grundler, W. and Keilmann, F., "Nonthermal effects of millimetre microwaves on yeast growth.," *Z Naturforsch C Biosci*, vol. 33, no. 1-2, p. 8, 1978.
- [92] Kwon, M. S. *et al.*, "GSM mobile phone radiation suppresses brain glucose metabolism," *Journal of Cerebral Blood Flow & Metabolism*, vol. 31, no. 12, p. 9, 2011.
- [93] French, P. W., Penny, R., Laurence, A. L., and McKenzie, D. R., "Mobile phones, heat shock proteins and cancer.," *Differentiation*, vol. 67, no. 4-5, p. 5, 2001.
- [94] Cancer, I. A. f. R. o., "IARC Classifies Radiofrequency Electromagnetic Fields as Possibly Carcinogenic to Humans," in *Press Release N 208*, ed: World Health Organization, 2011.
- [95] Belyaev, I. Y. *et al.*, "915 MHz microwaves and 50 Hz magnetic field affect chromatin conformation and 53BP1 foci in human lymphocytes from hypersensitive and healthy persons," *Bioelectromagnetics*, vol. 26, no. 3, p. 13, 2005.
- [96] Belyaev, I. Y., Markovà, E., Hillert, L., Malmgren, L. O. G., and Persson, B. R. R., "Microwaves from UMTS/GSM mobile phones induce long-lasting inhibition of 53BP1/gamma-H2AX DNA repair foci in human lymphocytes," *Bioelectromagnetics*, vol. 30, no. 2, p. 13, 2009.
- [97] Jeffrey, S., "Cell Phone Use Affects Brain Glucose Metabolism," in *Medspace Medical News, Neurology News*, ed, 2011.
- [98] Elwood, J. M., "Epidemiological studies of radio frequency exposures and human cancer," *Bioelectromagnetics Supplement*, vol. 6, p. 11, 2003.
- [99] Hardell, L., Carlberg, M., and Mild, K. H., "Case-control study of the association between the use of cellular and cordless telephones and malignant brain tumors diagnosed during 2000-2003," *Environmental Research*, vol. 100, no. 2, p. 10, 2006.
- [100] Breckenkamp, J., Berg, G., and Blettner, M., "Biological effects on human health due to radiofrequency/microwave exposure: a synopsis of cohort studies," *Radiation and Environmental Biophysics*, vol. 42, no. 3, p. 14, 2003.
- [101] Zhao, Y., Ma, H.-b., Song, J.-p., Yang, Y.-H., Pu, J.-s., and Zheng, J.-q., "Effects of microwave irradiation on ATPase activity and voltage dependent ion channel of rat hippocampus cell membrane," *Space Medico Medicine Engineering*, vol. 16, no. 1, p. 5, 2003.
- [102] Alekseev, S. I. and Ziskin, M. C., "Millimeter microwave effect on ion transport across lipid bilayer membranes," *Bioelectromagnetics*, vol. 16, no. 2, p. 8, 1995.
- [103] Blackman, C., Elder, J. A., Weil, C. M., Benane, S. G., Eichinger, D. C., and House, D. E., "Induction of calcium-ion efflux from brain tissue by radio-frequency radiation: Effects of modulation frequency and field strength," *Radio Science*, vol. 14, no. 6S, p. 6, 1979.
- [104] Adey, W. R., Bawin, S. M., and Lawrence, A. F., "Effects of weak amplitude-modulated microwave fields on calcium efflux from awake cat cerebral cortex," *Bioelectromagnetics*, vol. 3, no. 3, p. 13, 1982.
- [105] Chiang, H., Hu, G., and Xu, Z., "Effects of extremely low frequency magnetic fields on gap junctional intercellular communication and its mechanism," *Progress in Natural Science*, vol. 12, no. 3, p. 4, 2002.
- [106] Campisi, A. *et al.*, "Reactive oxygen species levels and DNA fragmentation on astrocytes in primary culture after acute exposure to low intensity microwave electromagnetic field," *Neuroscience Letters*, vol. 473, no. 1, p. 4, 2010.

- [107] Cleary, S. F., Cao, G., and Liu, L.-M., "Effects of isothermal 2.45 GHz microwave radiation on the mammalian cell cycle: comparison with effects of isothermal 27 MHz radiofrequency radiation exposure," *Bioelectrochemistry and Bioenergetics*, vol. 9, no. 2, p. 7, 1996.
- [108] Pirogova, E., Cosic, I., Fang, J., and Vojisavljevic, V., "Use of infrared and visible light radiation as modulator of protein activity " *Estonian Journal of Engineering*, vol. 14, no. 2, p. 14, 2008.
- [109] Hamad S. Alsuhaime, Vuk Vojisavljevic, and Pirogova, E., "Effects of low power microwaves at 1.8, 2.1, and 2.3 GHz on I-Lactic dehydrogenase and Glutathione peroxidase enzymes," *Journal of Electromagnetic Waves and Applications*, vol. 28, no. 14, p. 9, 2014.
- [110] Vojisavljevic, V., Pirogova, E., and Cosic, I., "The effect of electromagnetic radiation (550-850 nm) on l-lactate dehydrogenase kinetics," *International Journal of Radiation Biology*, vol. 83, no. 4, p. 10, 2007.
- [111] Volkow, N. D. *et al.*, "Effects of Cell Phone Radiofrequency Signal Exposure on Brain Glucose Metabolism," *Journal of American Medical Association*, vol. 305, no. 8, p. 6, 2011.
- [112] Black, B., Granja-Vazquez, R., Johnston, B. R., Jones, E., and Romero-Ortega, M., "Anthropogenic Radio-Frequency Electromagnetic Fields Elicit Neuropathic Pain in an Amputation Model," *PLoS/ONE*, p. 17, 2016.
- [113] Zhang, G. *et al.*, "Effects of cell phone use on semen parameters: Results from the MARHCS cohort study in Chongqing, China," *Environment International*, vol. 91, p. 6, 2016.
- [114] Yu` Ksel, M., Nazirog`lu, M., and Okan, M. O. z., "Long-term exposure to electromagnetic radiation from mobile phones and Wi-Fi devices decreases plasma prolactin, progesterone, and estrogen levels but increases uterine oxidative stress in pregnant rats and their offspring.," *Endocrine*, vol. 52, no. 2, p. 11, 2016.
- [115] Dutta, S. K., Subramoniam, A., Ghosh, B., and Parshad, R., "Microwave radiation-induced calcium ion efflux from human neuroblastoma cells in culture," *Bioelectromagnetics*, vol. 5, no. 1, 1984.
- [116] Shckorbatov, Y. G. *et al.*, "Application of intracellular microelectrophoresis to analysis of the influence of the low-level microwave radiation on electrokinetic properties of nuclei in human epithelial cells," *Electrophoresis*, vol. 23, no. 13, 2002.
- [117] Deshmukh, P. S. *et al.*, "Detection of Low Level Microwave Radiation Induced Deoxyribonucleic Acid Damage Vis-à-vis Genotoxicity in Brain of Fischer Rats," *Toxicology International*, vol. 20, no. 1, p. 6, 2013.
- [118] Paulraj, R. and Behari, J., "Biochemical Changes in Rat Brain Exposed to Low Intensity 9.9 GHz Microwave Radiation," *Cell Biochemistry and Biophysics*, vol. 63, no. 1, p. 6, 2012.
- [119] Vladimirovna, L. A., Stanislavovich, B. S., and Vladimirovich, T. I., "Production of cytokines, soluble forms of costimulatory molecules and nitric oxide in patients with coronary heart disease under the influence of nonthermal microwave irradiation with a frequency of 1 GHz " *European Journal of Biomedical and Life Sciences*, 2016.
- [120] Banik, S., Bandyopadhyay, S., and Ganguly, S., "Bioeffects of Microwave—A Brief Review," *Biosource Technology*, vol. 87, p. 5, 2003.
- [121] J, W., "Electromagnetic field effects on cells of the immune system: the role of calcium signalling," *FASEB Journal*, 1992.
- [122] FJ, P., "Use of calcium channel antagonist as magnetoprotective agents," *Radiation Research*, vol. 122, pp. 24-28, 1990.

- [123] Pilla, A. A., "Electromagnetic field instantaneously modulate nitric oxide signalling in challenged biological systems," *Biochemical and Biophysical Research Communications*, vol. 426, no. 3, p. 4, 2012.
- [124] Patapoutian, A., Peier, A. M., Story, G. M., and Viswanath, V., "ThermoTRP channels and beyond: mechanisms of temperature sensation," *Nature Reviews Neuroscience*, vol. 4, p. 11, 2003.
- [125] Fragopoulou, A. *et al.*, "Scientific panel on electromagnetic field health risks: consensus points, recommendations, and rationales," *Review on Environmental Health*, vol. 25, no. 4, p. 11, 2010.
- [126] Veeldersa, M., Brücknerb, S., Ottc, D., Unverzagt, C., Möschb, H.-U., and Essen, L.-O., "Structural basis of flocculin-mediated social behavior in yeast," *Proceedings of National Academy of Science of the United States of America*, vol. 107, no. 52, p. 6, 2010.
- [127] "What effects do mobile phones have on people's health?," World Health Organisation (WHO), Denmark 2006.
- [128] Phillips, J. L., Ivaschuk, O., Ishida-Jones, T., Jones, R. A., Campbell-Beachler, M., and Haggren, W., "DNA damage in Molt-4 T-lymphoblastoid cells exposed to cellular telephone radiofrequency fields in vitro," *Bioelectrochemistry and Bioenergetics*, vol. 45, no. 1, p. 8, 1998.
- [129] Panagopoulos, D. J., Karabarbounis, A., and Margaritis, L. H., "Effect of GSM 900MHz Mobile Phone Radiation on the Reproductive Capacity of *Drosophila Melanogaster*," *Electromagnetic Biology and Medicine*, vol. 23, no. 1, p. 15, 2004.
- [130] Malyapa, R. S. *et al.*, "Measurement of DNA damage after exposure to electromagnetic radiation in the cellular phone communication frequency band (835.62 and 847.74 MHz)," *Radiation Research*, vol. 148, no. 6, p. 10, 1997.
- [131] Valbonesi, P., Franzellitti, S., Bersani, F., Contin, A., and Fabbri, E., "Activity and expression of acetylcholinesterase in PC12 cells exposed to intermittent 1.8 GHz 217-GSM mobile phone signal," *International Journal of Radiation Biology*, vol. 92, no. 1, p. 10, 2015.
- [132] Tomomi Kurashige, Mika Shimamura, and Nagayama, Y., "Differences in the quantification of DNA double-strand breaks assessed by 53BP1/ γ H2AX focus formation assays and the comet assay in mammalian cells treated with irradiation and N-acetyl-L-cysteine," *Journal of Radiation Research*, vol. 57, no. 3, pp. 312–317, 2016.
- [133] Zeni, O. *et al.*, "Lack of genotoxic effects (micronucleus induction) in human lymphocytes exposed in vitro to 900 MHz electromagnetic fields," *Radiation Research*, vol. 160, no. 2, p. 8, 2003.
- [134] ICNIRP, "Review of the scientific evidence on dosimetry, biological effects, epidemiological observations, and health consequences concerning exposure to high-frequency electromagnetic fields (100 kHz to 300 GHz) " International Commission on Non-Ionizing Radiation Protection, Germany 2009.
- [135] "Electromagnetic fields and public health: mobile phones," vol. 2014, ed: World Health Organisation, 2014, p. Fact sheet N°193.
- [136] Hussein, S., El-Saba, A. A., and Gala, M. K., "Biochemical and histological studies on adverse effects of mobile phone radiation on rat's brain," *Journal of Chemical Neuroanatomy*, vol. 78, p. 9, 2016.
- [137] Vijayalaxmi and Prihoda, T., "Genetic Damage in Mammalian Somatic Cells Exposed to Radiofrequency Radiation: A Meta-analysis of Data from 63 Publications (1990–2005)," *Radiation Research*, vol. 169, no. 5, p. 14, 2008.

- [138] Fuqiang Xing, Qiuqiang Zhan, Yiduo He, Jiasheng Cui, Sailing He, and Wang, G., "1800MHz Microwave Induces p53 and p53-Mediated Caspase-3 Activation Leading to Cell Apoptosis In Vitro," *PLoS One*, Research Article 2016.
- [139] Chen, H., Qu, Z., and Liu, W., "Effects of Simulated Mobile Phone Electromagnetic Radiation on Fertilization and Embryo Development," *Fetal and Pediatric Pathology*, vol. 1, no. 7, p. 7, 2016.
- [140] Tang, J. *et al.*, "Exposure to 900 MHz electromagnetic fields activates the mep-1/ERK pathway and causes blood-brain barrier damage and cognitive impairment in rats," *Brain Research*, vol. 1601, p. 10, 2015.
- [141] Eris, A. H. *et al.*, "Effect of Short-term 900 MHz low level electromagnetic radiation exposure on blood serotonin and glutamate levels.," *Bratislava Medical Journal*, vol. 116, no. 2, p. 3, 2015.
- [142] Li, H.-J. *et al.*, "Alterations of cognitive function and 5-HT system in rats after long-term microwave exposure.," *Physiology & Behavior*, vol. 140, p. 11, 2015.
- [143] Zothansiam, Zosangzuali, M., Lalramdinpuui, M., and Jagetia, G. C., "Impact of radiofrequency radiation on DNA damage and antioxidants in peripheral blood lymphocytes of humans residing in the vicinity of mobile phone base stations," *Electromagnetic Biology and Medicine*, vol. 36, no. 3, p. 11, 2017.
- [144] Wyde, M. *et al.*, "Report of Partial Findings from the National Toxicology Program Carcinogenesis Studies of Cell Phone Radiofrequency Radiation in Hsd : Sprague Dawley® SD rats (Whole Body Exposures)," US National Toxicology Program 2016.
- [145] Leszczynski, D., "Brief Report on the Gaps in the Knowledge about the Health Effects of the RF-EMF Exposures," ed, 2017, p. 7.
- [146] Jain, S., Vojisaveljevic, V., and Pirogova, E., "Conformational Changes in Conotoxin Exposed to Static Electric Fields: A Molecular Modeling Study," presented at the ICMMT, Pune, India, 2016.
- [147] English, N. J. and Waldrona, C. J., "Perspectives on external electric fields in molecular simulation: progress, prospects and challenges " *The Journal of Physical Chemistry Chemical Physics*, Perspective vol. 17, no. 19, p. 34, 2015.
- [148] Carl Caleman and Spoel*, D. v. d., "Picosecond Melting of Ice by an Infrared Laser Pulse: A Simulation Study," *Molecular Dynamics Simulations*, vol. 47, p. 4, 2008.
- [149] Jr., A. D. M., "Empirical force fields for biological macromolecules: overview and issues.," *Journal of Computational Chemistry*, vol. 25, no. 13, p. 11, 2004.
- [150] William L. Jorgensen, Jayaraman Chandrasekhar, and Madura, J. D., "Comparison of simple potential functions for simulating liquid water," *The Journal of Chemical Physics*, vol. 79, no. 2, 1983.
- [151] Berendsen, H. J. C., Postma, J. P. M., Van Gunsteren, W. F., DiNola, A., and Haak, J. R., "Molecular dynamics with coupling to an external bath," *The Journal of Chemical Physics*, vol. 81, no. 8, 1998.
- [152] Petersen, H. G., "Accuracy and efficiency of the particle mesh Ewald method," *The Journal of Chemical Physics* vol. 103, no. 9, 1998.
- [153] Al-Naymat, G., Chawla, S., and Taheri, J., "Sparse DTW: A Novel Approach to Speed up Dynamic Time Warping," in *Eighth Australasian Data Mining Conference (AusDM'09)*, Melbourne, 2009, vol. 101, p. 11: Australian Computer Society, Inc.
- [154] Sakoe, H. and Chiba, S., "Dynamic Programming Algorithm Optimization for Spoken Word Recognition " *IEEE Transactions on Acoustics, Speech, and Signal Processing*, vol. 26, no. 1, p. 8, 1978.
- [155] Frishman D1 and P, A., "Knowledge-based protein secondary structure assignment.," *Proteins*, vol. 23, no. 4, pp. 566-579, 1995.
- [156] Humphrey W, Dalke A, and K., S., "VMD: visual molecular dynamics.," *J Mol Graph*, vol. 14, no. 1, pp. 27-28, 1996.

- [157] Basconi, J. E. and Shirts, M. R., "Effects of Temperature Control Algorithms on Transport Properties and Kinetics in Molecular Dynamics Simulations," *Journal of Chemical Theory and Computation*, vol. 9, no. 7, p. 13, 2013.
- [158] Lindorff-Larsen, K. *et al.*, "Improved side-chain torsion potentials for the Amber ff99SB protein force field," *Proteins*, vol. 78, no. 8, p. 8, 2010.
- [159] Crawford, M. L., "Generation of Standard EM Fields Using TEM Transmission Cells," *IEEE Transactions*, vol. EMC-16, p. 6, 1974.
- [160] Boriraksantikul, N., "TEM Cell Design to Study Electromagnetic Radiation Exposure from Cellular Phones," Master of Science, Faculty of the Graduate School, University of Missouri, 2008.
- [161] A. Nothofe, M. Alexander, D. Bozec, A. Marvin, and McCormack, L., "The use of GTEM cells for EMC measurements: Measurement, Good Practice Guide," *Teddington, Middlesex, United Kingdom*, vol. 65, 2003.
- [162] "TC-5060 UHF TEM Cell, Operating Manual," in *Tescom Co, Pty*, ed, 2005.
- [163] Valvona, C. J., Fillmore, H. L., Nunn, P. B., and Pilkington, G. J., "The Regulation and Function of Lactate Dehydrogenase A: Therapeutic Potential in Brain Tumor," *Brain Pathology*, vol. 26, p. 14, 2016.
- [164] Ganesha Rai *et al.*, "Discovery and Optimization of Potent, Cell-Active Pyrazole-Based Inhibitors of Lactate Dehydrogenase (LDH)," *Journal of Medical Chemistry*, vol. 60, no. 22, p. 20, 2017.
- [165] Ding, C., "Catalyzing the Knowledge of Catalase: Investigating the Effect of Substrate Concentration on Reaction Rates Involving Catalase," in *AP/IB Biology 2013*, p. 19.
- [166] Forsburg, S. L., "The yeasts *Saccharomyces Cerevisiae* and *Schizosaccharomyces pombe*: models for cell biology research " *Gravitational and Space Biology, Journal of the American Society For Gravitational And Space Research*, vol. 18, no. 2, p. 8, 2005.
- [167] Lin, K.-W., Yang, C.-J., Lian, H.-Y., and Cai, P., "Exposure of ELF-EMF and RF EMF Increase the Rate of Glucose Transport and TCA Cycle in Budding Yeast," *Frontiers in Microbiology*, vol. 7, p. 15, 2016.
- [168] Fong, S. Y., Piva, T., Dekiwadia, C., Urban, S., and Huynh, T., "Comparison of cytotoxicity between extracts of *Clinacanthus nutans* (Burm. f.) Lindau leaves from different locations and the induction of apoptosis by the crude methanol leaf extract in D24 human melanoma cells.," *BMC Complementary and Alternative Medicine*, vol. 16, no. 368, p. 12, 2016.
- [169] Spurr, A. R., "A low-viscosity epoxy resin embedding medium for electron microscopy," *Journal of Ultrastructure Research*, vol. 26, no. 1-2, p. 13, 1969.
- [170] Coelho, M. A. Z. *et al.*, "Effect of hyperbaric stress on yeast morphology: study by automated image analysis," *Applied Microbiology and Biotechnology*, vol. 66, no. 3, p. 7, 2004.
- [171] Schneider, C. A., Rasband, W. S., and Eliceiri, K. W., "NIH Image to ImageJ: 25 years of image analysis," *Nature Methods | Historical Commentary*, vol. 9, no. 7, p. 5, 2012.
- [172] Pons, M. N., Vivier, H., Remy, J. F., and Dodds, J. A., "Morphological Characterization of Yeast by Image Analysis," *Biotechnology and Bioengineering*, vol. 42, no. 11, p. 8, 1993.
- [173] Pâques, F. and Haber, a. E. H., "Multiple pathways of recombination induced by double-strand breaks in *Saccharomyces cerevisiae*," *Microbiology and Molecular Biology Reviews*, vol. 63, no. 2, p. 56, 1999.

- [174] Xing, F., Zhan, Q., He, Y., Cui, J., He, S., and Wang, G., "1800MHz Microwave Induces p53 and p53-Mediated Caspase-3 Activation Leading to Cell Apoptosis In Vitro," *PLOS/one*, Research Article p. 18, 2016.
- [175] Gos, P., Eicher, B., Kohli, J., and Heyer, W. D., "No mutagenic or recombinogenic effects of mobile phone fields at 900 MHz detected in the yeast *Saccharomyces cerevisiae*," *Bioelectromagnetics*, vol. 21, no. 7, p. 9, 2000.
- [176] Ahlbom, A., Green, A., Kheifets, L., Savitz, D., and Swerdlow, A., "Epidemiology of health effects of radiofrequency exposure," *Environmental Health Perspectives*, vol. 112, no. 17, p. 14, 2004.
- [177] Pacini, S., Ruggiero, M., Sardi, I., Gulisano, M., Gulisano, F., and Aterini, S., "Exposure to global system for mobile communication (GSM) cellular phone radiofrequency alters gene expression, proliferation, and morphology of human skin fibroblasts.," *Oncology Research Featuring Preclinical and Clinical Cancer Therapeutics* vol. 13, p. 6, 2002.
- [178] Alsuhaime, H. S., Vojisavljevic, V., and Pirogova, E., "Effects of low power microwave radiation on the biological activity of Collagenase enzyme and growth rate of *S. Cerevisiae* yeast," in *The International Society for Optical Engineering 8923 · November 2013*, 2013, vol. 8923, p. 6.
- [179] Grundler, W., "Intensity- and frequency-dependent effects of microwaves on cell growth rates," *Journal of Electroanalytical Chemistry*, vol. 27, no. 3, p. 5, 1992.
- [180] Rodney P. O'Connor, Steve D. Madison, Philippe Leveque, H. Llewelyn Roderick, and Bootman, M. D., "Exposure to GSM RF Fields Does Not Affect Calcium Homeostasis in Human Endothelial Cells, Rat Pheochromocytoma Cells or Rat Hippocampal Neurons," *PLOS/one*, vol. 5, no. 7, p. 16, 2010.
- [181] Liedtke, W. *et al.*, "Vanilloid Receptor-Related Osmotically Activated Channel (VR-OAC), a Candidate Vertebrate Osmoreceptor," *cell*, vol. 103, no. 3, p. 10, 2000.
- [182] Jin, M. *et al.*, "Determinants of TRPV4 Activity following Selective Activation by Small Molecule Agonist GSK1016790A," *PLOSone*, vol. 6, no. 2, p. 10, 2011.
- [183] Baratchi S, Almazi JG, Darby W, Tovar-Lopez FJ, Mitchell A, and P., M., "Shear stress mediates exocytosis of functional TRPV4 channels in endothelial cells.," *Cellular and Molecular Life Sciences*, Research Article vol. 73, no. 3, pp. 649-666, 20 August 2015 2016.
- [184] Min Jin *et al.*, "Determinants of TRPV4 Activity following Selective Activation by Small Molecule Agonist GSK1016790A," *PLosOne*, vol. 6, no. 2, p. 10, 2011.
- [185] Wegierski T, Lewandrowski U, Mueller B, Sickmann A, and G, W., "Tyrosine phosphorylation modulates the activity of TRPV4 in response to defined stimuli," *J. Biol Chem*, vol. 284, no. 5, pp. 2923-2933, 2009.
- [186] Daniel P. Poole *et al.*, "Protease-activated Receptor 2 (PAR2) Protein and Transient Receptor Potential Vanilloid 4 (TRPV4) Protein Coupling Is Required for Sustained Inflammatory Signaling," *Journal of biological chemistry*, vol. 288, pp. 5790 –5802, 2013.
- [187] Belyaev, I., "Non-thermal Biological Effects of Microwaves " *Microwave Review*, Review paper p. 17, 2005.
- [188] Sarimov, R., Malmgren, L. O. G., Markova, E., Persson, B. R. R., and Belyaev, I. Y., "Nonthermal GSM microwaves affect chromatin conformation in human lymphocytes similar to heat shock," *IEEE Transactions on Plasma Science*, vol. 32, no. 4, p. 9, 2008.
- [189] Pomerai, D. d. *et al.*, "Non-thermal heat-shock response to microwaves," *Nature*, vol. 405, p. 2, 2000.